

4-2015

Photophysiological Studies of Cyanobacterial Mats in Submerged Sinkholes of Lake Huron

Michael Snider
Grand Valley State University

Follow this and additional works at: <https://scholarworks.gvsu.edu/theses>



Part of the [Biology Commons](#)

ScholarWorks Citation

Snider, Michael, "Photophysiological Studies of Cyanobacterial Mats in Submerged Sinkholes of Lake Huron" (2015). *Masters Theses*. 757.

<https://scholarworks.gvsu.edu/theses/757>

This Thesis is brought to you for free and open access by the Graduate Research and Creative Practice at ScholarWorks@GVSU. It has been accepted for inclusion in Masters Theses by an authorized administrator of ScholarWorks@GVSU. For more information, please contact scholarworks@gvsu.edu.

Photophysiological Studies of Cyanobacterial Mats in Submerged Sinkholes of Lake
Huron

Michael Snider

A Thesis Submitted to the Graduate Faculty of

GRAND VALLEY STATE UNIVERSITY

In

Partial Fulfillment of the Requirements

For the Degree of

Master of Science in Biology

Annis Water Resources Institute

March 2015

ACKNOWLEDGEMENTS

Thank you to my adviser, Dr. Bopi Biddanda, for his hard work and careful guidance through my Master's Degree. Thank you also to the rest of the Biddanda Lab – Tony Weinke, Tom Holcomb, Leon Gereaux, Liz Sommers, Adam McMillan, Steve Long, Nicole Horne, and Scott Kendall.

A special thank you to Dr. Ralph Smith for selflessly lending vital equipment that greatly enhanced the outcome of this research. This work also would not have been possible without the help of the NOAA boat crew and Thunder Bay National Marine Sanctuary dive team.

Lastly, I would like to thank the members of my committee for their help and constructive criticism throughout the planning and conducting of this project, and preparing this manuscript.

This work was made possible through a Grand Valley State University Presidential Grant, funding from the Michigan Space Grant Consortium, and funding from Annis Water Resources Institute.

TABLE OF CONTENTS

LIST OF TABLES.....	7
LIST OF FIGURES.....	11
I. INTRODUCTION.....	19
LITERATURE CITED.....	32
II. Field Observations of Hydrology and Photophysiology of Cyanobacterial Mats in Submerged Sinkhole Ecosystems of Lake Huron Around Alpena, MI.....	36
INTRODUCTION.....	38
MATERIALS AND METHODS.....	48
<i>Study Sites</i>	48
<i>Sampling</i>	52
<i>Field Measurements</i>	52
<i>Statistical analyses</i>	55
RESULTS.....	57
DISCUSSION.....	67
<i>Water chemistry is similar among study sites</i>	67
<i>PAR is an important driver in mat ecosystems</i>	68
<i>Seasonality of biological parameters</i>	69
<i>Physical differences of study sites influence biological parameters</i>	74
<i>Conclusion</i>	78
LITERATURE CITED.....	79

III.	Experimental Studies of Lake Huron Sinkhole Mats Under	
	Variable Light, Oxygen and Sulfide Conditions.....	84
	INTRODUCTION.....	86
	MATERIALS AND METHODS.....	89
	<i>Sampling</i>	89
	<i>Mat slurry – stock preparation</i>	89
	<i>Calibration studies</i>	91
	<i>Filter study</i>	91
	<i>Photosynthetic inhibitors</i>	94
	<i>Cell motility</i>	95
	<i>Measurements</i>	97
	<i>Statistical analyses</i>	98
	RESULTS.....	99
	<i>Microscopy</i>	102
	<i>Calibration studies</i>	103
	<i>Filter studies</i>	105
	<i>Inhibitor studies</i>	120
	<i>Cell motility experiment</i>	131
	DISCUSSION.....	133
	<i>Mats are dominated by two morphotypes</i>	133
	<i>Calibration studies demonstrate</i> <i>stability of Fv/Fm</i>	134
	<i>Light and redox studies show high levels of</i> <i>cyanobacterial versatility</i>	135

	<i>Sulfide tolerance of sinkhole cyanobacteria</i>	141
	<i>Cell motility</i>	143
	<i>Conclusion</i>	144
	LITERATURE CITED.....	146
IV.	SYNTHESIS.....	151
	<i>Microbial mats show seasonally variable photosynthetic characterist</i>	152
	<i>Microbial mats tolerate extreme redox changes</i>	156
	<i>Sinkhole cyanobacteria have moderate sulfide tolerance</i>	157
	<i>Photophysiological filament motility and sedimentary carbon burial</i>	158
	LITERATURE CITED.....	160

LIST OF TABLES

TABLE	PAGE
<p>1. Chemical analysis of water from the Alpena Fountain (FT), El Cajon (EC) and Middle Island Sinkhole (MIS). Data source for calcium at EC site*: Moreau (1983). Values below the limit of detection indicated by a “<”, followed by the instrument limit of detection. “na”: not analyzed.....</p>	39
<p>2. Year-long average of physical parameters of site water. MIS column represents data taken from the groundwater layer. These parameters don’t have a strong influence from the surrounding area/seasonality.....</p>	40
<p>3. Data from winter months at MIS when sampling was not possible. Data was logged by a YSI deployed in the alcove.....</p>	40
<p>4. Average year-long light measurements (units: $\mu\text{mol s}^{-1} \text{m}^{-2}$) comparing surface PAR, PAR reaching the cyanobacterial mat (“Bottom PAR”: note that this is the light climate the mats experience. These data are given in italics to highlight this aspect), and the percent of surface PAR that reaches the cyanobacterial mat. Yearlong averages are indicated in the total section.....</p>	41
<p>5. Year-long pigment data for all three sites (A, B– FT; C, D – EC; E, F – MIS). Left column (A, C, E) show pigment data (Chl – chlorophyll, PE – phycoerythrin, PC – phycocyanin). Right column (B, D, F) shows photosynthetic yield. Data points slightly offset due to overlapping points. Note that the scale for pigment concentration is different for each site, while yield (F_v'/F_m') is constant (right side).....</p>	44

6. Average biological parameters for each site from 2012 – 2013 (units – yield: unitless; pigments (Chl, Phycoerythrin, Phycocyanin): $\mu\text{g} / \text{g}$ dry weight). Right hand column shows the p-value for ANOVA test run for the parameter in that column between the different sites, with significant values bolded ($\alpha = 0.05$), and the site(s) average value that was statistically different from the others via *post hoc* Tukey HSD test stated.....45

7. Carbon biomass Figures for the 2012 year. “%C” is the total carbon (g) in drymass of sample (g). C:N is the ratio of carbon to nitrogen atoms found in the sample, while C:Chl, C:PE, and C:PC are the ratios of carbon atoms to chlorophyll, phycoerythrin and phycocyanin, respectively.....46

8. P-values of regression analyses between various parameters at all sites for the whole sampling period (2012 — 2013; n = 21, 30, and 17 for FT, EC and MIS, respectively). Statistically significant values are bolded ($\alpha = 0.05$). Missing values (“--”) indicated due to redundant values and tests that result in identity (i.e. Chl and Chl).....47

9. Results of linear regression analysis (p – values; $\alpha = 0.05$, significant values bolded) between F_v'/F_m' and different data sources for PAR measurements. Surface PAR and Bottom PAR data values were collected on site with the LiCor meter, while “Weather Station” data was obtained from the Ameriflux database (UMBS station).....48

10. List of filter treatments used in the light filter study. +F and –F indicate the presence or absence, respectively, of a blue filter screen, and +D and –D the presence or absence of a neutral density filter, respectively (in the case of 2D, 2 neutral density filters were used). D refers to layers of neutral density filters that cut PAR by ~50%. Treatments are named based on the % light going past the filters and is available to the mats.....75

11. p-value Results of Shapiro Wilk tests ($\alpha = 0.05$) for each FT treatment group. Values less than 0.05 are shown in bold and signify samples with non-normal distributions. Nitrogen purged samples are shown at left and oxygenated samples at right.....	87
12. Resulting p-values from Kruskal Wallis tests applied to FT filter comparisons ($\alpha = 0.05$). Significant values shown in bold and indicate that there was some effect on the measured parameter between filter treatments (groupings indicated in Figure 8).....	89
13. p-values for Kruskal Wallis tests comparing FT nitrogen purged, oxygenated and control group samples ($\alpha = 0.05$). Significant values shown in bold.....	90
14. p-value Results of Shapiro Wilk tests ($\alpha = 0.05$) for each EC treatment group. Values less than 0.05 are shown in bold and signify samples with non-normal distributions. Nitrogen purged samples are shown at left and oxygenated samples at right.....	92
15. Resulting p-values from Kruskal Wallis tests applied to EC filter comparisons ($\alpha = 0.05$). Significant values shown in bold and indicate that there was some effect on the measured parameter between filter treatments (groupings indicated in Figure 11).....	94
16. p-values for Kruskal Wallis tests comparing EC nitrogen purged, oxygenated and control group samples ($\alpha = 0.05$). Significant values shown in bold.....	95
17. p-value Results of Shapiro Wilk tests ($\alpha = 0.05$) for each MIS treatment group. Values less than 0.05 are shown in bold and signify samples with non-normal distributions. Nitrogen purged samples are shown at left and oxygenated samples at right.....	97

18. Resulting p-values from Kruskal Wallis tests applied to EC filter comparisons ($\alpha = 0.05$). Significant values shown in bold and indicate that there was some effect on the measured parameter between filter treatments (groupings indicated in Figure 14).....	99
19. p-values for Kruskal Wallis tests comparing EC nitrogen purged, oxygenated and control group samples ($\alpha = 0.05$). Significant values shown in bold.....	100
20. Top - Shapiro Wilk Test p-value results for FT inhibitor studies. Significant results shown in bold and indicate non-normal sample distribution. Bottom - Kruskal Wallis test p-value results for inhibitor additions to FT samples ($\alpha = 0.05$). Significant values shown in bold, and indicate an effect of either H ₂ S and/or DCMU (the distinction between which treatment caused a positive test result is indicated by an “*” in Figure 17).....	103
21. Top - Shapiro Wilk Test p-value results for EC inhibitor studies. Significant results shown in bold and indicate non-normal sample distribution. Bottom - Kruskal Wallis test p-value results for inhibitor additions to EC samples ($\alpha = 0.05$). Significant values shown in bold, and indicate an effect of either H ₂ S and/or DCMU (the distinction between which treatment caused a positive test result is indicated by an “*” in Figure 20).....	107
22. Top: Shapiro Wilk Test p-value results for MIS inhibitor studies. Significant results shown in bold and indicate non-normal sample distribution. Bottom: Kruskal Wallis test p-value results for inhibitor additions to MIS samples ($\alpha = 0.05$). Significant values shown in bold, and indicate an effect of either H ₂ S and/or DCMU (the distinction between which treatment caused a positive test result is indicated by an “*” in Figure 23). Note that the global Kruskal Wallis test found a positive p-value (>0.05) for chlorophyll, but the <i>post hoc</i> pairwise Wilcoxon test found no significant differences.....	111

LIST OF FIGURES

FIGURE	PAGE
1. Side-on view of Middle Island Sinkhole. Arrows indicate the flow of groundwater beginning from the vent source in the Alcove which then spills over the Alcove Wall and into the Arena. While purple mat growth is typically present in the Alcove and Alcove Wall, the Arena is the main site for purple growth, including fingers.....	3
2. View of Arena landscape covered in purple microbial mat. Some finger structures are in view. Picture compliments of Taney Casserley, NOAA.....	4
3. Vertical water column profile at Middle Island Sinkhole from July 2013. All 4 parameters change suddenly at 23m indicating the groundwater/ambient water interface (DO in mg/L; pH; Conductivity in S/cm; Temperature in C°).....	4
4. Vertical profile of Middle Island mats. Purple cyanobacteria dominate the upper layer, giving the mats their distinctive purple color, while sulfur oxidizers and archeans (including methanogens) lie below. Each layers respective chemical profile is displayed at the right (graphic from Nold <i>et al.</i> 2010a).....	6
5. Timeline of significant chemical and biological events of Earth's biosphere. Top panel shows atmospheric oxygen levels, and the bottom panel shows major chemical components of the oceans. Pink areas represent a mixture of iron and sulfide, while light blue represents lower oxygenated waters (source: Kendall 2013).....	9
6. Conceptual diagram of the relationship between photosynthetically active radiation (PAR) and F_v'/F_m'	11

7. Light absorption spectra of photosynthetic pigments. Chlorophyll absorbs on the edges of photosynthetically active radiation (PAR), while the accessory pigments phycoerythrin and phycocyanin (and to a lesser extent β -carotene) fill in the middle range where chlorophyll absorption is minimal (Figure: Kaiser *et al.* 2005).....22

8. Diagram of de-excitation pathways of absorbed light energy. A decrease in any pathway would be offset by increases in the others. When the ‘photosynthesis’ pathway is backed up due to over reduction, energy begins flowing into the fluorescence and heat pathways.....24

9. Overview of the photosynthetic process. Electrons (path in dotted line) enter the system from H₂O at PSII with energy input from light, and are then transported from PSII to ETC via plastoquinones a and b (q_b/q_a). When the plastoquinone pool is over reduced, electrons can no longer be transported away from PSII. This can be problematic under constant illumination because energy will continually enter PSII. This excess energy needs to then be dissipated as heat, fluorescence, or electron resonance in order to avoid cellular damage.....25

10. Conceptual model of light intensity present within each sampling location. These differences exist due to differences in the amount of light that is filtered out by differing water column depths, ranging from 0% at the Fountain and nearly 95% at Middle Island Sinkhole.....28

11. Light attenuation in Lake Kinneret. At 20m depth, the wavelengths with the most remaining energy are in a small range between 500 and 600nm. However, note that the amount of available light in this narrow range of PAR wavelengths is drastically reduced compared to that available at the surface (Figure: Dubinsky and Berman 1979).....29

12. Map of study sites. Inset – Alpena Country, located in the Northeast region of Michigan’s lower peninsula (45° 3.746’N 83° 25.873’W). 1: Middle Island Sinkhole (MIS); 2: El Cajon (EC); 3: Fountain (FT).....	31
13. Top left: The Fountain (FT). A 600 foot well provides the groundwater for a community of cyanobacteria. Top right: looking down into the fountain where cyanobacterial mats grow. Middle left: El Cajon (EC), (Alpena, MI. 45° 5.121’N 83° 19.466’W). EC has a centrally located vent that discharges groundwater. Middle right: Underwater close up of cyanobacteria growing at EC. Bottom Left: Aerial view of Middle Island Sinkhole (MIS), (Lake Huron, near Alpena, MI. 45° 11.924’N 83° 19.664’W). Bottom right: Cyanobacteria growing at the bottom of MIS and two raised “finger” structures.....	32
14. NOAA Diver taking DIVING-PAM measurements at Middle Island Sinkhole.....	36
15. Close up views of DIVING-PAM measurements at FT (left), EC (middle), and MIS (right).....	36
16. Year-long pigment data for all three sites (A, B– FT; C, D – EC; E, F – MIS). Left column (A, C, E) show pigment data (Chl – chlorophyll, PE – phycoerythrin, PC – phycocyanin). Right column (B, D, F) shows photosynthetic yield. Data points slightly offset due to overlapping points. Note that the scale for pigment concentration is different for each site, while yield (F_v'/F_m') is constant (right side).....	44
17. Seasonal trend in photosynthetic yield for all 3 study sites. F_v'/F_m' shows an inverse relationship with PAR (PAR data source: Oak Ridge National Laboratory, Ameriflux, site: UMBS).....	52
18. Regression analyses comparing pigment content (x-axes, chlorophyll, phycoerythrin and phycocyanin, left to right) and F_v'/F_m' (y-axes). Top Row: FT samples, Middle Row: EC samples, Bottom Row: MIS samples. P-values for these comparisons located in Table 7.....	55

19. Top Row – (left) FT samples have a browner color during the summer than the vividly purple EC and MIS samples, but look more purple during the winter (right); Middle Row– El Cajon samples (<i>in situ</i>); Bottom Row – (left) Middle Island sample collected in a core tube, and (right) <i>in situ</i>	59
20. Samples were distributed into vials and placed in a matrix organizer underneath a common light source (top; upright cores on sides of incubator are MIS samples). Close up view of samples in scintillation vials (bottom: FT, EC and MIS samples, respectively).....	72
21. Tubing delivers nitrogen to samples and displaces oxygen. Tubing was connected to needles which delivered the nitrogen across a sealed membrane into each vial. The oxygen was then displaced and exited the vials via another needle open to room air.....	76
22. Phototactic cyanobacteria can move to form the shape of oncoming light through an aluminum foil cutout. Left: The ‘before,’ cyanobacteria are homogenously distributed around a petri dish. Middle: A petri dish lid covered with aluminum foil has an “A” cutout to allow light through to the cyanobacteria. Right: After several hours, the cyanobacteria have conformed to the same shape as the aluminum foil cutout. Bottom: Diagram of cutout used in this motility experiment.....	78
23. Recording DIVING-PAM measurements in the laboratory. The probe was placed into each vial and steadily held roughly 5mm from the mat surface and for each measurement.....	79
24. FT samples at 5X (top left), and 400X (top right), EC samples at 6.7X (middle left) and 400X (middle right), and MIS samples at 6.7X (bottom left) and 400X (bottom right).....	84
25. Yield was measured for a full 24hr period with FT (A) and EC (B) samples to observe the effect of continuous illumination. The only effect seen from ANOVA tests was an increase at 6hr for EC (indicated by “*”), while no significant differences were found for FT (p = 0.005, 0.901, respectively). N = 4 for each time point.....	85

26. Stock solution concentration effect on Fv/Fm for FT (A) and EC (B). Volume indicates amount of slurry stock mixed with groundwater to make a total volume of 15mL (0mL of groundwater in the case of 15mL stock). No effect of volume was seen for EC ($p = 0.112$), but there was for FT ($p = 0.024$) for the 6mL treatment.....86
27. Comparisons of filter treatments for FT samples, grouped by all measured parameters: Fv/Fm, chlorophyll (Chl), phycoerythrin (PE), and phycocyanin (PC). The top row shows samples that were purged with nitrogen, and the bottom row shows samples that were fully oxygenated. Bars represent the average of the entire course of the experiment. Error bars represent standard error of the mean. Letters are shown above to indicate statistically significant different groups.....88
28. Comparisons between FT nitrogen purged and oxygenated samples for Fv/Fm (A), chlorophyll (B), phycoerythrin (C), and phycocyanin (D) over the course of the experiment at top left, top right, bottom left and bottom right, respectively. An “*” is displayed above treatments where N₂ and O₂ were found to be statistically different via *post hoc* Wilcoxon tests.....89
29. Plots of filter experiment for FT. Time (x axis) begins with the control that has had no exposure to filters. Time points were taken 24hr apart for 5 days after the control time point. Each Figures compares anoxic and oxic treatment groups for each filter treatment (horizontal rows; treatment indicated at left).....91
30. Comparisons of filter treatments for EC samples, grouped by all measured parameters: Fv/Fm, chlorophyll (Chl), phycoerythrin (PE), and phycocyanin (PC). The top row shows samples that were purged with nitrogen, and the bottom row shows samples that were fully oxygenated. Bars represent the average of the entire course of the experiment. Error bars represent standard error of the mean. Letters are shown above to indicate statistically significant different groups.....93

31. Summary graphs of EC filter studies representing average photosynthetic yield, chlorophyll, phycoerythrin, and phycocyanin over the course of the experiment at top left, top right, bottom left and bottom right, respectively. These plots ignore the effect of time.....94

32. Plots of filter experiment for EC. Time (x axis) begins with the control that has had no exposure to filters. Time points were taken 24hr apart for 5 days after the control time point. Each Figures compares anoxic and oxic treatment groups for each filter treatment (horizontal rows; treatment indicated at left).....96

33. Comparisons of filter treatments for MIS samples, grouped by all measured parameters: Fv/Fm, chlorophyll (Chl), phycoerythrin (PE), and phycocyanin (PC). The top row shows samples that were purged with nitrogen, and the bottom row shows samples that were fully oxygenated. Bars represent the average of the entire course of the experiment. Error bars represent standard error of the mean. Letters are shown above to indicate statistically significant different groups.....98

34. Summary graphs of MIS filter studies representing average photosynthetic yield, chlorophyll, phycoerythrin, and phycocyanin over the course of the experiment at top left, top right, bottom left and bottom right, respectively. These plots ignore the effect of time.....100

35. Plots of filter experiment for MIS. Time (x axis) begins with the control that has had no exposure to filters. Time points were taken 24hr apart for 5 days after the control time point. Each figure compares anoxic and oxic treatment groups for each filter treatment (horizontal rows; treatment indicated at left).....101

36. Measured Fv/Fm, chlorophyll (Chl), phycoerythrin (PE), and phycocyanin (PC) from addition of H₂S (25 - 50μM), DCMU (10μM), and a control on FT samples. Bars represent the average of all time points taken through the duration of the experiment and error bars represent the standard error of the mean. An “*” signifies a statistically significant group.....102

37. Time series results of FT inhibitor results. A.) Fv/Fm, B.) Chlorophyll, C.) Phycoerythrin, D.) Phycocyanin. H ₂ S: (●), DCMU: (■), Control: (◇). When applicable, the treatment that had a significant effect is marked above the time point with a symbol denoting which treatment had the effect (S: H ₂ S; and D: DCMU).....	104
38. Time series of addition of increased inhibitor concentrations for FT samples. Two baseline, non-affected time points were measured before addition of inhibitors.....	105
39. Measured Fv/Fm, chlorophyll (Chl), phycoerythrin (PE), and phycocyanin (PC) from addition of H ₂ S (25 - 50μM), DCMU (10μM), and a control on EC samples. Bars represent the average of all time points taken through the duration of the experiment and error bars represent the standard error of the mean. An “*” signifies a statistically significant group.....	106
40. Time series results of EC inhibitor results.. A.) Fv/Fm, B.) Chlorophyll, C.) Phycoerythrin, D.) Phycocyanin. H ₂ S: (●), DCMU: (■), Control: (◇).When applicable, the treatment that had a significant effect is marked above the time point with a symbol denoting which treatment had the effect (S: H ₂ S; and D: DCMU).....	108
41. Time series of addition of increased inhibitor concentrations for EC samples. Two baseline, non-affected time points were measured before addition of inhibitors. Later time points for DCMU are missing as samples were too few after many cultures died.....	109
42. Measured Fv/Fm, chlorophyll (Chl), phycoerythrin (PE), and phycocyanin (PC) from addition of H ₂ S (25 - 50μM), DCMU (10μM), and a control on MIS samples. Bars represent the average of all time points taken through the duration of the experiment and error bars represent the standard error of the mean. An “*” signifies a statistically significant group.....	110
43. Time series results of MIS inhibitor results.. A.) Fv/Fm, B.) Chlorophyll, C.) Phycoerythrin, D.) Phycocyanin. H ₂ S: (●), DCMU: (■), Control: (◇). When applicable, the treatment that had a significant effect is marked above the time point with a symbol denoting which treatment had the effect (S: H ₂ S; and D: DCMU).....	112

44. Time series of addition of increased inhibitor concentrations for MIS samples. Two baseline, non-affected time points were measured before addition of inhibitors. No DCMU treatments are presented as samples in this group were too few after samples died.....	113
45. Time series results from cell motility experiment. This study was conducted for one hour and Fv/Fm was measured at 10min intervals in both the light sections and dark sections of the petri dish.....	114
46. Emission spectra of incandescent light bulbs at three different wattage ratings. The bulb used in this study was a 40W bulb, close to the 60W bulb represented in the figure. The visible spectrum is colored gray. (MacIsaac 1999).....	121
47. Control groups for samples from the three study sites. These values represent parameters measured in the lab, but before experimental treatments were applied.....	122
48. Overview of seasonality of Fv'/Fm' measured <i>in situ</i> in three sinkhole ecosystems.....	135
49. Top -- Conceptual diagrams of the relationship between chlorophyll, PAR, and Fv'/Fm'. Bottom – theoretical model of regulatory response to changes in PAR to maintain homeostasis. As PAR increases, Fv'/Fm' decreases. The response is to decrease chlorophyll pigment which then increases Fv'/Fm'	136
50. Comparison of Fv'/Fm' values between my study and other studies around the world. Source: Zanzibar (Lugomela <i>et al.</i> 2005), <i>Acaryochloris</i> (Kuhl <i>et al.</i> 2005), Aubi Dabi, Brazil and Spain (Al-Najjar <i>et al.</i> 2014).....	137
51. Timeline of Earth history showing atmospheric levels of molecular oxygen, significant biological landmarks, and the predominant type of photosynthesis. Cyanobacteria are believed to be responsible for the sharp rise in O ₂ 2.3bya, known as the Great Oxidation Event (Biddanda <i>et al.</i> 2012).....	139

INTRODUCTION

Nearly all primary biomass production on Earth is powered by solar energy through the process of photosynthesis. This complex photophysiological pathway provides oxygen for aerobic organisms to breathe, organic carbon for food, and even the carbon in ancient fossil fuels. The sunlight-dependent photosynthetic process has shaped the biogeochemistry and life on our planet from the depths of the ocean to terrestrial habitats over several billion years (Field *et al.* 1998; Blankenship *et al.* 1992). Photosynthesis is a complex process by which inorganic carbon (CO₂) is reduced using the energy harnessed by light (Hohmann-Marriott and Blankenship 2011). A great deal is known about photosynthesis, yet some pieces remain to be understood (like the water splitting mechanism). This process has evolved through a long, convoluted history in which several pieces (such as macromolecular structures, light harvesting pigments, and electron transport chain complexes) have been genetically shuffled around repeatedly between groups of organisms, namely through horizontal gene transfer, making a clear evolutionary map difficult to discern (Xiong and Bauer 2002). Recently discovered cyanobacteria-dominated ecosystems found in Lake Huron sinkholes that mimic Precambrian conditions may present insightful flashbacks along that long evolutionary history.

The Lake Huron Basin of the Great Lakes is pockmarked with sinkholes – karst depressions in the lake floor, or in many cases sheer drop-offs up to 25m deep (Biddanda *et al.* 2006; Coleman 2002). These sinkholes are caused by the dissolution of the limestone due to the porous nature of these limestone rich bedrock layers that allow high water flow through the rock which gradually causes dissolution and erosion. Eventually

the overlying weight is too much and the lake floor caves in on itself – resulting in submerged sinkholes with groundwater venting on the lake floor (Biddanda *et al.* 2009).

The physical conditions of these sinkholes cause a drastically altered hydrological lakescape due to the continued flow of groundwater that now brings in the dissolved minerals from the surrounding aquifer. The water temperature is slightly higher than surrounding lake water and relatively stable across the entire year due to continued input from underneath the lake where the water is immune to ambient temperature effects. In a similar manner, the water chemistry within sinkholes containing groundwater more closely resembles the chemical makeup of the 400 million year old bedrock aquifer. Most notably, the groundwater from these sinkholes contains levels of conductivity and chloride ~10 times higher than surrounding lake water and typical freshwater values, sulfate concentrations ~100 times higher, and, predictably, lacks detectable oxygen (Ruberg *et al.* 2008; Biddanda *et al.* 2009). The stark temperature, salinity and chemical differences between the groundwater and lake water causes a sharp physical-chemical gradient where mixing is minimal. This results in the venting groundwater remaining as a distinct layer at the very bottom of a sinkhole.

While these conditions are certainly uncommon and relatively harsh, life is abundant and thriving. In one sinkhole, a sprawling, vivid purple carpet of microbial life blankets the lake bed near a groundwater vent, extending outwards roughly 200m. Several locations have been discovered in and around Lake Huron with similar physico-chemical conditions, and it is likely that more exist.

Middle Island Sinkhole (Lake Huron; 45 11.927°N 83 19.674°W) is one such feature that harbors this peculiar microbial system. This sinkhole is located 4km off the

coast of Michigan, just north of Alpena. The depression is 23m at its greatest depth, and has high conductivity and high sulfur water lacking oxygen that steadily seeps in through a vent and spills out over the landscape (Figure 1). Purple microbial mats sprawl out across the bottom, dotted by stalagmite-like structures of raised mat (called fingers) that are filled with microbially-produced gasses (Nold *et al.* 2010a). This alien looking benthic landscape is perennially bathed in roughly 1m of venting groundwater (Figure 2). Groundwater mixing is minimal, especially closer to the source, creating a steep gradient (Figure 3).

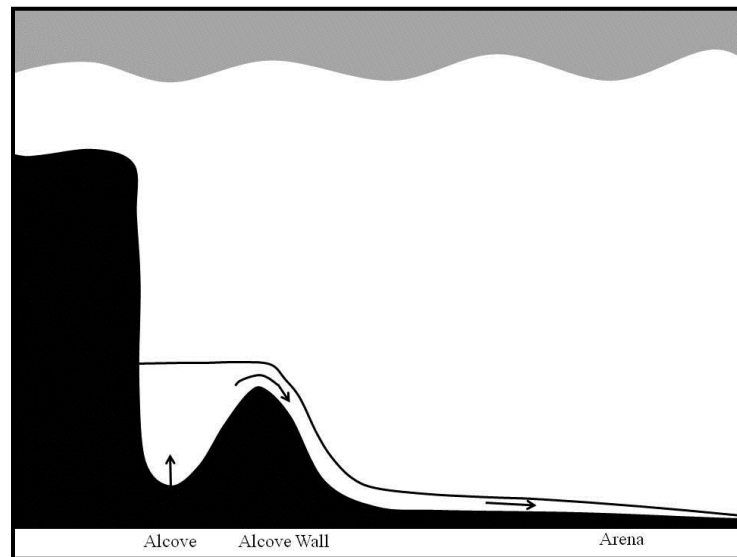


Figure 1: Side-on view of Middle Island Sinkhole. Arrows indicate the flow of groundwater beginning from the vent source in the Alcove which then spills over the Alcove Wall and into the Arena. While purple mat growth is typically present in the Alcove and Alcove Wall, the Arena is the main site for purple growth, including fingers.



Figure 2: View of Arena landscape covered in purple microbial mat. Some finger structures are in view. Picture compliments of Taney Casserley, NOAA.

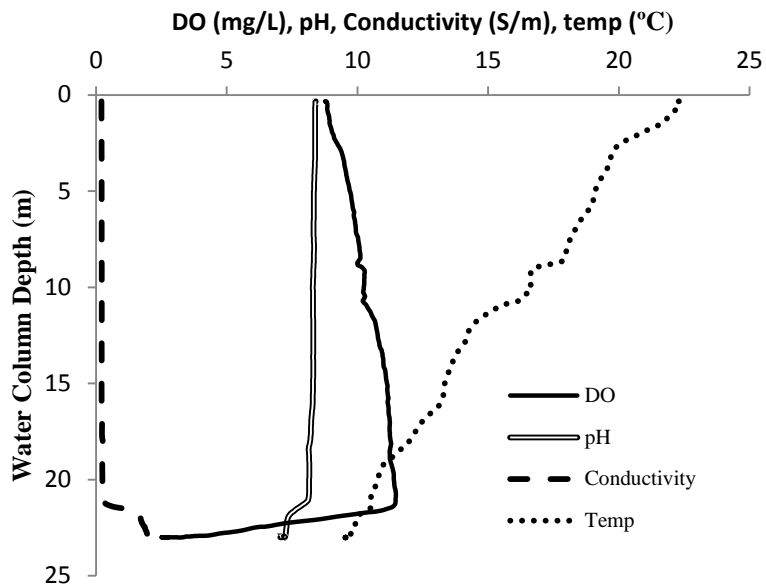


Figure 3: Vertical water column profile at Middle Island Sinkhole from July 2013. All 4 parameters change suddenly at 23m indicating the groundwater/ambient water interface (DO in mg/L; pH; Conductivity in S/cm; Temperature in C°).

The organisms that constitute these purple microbial mats are layered vertically (Figure 4), creating a tightly coupled metabolic cycle. Microbial metabolism here is elevated due in part to the increased and constant temperature (Biddanda and Cotner, 2002). The uppermost purple layer is dominated by photosynthetic cyanobacteria; specifically 2 groups – *Phormidium autumnalae*-like and a *Planktothrix*-like cyanobacteria. In a shotgun metagenomics study done by Voorhies *et al.* (2012), one *Phormidium*-like genotype made up roughly 70% of DNA sequences, while another *Phormidium*-like group and the *Planktothrix*-like (then referred to as an *Oscillatoria* at the time of publication) also contributed sequences found in the top layer of the mat.

A white layer roughly 0.2 cm below the purple layer contains sulfur oxidizers like filamentous *Thiothrix* and ϵ -*Proteobacteria* that have yellow inclusion granules. This layer oxidizes H₂S formed in the underlying sulfate reducing layer. There is some observational evidence that these sulfide oxidizers migrate towards the top of the mat during the night rendering the mats whitish (Biddanda *et al.* 2012, Nold *et al.* 2010a).

The underlying layer is a thin white crystalline carbonate section whose dominant metabolism is the reduction of sulfate from the venting groundwater to H₂S. This is evident from the concurrent drop of sulfate and organic acids at this layer, as well as the occurrence of carbonate secretion in sulfate reducing stromatolites (Nold *et al.* 2010a; Reid *et al.* 2000). This H₂S is then cycled back to sulfate by either the sulfide oxidizing layer, or the top photosynthetic layer (discussed below).

Dark organic rich sediment exists below the microbial mat, and extends down roughly 20m before hitting bedrock. Methanogenic archaeans and methane gas are present while Eukaryotes are scarce in the depths of the sediments (Nold *et al.* 2010b).

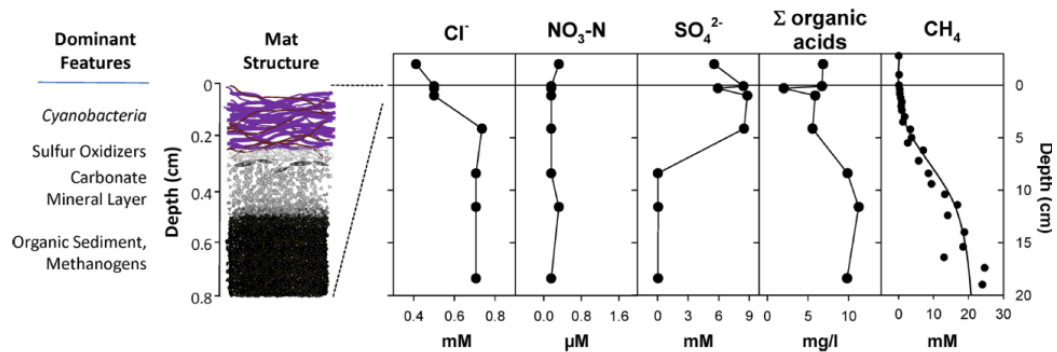


Figure 4: Vertical profile of Middle Island mats. Purple cyanobacteria dominate the upper layer, giving the mats their distinctive purple color, while sulfur oxidizers and archeans (including methanogens) lie below. Each layers respective chemical profile is displayed at the right (graphic from Nold *et al.* 2010a).

Nold *et al.* (2010a) studied the bacterial diversity, as well as the archeal and eukaryal diversity in another (Nold *et al.* 2010b) study. The surface layer of the mat contains a surprisingly low amount of genetic diversity – similar to that of oligotrophic waters. Further, while the other Great Lakes have relatively similar epilimnetic and hypolimnetic genetic profiles to lakes of similar trophic status, Middle Island Sinkhole sediments are significantly different from open lake sediments – characterized by great numbers of Cyanobacteria groups and to a lesser extent, *Bacteroidetes*, *Chloroflexi*, *Proteobacteria*, *Actinobacteria* and *Verrucomicrobiales*. This uniqueness lies more in relative abundances than presence/absence of groups, although some retrieved clones were only distantly related to those found in other aquatic habitats (Nold *et al.* 2010a; Nold *et al.* 2010b).

The paradox then exists that while genetic diversity (particularly in the very top portion of the mats) is dramatically low, functional diversity remains high (Voorhies *et al.* 2012). This is of particular interest considering the persistent anoxic/hypoxic conditions and high sulfate and hydrogen sulfide concentrations. How can so few microbe types carry out so many different ecological functions? The dominant physiology of the cyanobacteria layer is photosynthesis – though due to fluctuating redox conditions, there appears to be a dynamic interplay between oxygenic and anoxygenic photosynthesis. Exposure to sulfide, a photosystem II (PSII) inhibitor, would necessitate some sort of sulfide tolerance. Versatile photophysiology seems to be the answer to this dilemma. Cohen *et al.* (1986) describes several groups of sulfide tolerant cyanobacteria, ranging from minimal (less than 60 μ M) to types that seemed to actually benefit from sulfide, and it is often the case that many organisms containing a variety of sulfide physiologies would live together (Jorgensen *et al.* 1986).

Voorhies *et al.* (2012) characterized the genetic and metabolic diversity of the cyanobacterial layer in Middle Island Sinkhole. In this study, *in situ* light and dark chambers were used to show that the mats are net sinks for oxygen, which points to anoxygenic photosynthetic and chemosynthetic modes of production. C¹⁴ radiolabelling confirmed the presence of anoxygenic photosynthesis and chemosynthesis under sulfidic conditions, while oxygenic photosynthesis remained dominant under oxic conditions. Production values under sulfidic conditions were actually higher than when oxic (17 and 5.1 mg C L⁻¹ d⁻¹, respectively), showing that the mat community thrives on sulfide as opposed to simply tolerating it. The study showed that both prostrate and finger mats are largely dominated by the same *Phormidium-like* genotype, and *Oscillatoria-like* to a

lesser extent, and few other groups of cyanobacteria. These few dominating groups contain metabolic versatility that includes oxygenic and anoxygenic photosynthesis (and the apparent ability to rapidly switch between the two), chemosynthesis and possibly even sulfate reduction.

The mechanism by which cyanobacteria utilize oxygenic and anoxygenic photosynthesis has been described only in a few cyanobacterial communities. Oxygenic photosynthesis utilizes two distinct photosystems (PSII and PSI) in concert, while anoxygenic photosynthesis uses only one (PSI). When in oxygenated conditions, most cyanobacteria perform oxygenic photosynthesis, however, for some, exposure to sulfide simultaneously inhibits PSII, thus blocking oxygenic photosynthesis and stimulating anoxygenic photosynthesis (Cohen *et al.* 1975). The metabolic switch requires protein synthesis, and takes roughly 2hr to complete (Oren and Padan 1978). Although the exact mechanism by which the switch occurs is unknown, the genes and gene products that oxidize sulfide, sulfide quinone reductase (SQR), have been identified, and shown to work by transferring electrons from sulfide to the quinone pool in PSI (Bronstein *et al.* 2000).

This genetic trait is believed to stem from deep within life's history (Blankenship 1992, Falkowski *et al.* 2008). Cyanobacteria are believed to be the cause of a massive rise in atmospheric molecular oxygen levels nearly 2.4 billion years ago, which is now known as the Great Oxidation Event (GOE; Anbar *et al.* 2007; Frei *et al.* 2009, Figure 5). The GOE was a direct result of the rise of oxygenic photosynthesis and forced organisms to either cope with the oxidative cost of oxygen or recede to anaerobic habitats. In this time, O₂ rose from less than roughly 0.001% of modern levels to over 1% (3 orders of

magnitude) across a span of a few million years (a relatively short time on a geologic scale). Before this time, atmospheric oxygen was present, but only in very small

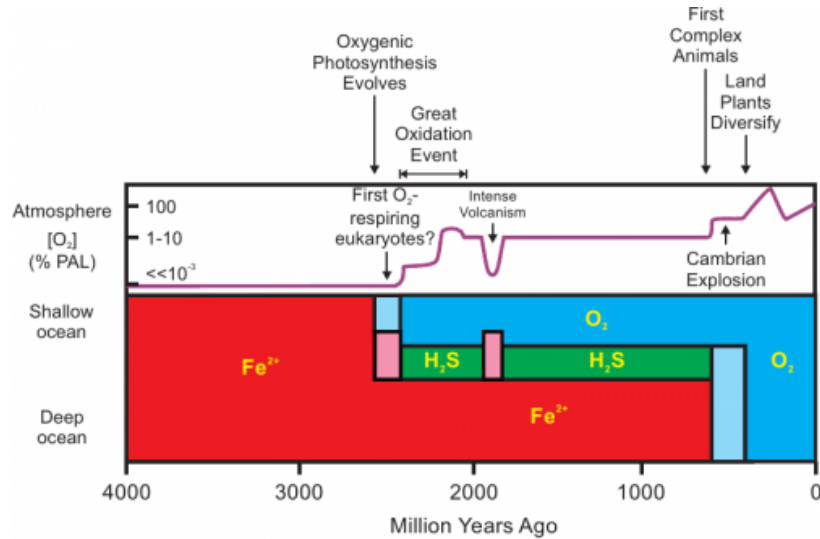


Figure 5: Timeline of significant chemical and biological events of Earth's biosphere. Top panel shows atmospheric oxygen levels, and the bottom panel shows major chemical components of the oceans. Pink areas represent a mixture of iron and sulfide, while light blue represents lower oxygenated waters (source: Kendall 2013).

quantities, and even when it began to appear it was quickly bound by iron containing compounds, methane, hydrogen and reduced forms of sulfur. Free atmospheric oxygen began accumulating once banded iron formations and red beds were unable to accumulate more oxygen. This oxygen transitional period lasted for roughly 1.8 billion years.

Physiologies that utilize oxygen as a respiratory electron acceptor for energy metabolism would have been highly advantageous during this mixed period. The ability

to not just tolerate, but utilize oxygen would have been a significant selective advantage considering the toxic effect of oxygen to obligate anaerobes (Fridovich 1998), as is the case in Middle Island Sinkhole. Further, the microbial mats and water conditions present in Middle Island Sinkhole may be an analog to the Precambrian making it an important system to understanding Earth history.

Other examples of extreme conditions containing cyanobacteria exist under permanently ice covered lakes of Antarctica. Here, *Phormidium*'s closest genetic analogue, *Phormidium autumnalae* (discussed above), lives in an ecosystem that is composed entirely of microbial life and previously thought to be largely devoid of microbial communities (Singh and Elster 2007). Here, cyanobacteria live in near freezing temperatures, performing important ecosystem functions that in some areas may be the only supply of organic carbon and nitrogen to the surrounding environment (Andersen *et al.* 2011; Vincent and Quesada 2012). Submerged mats underneath the ice can photosynthesize, and free living cyanobacteria are the typical biological pioneers of retreating ice sheets and meltwater streams.

The present study analyzes sulfur-metabolizing cyanobacteria-dominated microbial mats found in the extreme environments of submerged sinkholes in Lake Huron near Alpena, MI. While the genetics and robust physiology of these ecosystems have been recently researched, the diverse light climates under which these mats thrive have not been studied. The goal of this project was to gain an understanding of these organisms and how they are impacted by their environment to optimize their life strategy towards energy capture across a gradient of variable light intensity. The relationship between PAR and F_v'/F_m' , an indicator of physiological health, was explored (Figure 6).

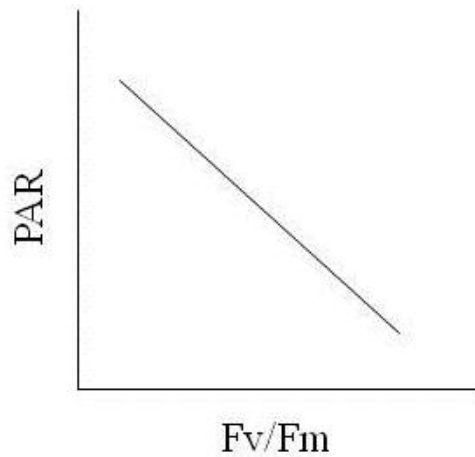


Figure 6: Conceptual diagram of the relationship between photosynthetically active radiation (PAR) and F_v'/F_m' .

Cyanobacteria similar to that found in Middle Island Sinkhole have been found in other nearby locations of Lake Huron containing similar physico-chemical conditions but with substantially different light levels (discussed below). This Lake Huron study increases our knowledge of the hardiness, sensitivity and adaptability of these ancient organisms that may serve as glimpses into the evolutionary history of photosynthesis and ancient Earth itself (Biddanda *et al.*, 2009). Other systems similar to those included in this study also have unique microbial life with sulfur metabolism, but are typically found in remote locations that are logistically and financially difficult to reach (Jorgensen *et al.* 1992; Jannasch and Mottl 1985; Cao *et al.* 2014) making these locations extremely valuable.

The present study analyzed microbial mats in Middle Island Sinkhole (MIS), El Cajon Bay (EC), and a nearby fountain (FT) for photosynthetic yield (F_v'/F_m') as well as chlorophyll, phycoerythrin and phycocyanin (all photosynthetic pigments) to assess the photosynthetic characteristics of mats found in different light conditions. My objective was to understand how photosynthetic efficiency and certain pigment levels changed in similar microbial mats found in habitats with different light conditions. It was found that PAR was an important driving factor at EC and MIS. PAR correlated with F_v'/F_m' and chlorophyll at EC, while PAR correlated with chlorophyll, phycoerythrin, phycocyanin and phycobillin:chlorophyll at MIS. At FT, only chlorophyll and F_v'/F_m' were significantly associated with one another (the association between F_v'/F_m' and PAR was arguably biologically relevant as well; $p = 0.055$). These data show that PAR has a stronger effect on the photosynthetic characteristics at the more shaded sites EC and MIS, while FT, being more exposed to the sun, only showed an association between chlorophyll and F_v'/F_m' . Chlorophyll normally has an inverse relationship with PAR. This relationship was not observed at FT due to the harsh effects of PAR at this site that varied daily with direct sun exposure, to low PAR at morning and evening due to shading by the surrounding buildings.

Laboratory experiments were conducted to further assess the photosynthetic characteristics of the microbial mats. Filters were used to change the light conditions to understand how the photosynthetic characteristics change when mats are subjected to new light conditions. This experiment was conducted with half of the samples grown in oxygenated and the rest in nitrogen purged vials to analyze the effect of oxygen's presence/absence on the measured photosynthetic parameters. Mats were grown using

photosynthetic inhibitors to understand their *in situ* sulfide tolerance and to determine if sulfide mediated PSII inhibition occurs *in situ*. Finally, mat samples were homogenized, disrupting the mat structure, distributed across a petri dish and analyzed for phototactic movement to better understand the association between motility and photosynthetic yield.

PAR was generally associated with increased yield, phycoerythrin and phycocyanin. Chlorophyll was only significantly increased with the higher PAR treatment for EC samples. Limited differences were measured between nitrogen purged and oxygenated samples. Photosynthetic yield was the most affected measured parameter, though no differences were detected for EC samples. In all instances where samples were a response was measured, the oxygenated sample had the higher photosynthetic yield or pigment concentration. Photosynthetic yield was found to be unaffected by the addition of H₂S in cyanobacteria from all sites up to 125µM (the highest treatment administered).

This study showed that chlorophyll was the main photosynthetic pigment that typically varied with PAR. It is well known that photosynthetic yield has an inverse relationship with PAR within normal sunlight ranges. This was seen at EC, weakly at FT (due to shading), and not observed at MIS (due to consistently low PAR). In the laboratory, increased PAR lead to increased photosynthetic yield likely due to insufficiently high PAR. Laboratory experiments showed that *in situ* mats likely were not photosynthetically inhibited by oxygen or sulfide conditions. Lastly, the motility experiment showed that phototactic movement of the cyanobacterial filaments likely played a very important role in light capture optimization *in situ*.

LITERATURE CITED

- Anbar, A., Y. Duan, T. Lyons, G. Arnold, B. Kendall, R. Creaser, A. Kaufman, G. Gordon, C. Scott, J. Garvin, and R. Buick. "A Whiff of Oxygen Before the Great Oxidation Event?" *Science* 317.5846 (2007): 1903-906. Print.
- Andersen, D., D. Sumner, I. Hawes, J. Webster-Brown, and C. Mckay. "Discovery of Large Conical Stromatolites in Lake Untersee, Antarctica." *Geobiology* 9.3 (2011): 280-93. Print.
- Biddanda, B., S. Nold, G. Dick, S. Kendall, J. Vail, S. Ruberg, and C. M. Green. "Rock, Water, Microbes: Underwater Sinkholes in Lake Huron Are Habitats for Ancient Microbial Life." *Nature Education Knowledge* 3:13 (2012). Web.
- Biddanda, B., and J. Cotner. "Love Handles in Aquatic Ecosystems: The Role of Dissolved Organic Carbon Drawdown, Resuspended Sediments, and Terrigenous Inputs in the Carbon Balance of Lake Michigan." *Ecosystems* 5.5 (2002): 431-45. Print.
- Biddanda, B., D. Coleman, T. Johengen, S. Ruberg, G. Meadows, H. Sumeren, R. Rediske, and S. Kendall. "Exploration of a Submerged Sinkhole Ecosystem in Lake Huron." *Ecosystems* 9.5 (2006): 828-42. Print.
- Biddanda, B., S. Nold, S. Ruberg, S. Kendall, T. Sanders, and J. Gray. "Great Lakes Sinkholes: A Microbiogeochemical Frontier." *EOS, Transactions American Geophysical Union* 90.8 (2009): 61. Web.
- Blankenship, R. "Origin and Early Evolution of Photosynthesis." *Photosynthesis Research* 33.2 (1992): 91-111. Web.

- Bronstein, M., M. Schutz, G. Hauska, E. Padan, and Y. Shahak. "Cyanobacterial Sulfide-Quinone Reductase: Cloning and Heterologous Expression." *Journal of Bacteriology* 182.12 (2000): 3336-344. Web.
- Cao, H., Y. Wang, O. Lee, X. Zeng, Z. Shao, and P. Qian. "Microbial Sulfur Cycle in Two Hydrothermal Chimneys on the Southwest Indian Ridge." *MBio* 5.1 (2014). Web.
- Cohen, Y., B. Jorgensen, N. Revsbech, and R. Poplawski. "Adaptation to Hydrogen Sulfide of Oxygenic and Anoxygenic Photosynthesis among Cyanobacteria." *Applied and Environmental Microbiology* 51.2 (1986): 398-407. Web.
- Cohen, Y., E. Padan, and M. Shilo. "Facultative Anoxygenic Photosynthesis in the Cyanobacterium *Oscillatoria Limnetica*." *Journal of Bacteriology* 123.3 (1975): 855-61. Web.
- Coleman, D. "Underwater Archaeology in Thunder Bay National Marine Sanctuary, Lake Huron—Preliminary Results from a Shipwreck Mapping Survey." *Marine Technology Society Journal* 36.3 (2002): 33-44. Print.
- Falkowski, P., T. Fenchel, and F. Delong. "The Microbial Engines That Drive Earth's Biogeochemical Cycles." *Science* 320 (2008): 1034-038. Web.
- Field, C., M. Behrenfeld, J. Randerson, and P. Falkowski. "Primary Production of the Biosphere: Integrating Terrestrial and Oceanic Components." *Science* 281 (1998): 237-40. Web.
- Frei, R., C. Gaucher, S. Poulton, and D. Canfield. "Fluctuations in Precambrian Atmospheric Oxygenation Recorded by Chromium Isotopes." *Nature* 461.7261 (2009): 250-53. Print.

- Fridovich, I. "Oxygen Toxicity: A Radical Explanation." *Journal of Experimental Biology* 201 (1998): 1203-209. Web.
- Hohmann-Marriott, Martin F., and Robert E. Blankenship. "Evolution of Photosynthesis." *Annual Review of Plant Biology* 62.1 (2011): 515-48. Web.
- Jannasch, H., and M. Mottl. "Geomicrobiology of Deep-Sea Hydrothermal Vents." *Science* 229.4715 (1985): 717-25. Print.
- Jorgensen, B., M. Isaksen, and H. Jannasch. "Bacterial Sulfate Reduction Above 100 C in Deep-Sea Hydrothermal Vent Sediments." *Science* 258.5089 (1992): 1756-757. Print.
- Jorgensen, B., Y. Cohen, and N. Revsbech. "Transition from Anoxygenic to Oxygenic Photosynthesis in a Microcoleus-Chthonoplastes Cyanobacterial Mat." *Applied and Environmental Microbiology* 51.2 (1986): 408-17. Web.
- Kendall, B. "Earth's Oxygen Revolution." University of Waterloo, 1 Mar. 2013. Web, <<https://uwaterloo.ca/wat-on-earth/news/earths-oxygen-revolution>>.
- Nold, S., J. Pangborn, H. Zajack, S. Kendall, R. Rediske, and B. Biddanda. "Benthic Bacterial Diversity in Submerged Sinkhole Ecosystems." *Applied and Environmental Microbiology* 76.1 (2010a): 347-51. Print.
- Nold, S., H. Zajack, and B. Biddanda. "Eukaryal and Archaeal Diversity in a Submerged Sinkhole Ecosystem Influenced by Sulfur-rich, Hypoxic Groundwater." *Journal of Great Lakes Research* 36.2 (2010b): 366-75. Print.
- Oren, A., and E. Padan. "Induction of Anaerobic, Photoautotrophic Growth in the Cyanobacterium *Oscillatoria Limnetica*." *Journal of Bacteriology* 133.2 (1978): 558-63. Web.

- Reid, R., P. Visscher, A. Decho, J. Stolz, B. Bebout, C. Dupraz, I. Macintyre, H. Paerl, J. Pinckney, L. Prufert-Bebout, T. Steppe, and D. DesMarais. "The Role of Microbes in Accretion, Lamination and Early Lithification of Modern Marine Stromatolites." *Nature* 406 (2000): 989-92. Web.
- Ruberg, S., S. Kendall, B. Biddanda, T. Black, S. Nold, W. Lusardi, R. Green, T. Casserley, E. Smith, G. Sanders, G. Lang, and S. Constant. "Observations of the Middle Island Sinkhole in Lake Huron – A Unique Hydrogeologic and Glacial Creation of 400 Million Years." *Marine Technology Society Journal* 42.4 (2008): 12-21.
- Singh, S., and J. Elster. "Cyanobacteria in Antarctic Lake Environments: A Mini-review." *Algae and Cyanobacteria in Extreme Environments* (2007): 303-20. Print.
- Vincent, W., and A. Quesada. "Cyanobacterial in High Latitude Lakes, Rivers and Seas." *Ecology of Cyanobacteria II: Their Diversity in Space and Time*. By Brian Whitton. Dordrecht: Springer, 2012. 371-86. Print.
- Voorhies, A., B. Biddanda, S. Kendall, S. Jain, D. Marcus, S. Nold, N. Sheldon, and G. Dick. "Cyanobacterial Life at Low O₂: Community Genomics and Function Reveal Metabolic Versatility and Extremely Low Diversity in a Great Lakes Sinkhole Mat." *Geobiology* 10.3 (2012): 250-67. Print.
- Xiong, J., and C. Bauer. "Complex Evolution of Photosynthesis." *Annual Review of Plant Biology* 53 (2002): 503-21. Print.

CHAPTER 2

Field Observations of Hydrology and Photophysiology of Cyanobacterial Mats in Submerged Sinkhole Ecosystems of Lake Huron around Alpena, MI

ABSTRACT

Recently discovered submerged sinkholes in Lake Huron on the coast of Michigan are extreme environments for microbial life. Physical conditions (PAR, temperature), chemical composition (conductivity, pH) and photophysiological parameters (photosynthetic yield, pigment concentration, C:N), were measured seasonally at three sites to understand the relationship between the physical environment and photophysiology of the cyanobacteria-dominated mats in these sinkholes. These 3 sites, “Fountain” (FT), “El Cajon” (EC) and “Middle Island” (MIS), exist across a natural light gradient ranging in depth from 0m to 23m. At all sites, the cyanobacterial mats were bathed in high conductivity, high sulfate water of roughly constant temperatures (~10°C year-round). Photophysiological results showed a strong seasonal trend at all 3 sites characterized by decreased photosynthetic yield (F_v'/F_m') during the summer months ($F_v'/F_m' = 0.25 - 0.40$; April – August) and increased yield during the winter months ($F_v'/F_m' = 0.70 - 0.75$; November – March). This expected relationship showed that PAR was a significant driving force of photosynthetic yield (linear regression p-values of 0.02, 0.07, and 0.03 for EC, FT and MIS, respectively). Chlorophyll also appeared to vary seasonally in a similar manner to yield. Chlorophyll trended with PAR only at EC, however. This can be explained by physical differences that between the study sites;

namely differences in shading. FT had the higher levels of PAR and the cyanobacteria at this site contained a significantly lower amount of chlorophyll (143 $\mu\text{g/g}$, 1122 $\mu\text{g/g}$ and 1532 $\mu\text{g/g}$ for FT, EC and MIS, respectively). The phycobilins were generally higher in concentration than chlorophyll at all sites. Carbon biosynthesis appeared to increase throughout the summer. Photosynthetic yield was statistically indistinguishable between sites suggesting that the mats are either genetically distinct communities optimized for each location, or they are genetically similar and simply acclimate their photophysiology to the local conditions. This study provides insight into the adaptive capabilities of cyanobacteria, showing how they respond to natural changes in the environment and are capable of inhabiting a wide range of physical environments. Furthermore, these findings regarding the variable pigment composition and photophysiology of sinkhole cyanobacteria found in habitats with a large range of PAR serve as another example of the high functional diversity present in these unique ecosystems that are otherwise characterized by surprisingly low taxonomic diversity.

INTRODUCTION

Cyanobacteria are ubiquitous and thus occupy a vast range of habitats with varying light intensities and comprise much of the microscopic organisms in oceans, lakes, and soils (Garcia-Pichel *et al.* 2003). Cyanobacteria are often the common inhabitant of extreme environments from permanently ice-covered lakes to thermal hot springs (Klatt *et al.* 2011; Olsson-Francis and Cockell 2009). With such a huge variation of niches filled across the planet, cyanobacteria exhibit an incredibly diverse and expansive evolutionary history, both morphologically and genetically as they must possess many different life strategies to fill these niches and optimize survival. Common cyanobacterial life strategies include sheath building, mat biofilm formation, motility, heterocysts and protective pigmentation or changes in photophysiology to make the best use of incident sunlight (Whitton 2012). The cyanobacteria in the present study are found across a wide range of light intensity and quality, so discussion will primarily focus on photophysiology.

Three main classes of photosynthetic pigment exist, and organisms commonly use differential expression of these pigment types as a method of light acclimation (MacIntyre *et al.* 2002). The most important pigment, chlorophyll *a*, is universal to all photosynthesizing organisms except for some photosynthetic bacteria where a close derivative, bacteriochlorophyll, replaces chlorophyll. It is considered to be the main photosynthetic pigment and is directly involved in the charge separation that liberates electrons that are then donated to electron transport chain ETC.

The second pigment class, carotenoids, are fat soluble compounds that are typically embedded in the thylakoid membrane. Some resonance may occur between carotenoids and chlorophylls, but carotenoids are typically associated with photoprotection (Bryant 1994). Although also found in all photosynthetic organisms, carotenoids are made up of many groups of pigments, each of which serve different functions, including some not directly related to photosynthesis. Some examples are myxozanthophyll, canthaxanthin (cold and high light protection), and scytonemin (secreted in filament sheaths; Vincent *et al.* 2004, Whitton 2012). Mycosprine amino acids (MAA) are also secreted to protect against UV damage (Ehling-Shulz and Scherer 1999).

The final pigment class, phycobilins, are water soluble accessory pigments found in cyanobacteria and red algae. Phycobilins typically include three specific pigments: phycocyanin, phycoerythrin, and allophycocyanin. These pigments are arranged in macromolecular protein-pigment complexes that specialize in harvesting wavelengths of light not captured by chlorophyll or carotenoids (Zhao *et al.* 2011; Figure 1). Phycoerythrin provides the characteristic red pigmentation seen in red algae, and helps absorb shorter wavelengths of light at increased depths. Cyanobacteria are able to rapidly vary phycobilin concentration in response to environmental changes (Grossman *et al.* 1993). As such, they are of particular interest in terms of these organisms' relationship with environmental parameters. Phycobilins are likely more crucial to light harvesting than even chlorophyll in cyanobacteria (Jorgenson *et al.* 1987).

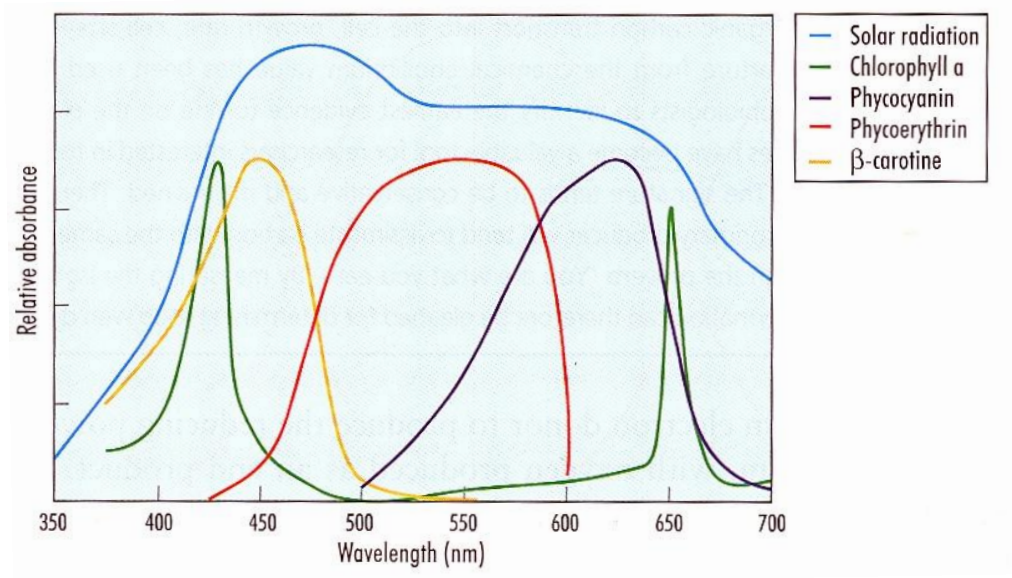


Figure 1: Light absorption spectra of photosynthetic pigments. Chlorophyll absorbs on the edges of photosynthetically active radiation (PAR), while the accessory pigments phycoerythrin and phycocyanin (and to a lesser extent β -carotene) fill in the middle range where chlorophyll absorption is minimal (Figure: Kaiser *et al.* 2005).

Photosynthetic organisms are physiologically dynamic as they must tolerate changes in available solar radiation both daily and seasonally. The cyanobacteria in this study inhabit relatively extreme conditions and must tolerate fluctuating illumination and chemical changes. Tolerating changes in illumination involves changes in pigment levels (above), which in turn changes overall photophysiology. Pigment content directly affects yield – when a cell has more pigment content, more light is absorbed. When too much

energy is absorbed, some of it must be released as fluorescence to prevent damage. Thus, constant regulation of pigment levels is vital.

Photosynthetic yield, which is also known as F_v'/F_m' , steady-state quantum yield or simply Y , is a non-invasive, instantaneous and integrated measure of several photosynthetic processes that serves as an index of how efficient a photosynthetic organism captures light energy. Thus, knowledge of photosynthetic yield helps quantify the photosynthetic condition or health of the organism. The theory behind fluorescence parameters is very complex and in many areas, its interpretation remains highly controversial (see Maxwell and Johnson 2000, Campbell *et al.* 1998). For the purposes of this study, the most important parameter is F_v'/F_m' (and in the next chapter, F_v/F_m , which is the potential or maximum fluorescence), which represents steady-state fluorescence (actual or achieved fluorescence).

Steady-state quantum yield (hereon referred to as yield or F_v'/F_m') measures fluorescence, which is one of three routes for light energy after being absorbed by a pigment – photochemistry (energy successfully put into driving photosynthesis), heat dissipation (energy reemitted and not used for photosynthesis), or it can be reemitted as light (referred to as fluorescence) – and the last pathway is measured for yield (Figure 2). An increase in one pathway means a decrease in the others, so we can measure energy transferred to photosynthesis indirectly by measuring fluorescence (an inversely proportional relationship). Each measurement consists of a burst of light that is sent to the sample, the sample then reemits some of the light as fluorescence, and the fluorometer measures the amount of fluorescence.

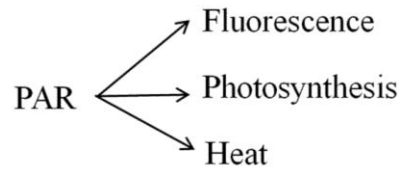


Figure 2: Diagram of de-excitation pathways of absorbed light energy. A decrease in any pathway would be offset by increases in the others. When the ‘photosynthesis’ pathway is backed up due to over reduction, energy begins flowing into the fluorescence and heat pathways.

The source of fluorescence occurs at the molecular level. Only so much light energy can be processed for photosynthesis at a time, and any additional energy must be dissipated to prevent cellular damage (Falkowski and Raven 1997). Photons of light provide the energy necessary to separate electrons from water. These electrons are then sent down the photosynthetic pathway to the electron transport chain. Under normal conditions these high energy electrons are passed from the chlorophyll a complex to reduce plastiquinone_b (q_b) and plastiquinone_a (q_a) to allow more electrons to be stripped from water at the chlorophyll. The plastiquinone pool then transports the electrons to ETC – this, however, is a slower process and is considered to be the rate limiting step for the light reactions. If the plastiquinone pool is saturated and completely reduced, there is no route for additional electrons to move down the photosynthetic pathway. The problem is that pigments will continue to collect light energy. These non-photochemical routes

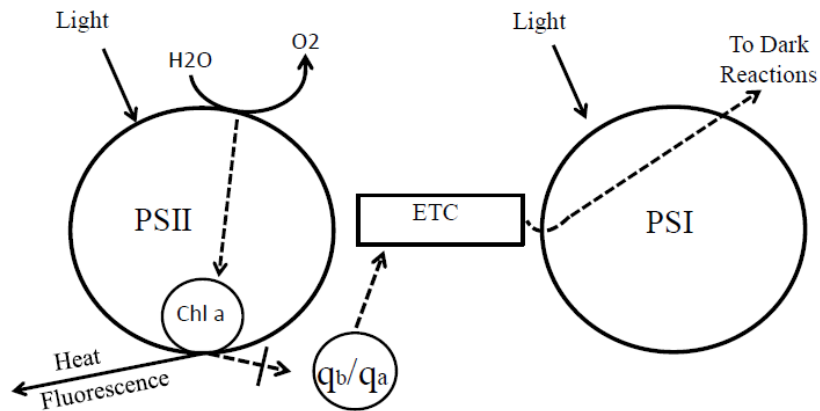


Figure 3: Overview of the photosynthetic process. Electrons (path in dotted line) enter the system from H₂O at PSII with energy input from light, and are then transported from PSII to ETC via plastiquinones a and b (q_b/q_a). When the plastiquinone pool is over reduced, electrons can no longer be transported away from PSII. This can be problematic under constant illumination because energy will continually enter PSII. This excess energy needs to then be dissipated as heat, fluorescence, or electron resonance in order to avoid cellular damage.

allow the energy to be diverted and prevent damage to the photosynthetic reaction center (Figure 3).

Conceptually, as the plastiquinone pool becomes saturated, the reaction centers close as they are unable to transfer electrons into the photosynthetic process. Photosynthetic efficiency then decreases because each reaction center is less likely to deliver electrons from water to ETC. The presence of any closed reaction centers leads to

an increase in fluorescence. This relationship is indicated by photosynthetic yield peaking at low light which can then only decrease as light increases because more reaction centers will be reduced. This should not be confused with the overall rate of photosynthesis – carbon assimilation increases to a saturation point with increasing light, and only decreases beyond that point due to photoinhibition. Light acquisition (the “light reactions”) generates reducing power used in carbon assimilation (the “dark reactions”) – the two are closely linked, yet the dark reactions can occur in the dark. Fluorescence analysis only looks at the first half of the photosynthetic process – the light reactions – though the dark reactions still play a critical role in photosynthesis. Many factors affect this overall process and consequently F_v'/F_m' values.

The advantage of modern fluorometers that use pulse amplitude modulation (PAM) is that photosynthetic yield can be measured in the field where high ambient sunlight would otherwise make measurements impossible (Heinz *et al.* 1998). This method makes the burst of light sent to the sample a series of quick successive pulses. The fluorescence given off by the samples follows this series of pulses and the instrument is tuned to measure that signal. In addition, wavelength specific modifications helps to fine-tune the measured signal.

Cyanobacteria are oxygenic photosynthesizers which means they contain both a type I and type II photosystem (PSI and PSII, respectively). The two systems work in concert to strip electrons from water and create a proton gradient to drive ATP synthesis. In addition, some cyanobacteria can shut down PSII and perform a bacteria-like anoxygenic photosynthetic pathway (discussed later).

Lugomela *et al.* (2005) found photosynthetic yield to increase with depth due to decreased PAR, but observed no apparent seasonality through the year for cyanobacterial mats found in sub-tidal zones. Lionard *et al.* (2012) found decreasing photosynthetic yield with increasing conductivity, and many studies have found *in situ* seasonality of Fv'/Fm' and pigment content (Bowker *et al.* 2002), but no such studies have been conducted in these sinkhole ecosystems.

The purpose of this study was to characterize how changes in light intensity and spectra affect the photophysiology of these cyanobacteria dominated mats. Communities of cyanobacteria at three separate locations across a natural light gradient (94 - 1879 $\mu\text{mol s}^{-1} \text{m}^{-2}$; Figure 4) were studied. Increased depth filters out light intensity and longer wavelengths of light according to the Beer-Lambert law in addition to planktonic light absorption (Stavn 1988, Figure 5), so all study sites contain cyanobacteria living in different light conditions due to differences in depth. I sought to investigate if mats in higher light conditions would have lower pigment levels, and if overall pigment levels would change in response to changes in PAR during summer and winter months. I also wanted to investigate if photosynthetic yield would differ between the different sites studied, and similarly if yield would stay stable or vary seasonally across the year at each site. To date, no other studies have analyzed the *in situ* pigment content or photosynthetic yield of these microbial mats. Pigment levels (chlorophyll, phycoerythrin and phycocyanin) as well as photosynthetic yield and C:N were measured to understand the photophysiology of these microbial systems.

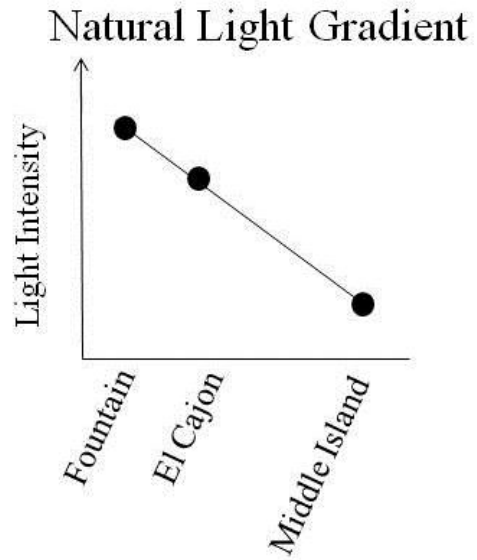


Figure 4: Conceptual model of light intensity present within each sampling location. These differences exist due to differences in the amount of light that is filtered out by differing water column depths, ranging from 0% at the Fountain and nearly 95% at Middle Island Sinkhole.

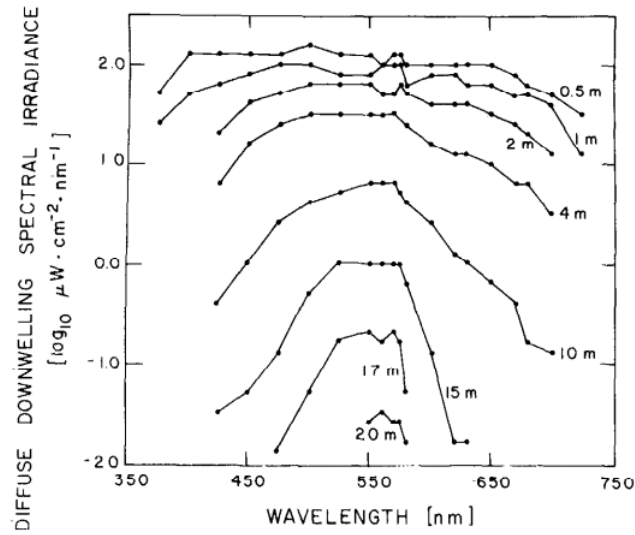


Figure 5: Light attenuation in Lake Kinneret. At 20m depth, the wavelengths with the most remaining energy are in a small range between 500 and 600nm. However, note that the amount of available light in this narrow range of PAR wavelengths is drastically reduced compared to that available at the surface (Figure: Dubinsky and Berman 1979).

MATERIALS AND METHODS

Study sites

Alpena Library Fountain

“The Fountain” (FT) is an artesian well located directly next to the Alpena County Library (45 3.747’N 83 25.872’W, Figures 6 and 7 top). Its location between two buildings provides shading in the morning and late evening, but the absence of any overlying water means direct sunlight can reach the cyanobacteria during midday. Water flows from the top of the fountain into an upper trough which overflows into a larger bottom basin and then to a single drain. This water comes from a high conductivity, sulfate-rich, oxygen-deprived source from a deep bedrock aquifer. Cyanobacterial mat growth is typically located around the perimeter of the bottom basin affixed to concrete, containing no underlying sediment. The mats at this location are a dull, brown color, though the individual filaments still appear purple under a microscope. White chemosynthetic growth is prevalent in the upper trough.

El Cajon Bay

“El Cajon” (EC) is a shallow (~1m) spring located in a small inlet of El Cajon Bay (45 5.120’N 83 19.467’W, Figures 6 and 7 middle). Sulfate-rich groundwater flows up from a vent and quickly mixes with the surrounding oxic waters. Some surface turbulence is visible under calm conditions from the upward flow of groundwater. The

source of this groundwater is believed to be the same as from the other sites studied. Cyanobacterial growth is prevalent inside the vent and up to roughly 3 meters out towards the rest of the bay where purple cyanobacterial growth thins out and appears to disappear to the naked eye. Growth is visible in and around the vent, on the surfaces of underwater plants, logs and debris, as well as underneath floating ‘rafts’ at the water surface. An unknown depth (>1 m) of rich organic matter lies underneath this area.

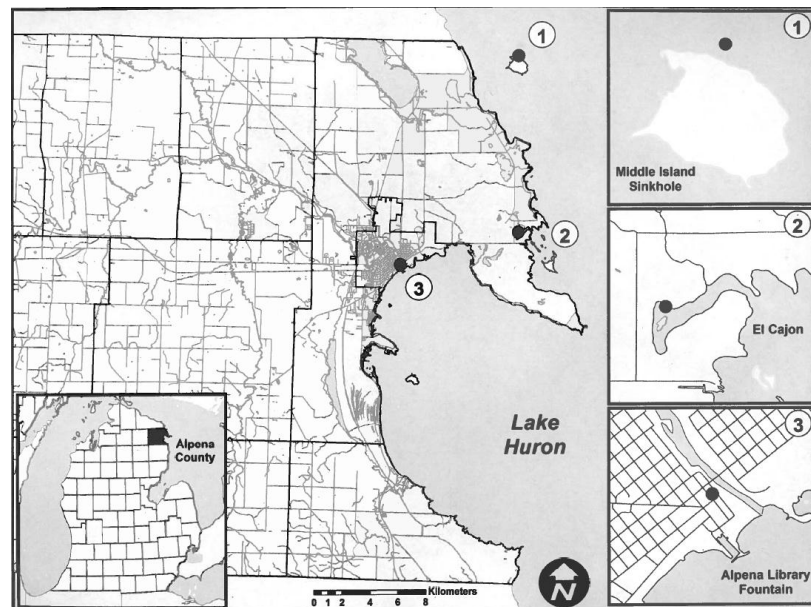


Figure 6: Map of study sites. Inset – Alpena County, located in the Northeast region of Michigan’s lower peninsula ($45^{\circ} 3.746'N$ $83^{\circ} 25.873'W$). 1: Middle Island Sinkhole (MIS); 2: El Cajon (EC); 3: Fountain (FT).



Figure 7: Top left: The Fountain (FT). A 600 foot well provides the groundwater for a community of cyanobacteria. Top right: looking down into the fountain where cyanobacterial mats grow. Middle left: El Cajon (EC), (Alpena, MI. $45^{\circ} 5.121'N$ $83^{\circ} 19.466'W$). EC has a centrally located vent that discharges groundwater. Middle right: Underwater close up of cyanobacteria growing at EC. Bottom Left: Aerial view of Middle Island Sinkhole (MIS), (Lake Huron, near

Alpena, MI. 45° 11.924'N 83° 19.664'W). Bottom right: Cyanobacteria growing at the bottom of MIS and two raised “finger” structures.

Middle Island Sinkhole

Middle Island Sinkhole (MIS) is a submerged, karst, bowl-shaped feature on the floor of Lake Huron (45 11.927'N 83 19.674'W, Figures 6 and 7 bottom). This sinkhole ecosystem is 23m deep where it receives roughly ~10% of surface illumination and has a significant portion of the long-wave red spectrum attenuated due to its depth. Two dominant cyanobacterial groups, a Phormidium-like and an Oscillatoria-like cyanobacteria make up the sprawling purple landscape, including raised finger structures created by microbial gasses produced within deep carbon-rich sediment (Voorhies *et al.* 2012; Nold *et al.* 2013, Figure 6 bottom right). The surrounding lake bed is roughly 2 m deep on the South end (neighboring Middle Island) with an almost sheer drop down into the sinkhole, and opens up towards the Northwest at about 23m depth. A point source vent discharges groundwater into a bowl located in what is known as the alcove, where, due to the groundwater's greater density, it collects and flows over the lip, spreading into the larger portion of the sinkhole. Many cracks in the lake bed act as small non-point sources of groundwater. However, the single point source vent within the alcove is believed to be the main source of groundwater in the sinkhole. The venting groundwater, remains well stratified due to thermo, pycno and chemoclines (Sanders *et al.* 2011).

Sampling

Samples were collected from each site for pigment extraction. FT samples were scraped from the large basin at the bottom of the fountain and hand collected into zip lock bags. EC samples were pulled off of plants and debris and placed into ziplock bags. SCUBA divers hand-collected prostrate mat samples at MIS using plastic coring tubes and rubber stoppers. Coring tubes were filled with approximately 15cm of sediment along with the cyanobacterial mats laying on top of the sediment in each sample. All samples from each site were stored on ice immediately following collection and during transportation to the laboratory. MIS mat material was removed from the sediments prior to analysis, and pigment samples were stored at -80°C until extraction (maximum of three months).

Samples were collected periodically from all three sites from April 2012 to August 2013. Exceptions included limited growth at the fountain due to Alpena Library maintenance cleaning, and ice cover and rough weather conditions on Lake Huron and around Middle Island during the colder months.

Field Measurements

Conductivity, DO, pH, and temperature were measured using a YSI 6600 multi-probe sonde (YSI incorporated, Yellow Springs, OH). Photosynthetically active radiation (PAR) was measured at the surface and greatest depth using a LiCor LI-192 Underwater Quantum Sensor (LiCor Biotechnology, Lincoln, Nebraska). YSI measurements were made at FT by dipping the sonde into a bucket with water collected from the fountain

because the water was not deep enough for sonde measurements, while at EC, measurements were taken at the groundwater source. At MIS, a YSI sonde was deployed in the center of the collection site during sampling and retrieved later. However, due to logistical reasons of operating at ~23 m and over a large and expansive area of the arena, measurements could not always be repeated at precisely the same location, though care was taken to ensure relative proximity to the alcove and a reference fenceline that is in place. Full water column profiles were obtained as well. A sonde was deployed at MIS and left to log data once daily throughout the winter (September 2012 to May 2013). Photosynthetic efficiency was measured at all sites at the time of collection using a Diving-PAM submersible fluorometer (Walz, Germany, Figure 8) before samples were collected. Measurements were taken in all areas of growth for all sites (Figure 9).

Water samples were collected, frozen immediately and submitted to Trace Analytical (Muskegon, MI) for water chemistry analysis for calcium, iron, magnesium, manganese (EPA 6000) SRP-P, SO₄ (EPA 300.0), Cl (EPA 300.0 / SM 4500 Cl⁻D & E), and NO₃-N (EPA 300.0 / 353.2).



Figure 8: NOAA Diver taking DIVING-PAM measurements at Middle Island Sinkhole.

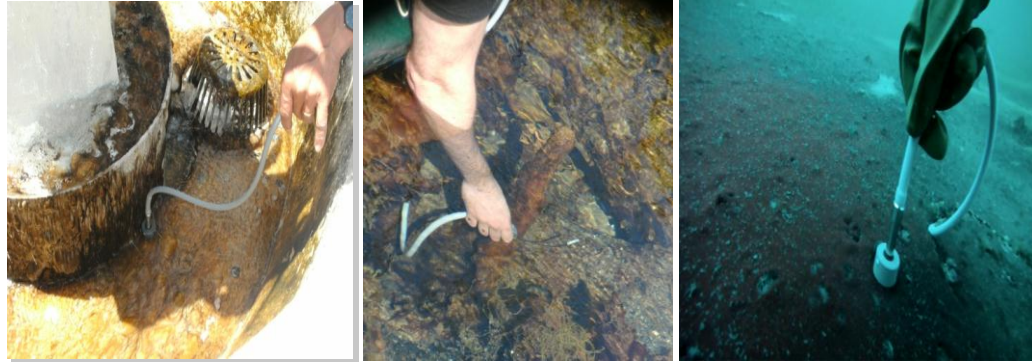


Figure 9: Close up views of DIVING-PAM measurements at FT (left), EC (middle), and MIS (right).

Phycobilin extractions (phycoerythrin and phycocyanin) were analyzed using a spectrophotometer according to Lawrenz *et al.* (2011). Extractions were performed on ice by two 30 second sonication pulses followed by a 24 hour extraction at 5°C in 0.1M phosphate buffer (pH 6.0). These samples were then centrifuged at a speed of 20,000RPM at 20min and the supernatant was analyzed in a spectrophotometer. Phycoerythrin was measured at 545nm and phycocyanin at 620nm, and both were scatter corrected by subtracting the absorbance of each sample at 750nm. Chlorophyll extractions were performed by sonification and extraction with dimethylformamide (DMF; Sharize *et al.* 1984). Phaeopigment correction and final chlorophyll calculations were conducted according to equations derived by Lorenzen (1967). Samples were measured for absorbance at 665nm, acidified and remeasured to correct for

pheopigments. All pigment determinations were standardized to dry weight after complete dryness in a dessicator.

Roughly 1mg (dry weight) samples were collected onto pre-weighed 25mm GF/F microfiber filters and submitted to the Marine Science Institute at the University of California, Santa Barbara for CHN analysis (Dumas combustion method). Filters were vacuumed to remove excess moisture, and then frozen at -80°C until ready for submission when they were then acidified using concentrated HCl to remove any calcium bicarbonate.

My PAR measurements were only taken on the days of sampling. In order to assess the affect of yearlong PAR (that I did not measure), long term PAR data was retrieved from <http://ameriflux.ornl.gov/> (courtesy Oak Ridge National Laboratory). Data used was from the UMBS station because this weather station site was the closest station that measured PAR over the sampling period.

Statistical Analyses

PAR and field measurements (yield, chlorophyll, phycoerythrin and phycocyanin) were divided into summer and winter seasons (May – September, October – April, respectively). Field measurements were compared between sites with ANOVA. Significant findings were followed by a *post hoc* Tukey test. Regression analyses were used to compare carbon content to nitrogen, chlorophyll, phycoerythrin and phycocyanin for all sites. Regression analyses were conducted between all measured field parameters (chlorophyll, phycoerythrin, phycocyanin, phycoerythrin:phycocyanin,

phycobilins:chlorophyll, F_v'/F_m' , and PAR). Regressions were conducted between F_v'/F_m' and the different sources of PAR data (surface PAR, bottom PAR, and weather station PAR) to show any differences in using these different sources of data.

RESULTS

Water parameters were measured at all sites and are displayed in Table 1. Iron and manganese were both below the limit of detection, while SRP and NO₃-N were below the limit of detection at FT. All sites have high SO₄ content, consistent with previous publications.

Table 1: Chemical analysis of water from the Alpena Fountain (FT). El Cajon (EC) and Middle Island Sinkhole (MIS). Data source for calcium at EC site*: Moreau (1983). Values below the limit of detection indicated by a “<”, followed by the instrument limit of detection. “na”: not analyzed.

Parameter	FT	EC	MIS
Calcium (mg/L)	450	384*	280
Iron (mg/L)	<0.20	na	<0.20
Magnesium (mg/L)	110	na	33
Manganese (mg/L)	<0.050	na	<0.050
SRP-P (mg/L)	<0.005	<0.005	0.005
SO ₄ (mg/L)	1056	1303	617
Cl (mg/L)	64	29	16
NO ₃ -N (mg/L)	<0.01	<0.01	2.42

Table 2: Year-long average of physical parameters of site water. MIS column represents data taken from the groundwater layer. These parameters don't have a strong influence from the surrounding area/seasonality.

	FT	EC	MIS
DO (mg/L)	3.68	1.02	0.89
Temperature (°C)	11.46	10.28	9.42
Conductivity (µS/cm)	2491	2431	1816
pH	7.27	7.12	7.29

Table 3: Data from winter months at MIS when sampling was not possible. Data was logged by a YSI deployed in the alcove.

Parameter	MIS Alcove
Temperature (°C)	9.2
Conductivity (µS/cm)	21780
Dissolved Oxygen (mg/L)	0.95

Table 4: Average year-long light measurements (units: $\mu\text{mol s}^{-1} \text{m}^{-2}$) comparing surface PAR, PAR reaching the cyanobacterial mat (“Bottom PAR”: note that this is the light climate the mats experience. These data are given in italics to highlight this aspect), and the percent of surface PAR that reaches the cyanobacterial mat. Yearlong averages are indicated in the total section.

	Parameter	FT	EC	MIS
Winter	Surface PAR	985	1575	--
	Bottom PAR	985	873	--
	% Remaining	<i>100</i>	<i>55</i>	--
Summer	Surface PAR	2356	2307	2218
	Bottom PAR	2356	1360	94
	% Remaining	<i>100</i>	<i>59</i>	<i>4</i>
Total	Surface PAR	1879	1824	2218
	Bottom PAR	<i>1879</i>	<i>1008</i>	<i>94</i>
	% Remaining	<i>100</i>	<i>54</i>	<i>4</i>

Physical parameters of the groundwater from each sample location are compared in Table 2. Despite being geographically separated, the measured parameters are quite similar. Three parameters were measured over the winter period at MIS (Table 3) to show physical parameters in the months in which sampling was not logistically feasible. PAR data for each site is shown in Table 4, highlighting the main differences in light climate for each site. Comparisons can be made between the summer (May through September)

and winter (October through April) in order to see the full effect of seasonality. Separating the data in this manner was important due to the lack of winter data for MIS. The summer had higher PAR values for both sites where full year sampling was possible. MIS had the highest degree of PAR filtering through the water column, followed by EC, and finally FT where there is virtually no water column. The degree to which PAR was filtered at EC was relatively unchanged between the summer and winter. Year-long F_v'/F_m' measurements are presented in Figure 10, showing chlorophyll, phycocyanin and phycoerythrin, as well as yield. Average values of summer and winter seasons of biological parameters are presented in Table 5. This was organized into summer and winter as well to assess the impact of seasonality. Results of an ANOVA tests showed that chlorophyll levels differed between sites (EC and MIS in one group, FT in the other and having a significantly lower value), while all other averaged year-long parameters were not significantly different. No differences were detected in the winter season between FT and EC.

Table 6 displays estimates of ratios of cellular carbon to pigment molecules as well as total percent weight of carbon by dry mass. All sites show the lowest cellular carbon in the spring followed by the highest in the mid-summer, and an intermediate value in the fall. Some values are missing at FT due to insufficient growth for pigment and CHN analyses.

The results of linear regression analyses of biological parameters and the resulting p-values are presented in Table 7. Chlorophyll content was significant when compared to PAR for EC and MIS (not FT), while all sites had significant comparisons between chlorophyll and F_v'/F_m' . Interestingly, FT has a significantly different chlorophyll value

(Table 5). PAR and F_v'/F_m' results were significant for EC and quite close to significance at FT (<0.001 , and 0.0552 , respectively). PAR is likely an important driving factor so several sources of PAR measurements were analyzed as well (Table 8), though these analyses yielded no change in significant test results.

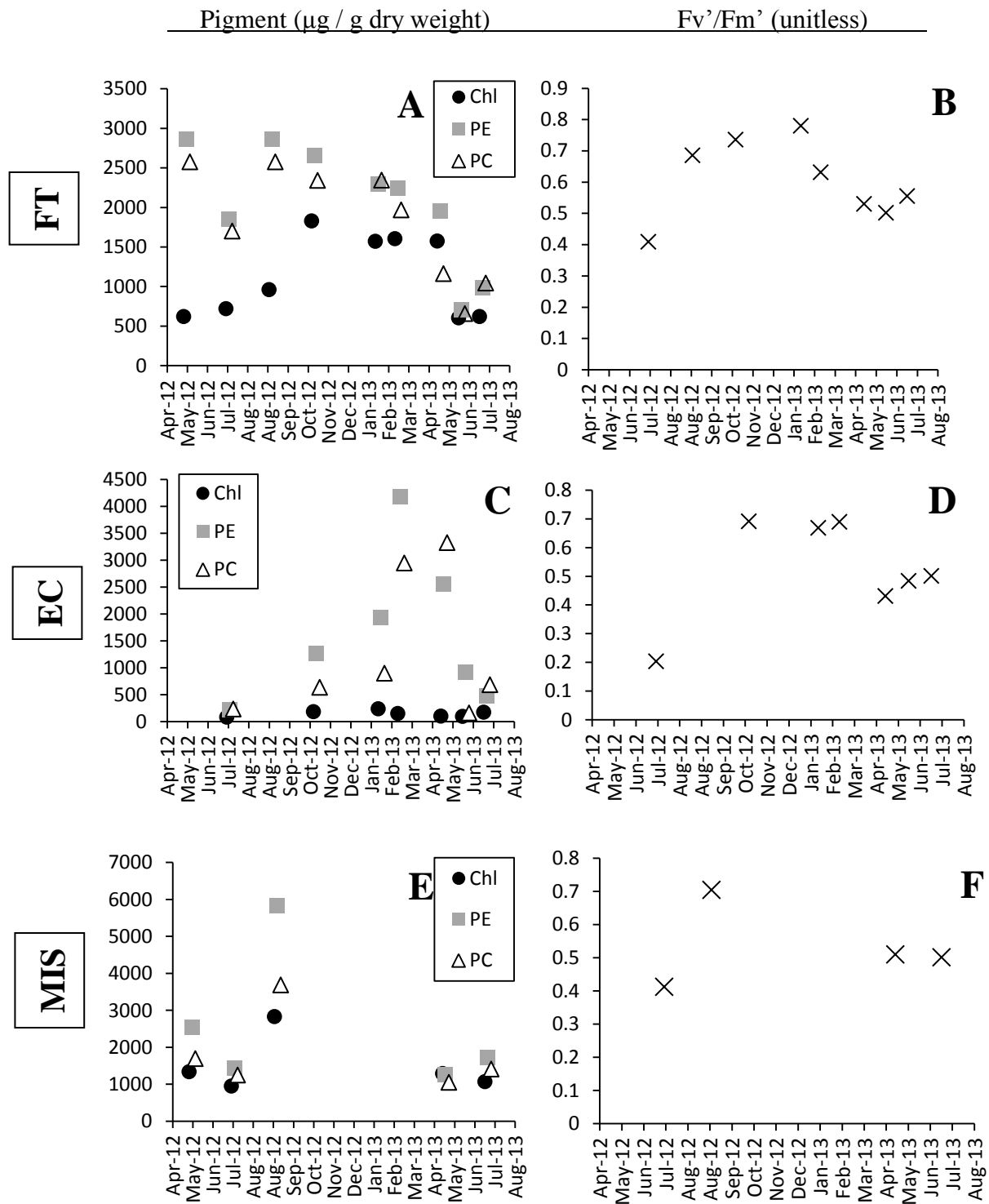


Figure 10: Year-long pigment data for all three sites (A, B– FT; C, D – EC; E, F – MIS). Left column (A, C, E) show pigment data (Chl – chlorophyll, PE – phycoerythrin, PC – phycocyanin). Right column (B, D, F) shows photosynthetic

yield. Data points slightly offset due to overlapping points. Note that the scale for pigment concentration is different for each site, while yield (Fv'/Fm') is constant (right side).

Table 5: Average biological parameters for each site from 2012 – 2013 (units – yield: unitless; pigments (Chl, Phycoerythrin, Phycocyanin): $\mu\text{g} / \text{g}$ dry weight). Right hand column shows the p-value for ANOVA test run for the parameter in that column between the different sites, with significant values bolded (alpha = 0.05), and the site(s) average value that was statistically different from the others via *post hoc* Tukey HSD test stated.

	Site	FT	EC	MI	p-value
Winter	Yield	0.68	0.72	--	0.504
	Chl	188	1668	--	<0.0001
	Phycoerythrin	2455	2396	--	0.928
	Phycocyanin	1489	2217	--	0.215
Summer	Yield	0.37	0.53	0.58	0.27
	Chl	110*	849	1532	0.0036
	Phycoerythrin	1038	1871	1893	0.233
	Phycocyanin	1098	1619	813	0.59
Total	Yield	0.52	0.6	0.53	0.606
	Chl	143*	1122	1532	<0.0001
	Phycoerythrin	1645	2046	1893	0.426
	Phycocyanin	1265	1818	813	0.375

Table 6: Carbon biomass Figures for the 2012 year. “%C” is the total carbon (g) in drymass of sample (g). C:N is the ratio of carbon to nitrogen atoms found in the sample, while C:Chl, C:PE, and C:PC are the ratios of carbon atoms to chlorophyll, phycoerythrin and phycocyanin, respectively.

	FT	EC	MIS
<u>May 2012</u>			
%C	15	9.7	17
C:N	9.2	5.8	6.3
C:Chl		155	125
C:PE		34	66
C:PC		38	99
<u>July 2012</u>			
%C	34	28	29
C:N	13	6.14	6.2
C:Chl	4492	382	307
C:PE	1559	149	203
C:PC	1491	162	234
<u>September 2012</u>			
%C	21	19	18
C:N	6.7	5.5	7.8
C:Chl		216	63
C:PE		79	7.9
C:PC		84	48

Table 7: P-values of regression analyses between various parameters at all sites for the whole sampling period (2012 — 2013; n = 21, 30, and 17 for FT, EC and MIS, respectively). Statistically significant values are bolded (alpha = 0.05). Missing values (“--“) indicated due to redundant values and tests that result in identity (i.e. Chl and Chl).

	Par	Yield	Chl
FT			
Chl	0.0741	0.0399	
PE	0.3640	0.1905	0.7083
PC	0.9252	0.6257	0.8799
PE:PC	0.9823	0.6869	0.8209
Phy:Chl	0.0926	0.1867	
Yield	0.0552		
EC			
Chl	0.0164	0.0543	
PE	0.1445	0.0569	0.2509
PC	0.0896	0.0277	0.4149
PE:PC	0.5580	0.7564	0.4445
Phy:Chl	0.2791	0.6401	
Yield	0.0009		
MIS			
Chl	0.0323	0.0315	
PE	0.0128	0.0706	0.0044
PC	0.0131	0.0695	0.0041
PE:PC	0.8628	0.5054	0.7418
Phy:Chl	0.0053	0.2004	
Yield	0.1762		

Table 8: Results of linear regression analysis (p – values; alpha = 0.05, significant values bolded) between F_v'/F_m' and different data sources for PAR measurements. Surface PAR and Bottom PAR data values were collected on site with the LiCor meter, while “Weather Station” data was obtained from the Ameriflux database (UMBS station).

	FT	EC	MIS
Surface PAR	0.1109	0.0243	0.8720
Bottom PAR	0.1109	0.0168	0.9772
Weather Station	0.0552	<0.0001	0.1762

DISCUSSION

Water chemistry is similar among study sites

Water chemistry values measured were similar to previous studies (Biddanda *et al.* 2006; Ruberg *et al.* 2005). YSI values (temperature, dissolved oxygen, conductivity) were quite similar among all three sites. Dissolved oxygen differed most at FT due to the very shallow (0-5cm) water level as well as relatively quick flow, both of which increase oxygen content from increased exposure to air. Despite this physical difference, oxygen values were still found to be very low overall (>4.0 mg/L). This may contribute to oxygen tolerance (discussed below, Ch. 3). For all parameters some variation may have occurred due to sampling at variable distances from the groundwater source. At MIS, the groundwater interface can fluctuate vertically, especially with increasing distance from the groundwater source. The physical conditions (temperature, water chemistry, pH, etc.) are quite stable across the year, including over the winter (Table 3) because the water input is not subject to ambient effects like weather. This shows the relative isolation of these ecosystems, with PAR being an exception. The winter data collected at MIS are the first recorded at this location over the cold months due to difficulties caused by ice-cover over the site. This data showed the extent to which the groundwater consistently maintains at steep gradient to ambient lake.

PAR is an important driver in mat ecosystems

Yearlong average PAR was highest at FT, though this also was the most variable site. This likely is due to the location of the fountain between two buildings as well as a second story skyway connecting the two buildings which cause the structure to have periods of either direct sunlight or shade. The high yearlong PAR was paired with the lowest yearlong F_v'/F_m' and a significantly lower level of chlorophyll. These are likely to be responses to high PAR to regulate photosynthesis. Increased pigmentation during high PAR can lead to cellular damage, and decreased pigmentation would lead to decreased F_v'/F_m' .

Despite EC and FT receiving relatively similar PAR levels in the winter, chlorophyll still differed significantly. This may be due to the 'spikes' of PAR that occur at FT – times of direct sunlight. EC mats may not receive as much PAR as indicated due to microhabitat structure – discussed below. The F_v'/F_m' and chlorophyll measured at EC and MIS were both significantly higher than FT likely because the level of PAR was much lower than at FT. The need for down regulation of chlorophyll would not be required with more moderate levels of PAR, especially at MIS where PAR was consistently low. The role of PAR variability likely is an important factor as well – PAR at FT can change rapidly due to variations in direct and indirect sunlight. Over pigmentation would therefore become problematic very quickly. MIS receives PAR at a considerably lower range than either FT or EC, and does not experience rapid changes in PAR. Relatively stable conditions may select for high and steady levels of pigmentation in MIS microbial mats.

Seasonality of biological parameters

Fv'/Fm' data revealed an apparent seasonal trend where recorded values were consistently higher during the colder low-light months and lower during the warmer high-light months (Figure 10, Figure 11). Similar findings have been made in other studies (Warner *et al.* 2002; Abdala-Diez *et al.* 2006; Hawes *et al.* 2014). Warner *et al.* (2002) found this trend in coral-associated diatoms at varying depths, and that more shallow measurements were more highly variable likely due to higher variation in PAR. Increased variability in shallow sites was not found in the present study, although this may be misleading due to differences in sites, discussed below (Figure 1, Table 5). Additionally, Warner *et al.* (2002) reported higher average Fv'/Fm' values at greater depth, whereas we found no trend with depth; indeed, photosynthetic yield was indistinguishable among sites over the course of the year, within the summer, and within the winter (Table 5). Abdala-Diez *et al.* (2006) found similar seasonal trends in a brown algae, as well as diel patterns where Fv'/Fm' was higher during low light periods of the day (morning and evening; a similar trend, but on a much shorter time scale) and reached a minimum at mid-day. Hawes *et al.* (2014) found an inverse relationship between PAR and Fv'/Fm' fluorescence in a similar microbial mat community that reside under ice covered lakes in Antarctica. While we were unable to make repeated measurements at the sites over the course of a day, the yearlong inverse relationship between PAR and yield remained, and thus it seems likely that a similar diel trend exists at our 3 study sites.

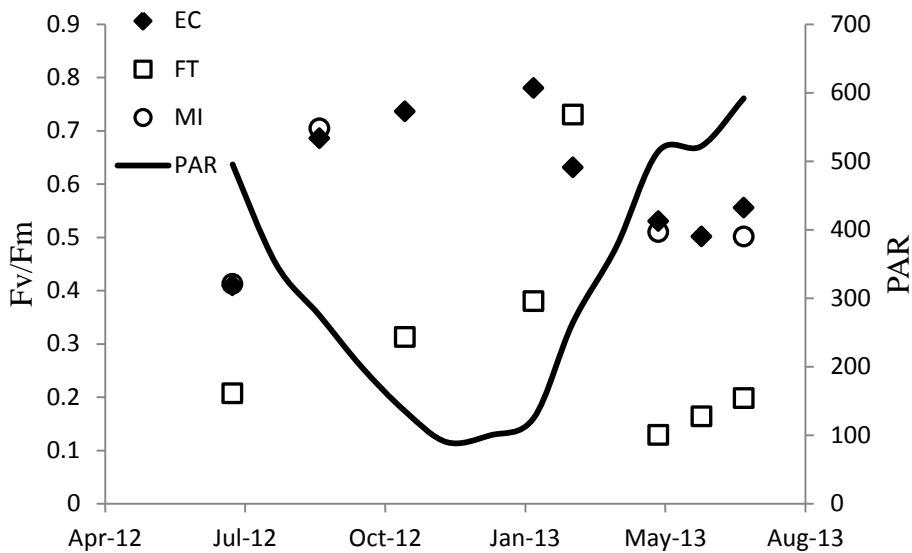


Figure 11: Seasonal trend in photosynthetic yield for all 3 study sites. F_v'/F_m' shows an inverse relationship with PAR (PAR data source: Oak Ridge National Laboratory, Ameriflux, site: UMBS).

Similarly, pigments appeared to vary seasonally. Chlorophyll had distinct high periods in the winter (November – April) at EC, though EC had a much higher level of chlorophyll all year. Chlorophyll was higher in the winter at FT, though chlorophyll was relatively low all year likely due to the extremely high levels of PAR. Chlorophyll was higher in the winter months likely as a result of lower PAR, meaning chlorophyll followed a relatively inverse relationship with PAR. Chlorophyll was lowest at FT due to high and variable sunlight (discussed above), while chlorophyll was highest at MIS due

to low and relatively stable PAR. Phycoerythrin and phycocyanin did not have as clear of a seasonal pattern especially at EC where phycobilins were highest around summer of 2012 but lowest in July 2013. It is unclear why this would be, as no drastic changes in PAR, temperature or other parameters occurred between 2012 and 2013. The relatively high concentration of phycobilin pigments likely contributes to the mats' purple color.

Seasonality in chlorophyll is a well-known phenomenon in phytoplankton communities (Niebauer et al 1995), and has been studied in cyanobacterial mats as well (Pinckney *et al.* 1995). However, most studies use chlorophyll as a measure of oxygenic phototrophic biomass by measuring chlorophyll per unit area. We opted to measure chlorophyll per unit dry mass to estimate cellular chlorophyll content as we were interested in cyanobacterial activity. Whereas chlorophyll per unit dry mass is related to the production of new biomass, it is more closely related to photophysiology. This allowed a measure that estimated the amount of chlorophyll that was independent of the size of the sample collected. While the top purple layer of the cyanobacterial mat was primarily cyanobacteria (qualitatively), it was not possible to exclude other organisms or small detrital particles were not present in the samples, which would artificially decrease the chlorophyll concentration.

In linear regression analyses, chlorophyll showed a positive relationship with PAR at EC and MIS but not FT, though caution should be taken in interpreting regression data from MIS due to low sample sizes. It is possible that cleaning of the fountain may have interfered with chlorophyll measurements. Regardless, these data seem to support the idea that chlorophyll levels are low during times of high PAR to avoid cellular damage from excess energy, while chlorophyll expression increases with decreasing light

levels at the other sites as PAR is not excessively high. So as PAR increases, pigments decrease, and, generally speaking, F_v'/F_m' typically negatively correlates with PAR (Figure 12). This relationship is theoretically maintained by controlling pigment concentration. This was true for EC only, although the p-value for FT is arguably biologically significant (0.0552). It is possible that this relationship did not hold at MIS simply due to such a low sample size ($n = 4$). Another explanation could be the greatly diminished role of variability in PAR reaching MIS mats (only $\pm 9 \mu\text{mol s}^{-1} \text{m}^{-2}$). This represents a range of 0 (darkness) to just over $100 \mu\text{mol s}^{-1} \text{m}^{-2}$, and likely even less during the darker months – this is a much smaller range than measured at the other sites. In that sense, MIS has a significantly diminished effect of seasonal PAR, so it is not surprising that yield wouldn't show a positive or negative relationship with PAR.

PAR measurements were essentially instantaneous and thus highly susceptible to effects of cloud cover, time of day and other possible factors. Weather station PAR data was used as an alternate method of measuring PAR to minimize these variables. However no statistical differences were detected in regression analyses between the use of our LiCor readings and the local weather station PAR data (Table 8). The benefit of the weather station data is that PAR for the whole day could be averaged to get a better value for the level of PAR at that point in the season, the obvious disadvantage is the geographic distance from the actual sites – roughly 70 miles.

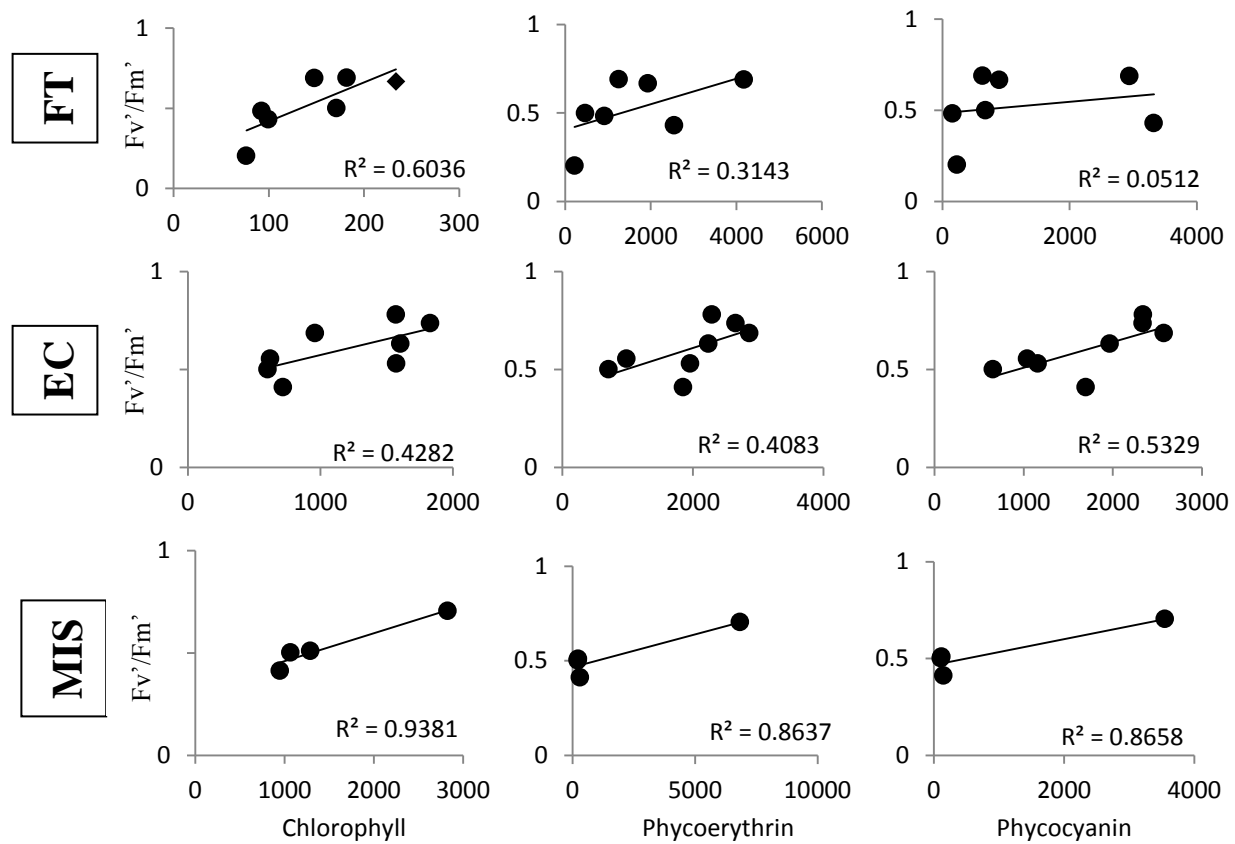


Figure 12: Regression analyses comparing pigment content (x-axes, chlorophyll, phycoerythrin and phycocyanin, left to right) and F_v'/F_m' (y-axes). Top Row: FT samples, Middle Row: EC samples, Bottom Row: MIS samples. P-values for these comparisons located in Table 7.

Carbon content data suggests that mats in all the three sites increase biomass into the summer, and drop off going into the fall period. FT mats had high C:pigment ratios,

showing generally lower cellular pigment levels, likely to compensate for over saturating PAR. EC and MIS were much more similar to one another in this regard. C:pigment ratios followed a similar C biomass trend – higher ratios were recorded in the middle of the high light summer month, suggesting that less cellular material was devoted to pigmentation. Higher carbon content suggests that the mats are actively photosynthesizing and sequestering carbon. This is despite lower photosynthetic efficiency – PAR is likely higher than necessary for optimal carbon assimilation.

Physical differences of study sites influence biological parameters

Comparing biological parameters between sites for photosynthetic yield and pigment concentration lead to only one statistical difference – chlorophyll at FT (for the summer and yearlong average). This likely stems from the physical conditions of FT, which changes from periods of direct sunlight (the highest PAR levels recorded) to shade, and contains the largest range of PAR to constantly adjust to. Higher levels of chlorophyll pigmentation would potentially cause photoinhibition above optimal levels of PAR and thus chlorophyll concentrations are considerably lower than at EC and MIS for both summer and winter. With the increased PAR present, the chlorophyll in FT mats would decrease either by decreased synthesis or increased degradation until a homeostatic balance is achieved, and would remain low so as not to absorb excess energy that could be detrimental. It is also possible that this statistical finding was due to non-cyanobacterial and non-photosynthetic growth that was more prevalent during the warm period.

The physical habitat at each site alters the amount of PAR. For example, F_v'/F_m' was similar at all sites despite a vast range of PAR reaching the mats at each location. Many EC samples were collected off of plants. Dense, cyanobacterial growth coated the plants from the base to water surface. At the water surface, large areas of detritus would often float (motionless) and the cyanobacterial growth would connect from the plants to the underside of the detrital rafts. Growth seemed to be most dense on the plants and the underside of the floating rafts – all relatively shaded areas. These conditions simultaneously act to decrease the incident angle of oncoming PAR for cyanobacteria on the plants, as well as creating shade for growth on the underside of the rafts and areas below rafts (which may include plants). The cyanobacteria could potentially take advantage of these physical features over small scales due to their incredible motility (Biddanda *et al.* 2012). Much of the growth at EC is located on the abundant plants around the spring. For those cyanobacteria located on or even near these plants, oxygen was likely able to be used, perhaps in only small amounts, that would provide the potential to benefit from respiration. The extent and benefit of this effect is unknown, however, and would be a worthwhile study. In terms of PAR, EC and MIS may be more similar in their light climates than previously realized because EC cyanobacteria can potentially relocate to areas of lower light, or at the least, preferentially grow in areas of lower light. MIS receives low light due to depth, while cyanobacteria in EC are able to relocate along microscales to optimize light harvesting. Considering that most cyanobacterial growth at EC is found in shaded areas it seems as if the incident PAR is much higher than needed. PAR and chlorophyll data collected at a more micro-scale would be needed to confirm this hypothesis.

Cyanobacteria at FT are exposed to high, direct PAR and must also maintain adhesion to the fountain bottom. The high water flow would wash mats down the drain if they were not clinging tightly to the bottom. This likely takes extra energy for cellular adhesive material. These reasons may also contribute to the visibly different appearance of FT mats compared to EC and MIS mats. FT mats are typically a browner, orange color instead of the vivid purple seen at the other sites. These samples appeared more purple during the winter, almost appearing scorched during the high light summer (Figure 13). The presence of carotenoids and other UV absorbing compounds such as microsporin-like amino acids may also help with warding off excess energy absorption as well as contribute to the darker appearance.

These cyanobacteria found in three very different light environments seem to employ different life strategies to survive. It is unknown how genetically different the communities from these sites are as of now. It is possible that the mats are versatile enough that the same community can thrive across a range of light conditions.

Alternatively, the communities could be distinguishable in their species composition such that each community has been optimized to the local conditions, as in the study of cyanobacterial communities in the tropics (Rascher *et al.*, 2003). The answers to these questions may be forthcoming from the ongoing genetic analysis. Interestingly, distinct communities were identified in microclimates in Rascher's study, which were also characterized by different rates of photosynthetic yield. The communities in this study can be divided into two groups based on their photosynthetic yield and pigment composition – EC and MIS in one group and FT in the other. These

two groups only differed in their chlorophyll content. Despite containing different levels of the main photosynthetic pigment, photosynthetic yield remained the same.



Figure 13: Top Row – (left) FT samples have a browner color during the summer than the vividly purple EC and MIS samples, but look more purple during the winter (right); Middle Row– El Cajon samples (*in situ*); Bottom Row – (left) Middle Island sample collected in a core tube, and (right) *in situ*.

Conclusion

This study examined three geographically separate and isolated locations with similar microbial communities occurring at different depths. All contain stable, persistent groundwater inputs that provide constant chemical conditions. PAR was found to be an important driver of chlorophyll levels at the two lower light locations, and the high light site contained significantly lower levels of chlorophyll to counteract the excessively high PAR. The difference in pigmentation did not significantly affect the photosynthetic yield between sites – the changes in pigmentation likely helps adjust yield. An apparent seasonal trend was seen most strongly in photosynthetic yield within each site – the winter (low PAR) had significantly higher yield than the summer (high PAR). Carbon content appeared to follow a seasonal trend as well, whereby increasing during the summer and tapering off near the end of the summer season.

LITERATURE CITED

- Abdala-Díaz, R. T., A. Cabello-Pasini, E. Pérez-Rodríguez, R. M. Conde Álvarez, and F. L. Figueroa. "Daily and Seasonal Variations of Optimum Quantum Yield and Phenolic Compounds in *Cystoseira Tamariscifolia* (Phaeophyta)." *Marine Biology* 148.3 (2006): 459-65. Print.
- Biddanda, B., D. Coleman, T. Johengen, S. Ruberg, G. Meadows, H. Sumeren, R. Rediske, and S. Kendall. "Exploration of a Submerged Sinkhole Ecosystem in Lake Huron." *Ecosystems* 9.5 (2006): 828-42. Print.
- Biddanda, B., S. Nold, G. Dick, S. Kendall, J. H. Vail, S. A. Ruberg, and C. M. Green. "Rock, Water, Microbes: Underwater Sinkholes in Lake Huron Are Habitats for Ancient Microbial Life." *Nature Education Knowledge* 9th ser. 2.12 (2012). Web.
- Bowker, M., S. Reed, J. Belnap, and S. Phillips. "Temporal Variation in Community Composition, Pigmentation, and Fv/Fm of Desert Cyanobacterial Soil Crusts." *Microbial Ecology* 43.1 (2002): 13-25. Print.
- Bryant, D. "Carotenoids in Cyanobacteria." *The Molecular Biology of Cyanobacteria*. Dordrecht: Kluwer Academic, 1994. 559-79. Print.
- Campbell, D., V. Hurry, A. Clarke, P. Gustafsson, and G. Oquist. "Chlorophyll Fluorescence Analysis of Cyanobacterial Photosynthesis and Acclimation." *Microbiological and Molecular Biology Reviews* 62.3 (1998): 667-83. Web.
- Dubinsky, Z., T. Berman. "Seasonal changes in the spectral composition of downwelling irradiance in Lake Kinneret (Israel)." *Limnology and Oceanography* 24.4 (1979): 652-663.

- Ehling-Schulz, M., and S. Scherer. "UV Protection in Cyanobacteria." *European Journal of Phycology* 34.4 (1999): 329-38. Print.
- USEPA. *Methods for chemical analysis of water and wastes*. 2nd ed. Method 365.2. U.S. Environmental Protection Agency, Washington, DC. 1983.
- Falkowski, P., and J. Raven. "Light Absorption and Energy Transfer in the Photosynthetic Apparatus." *Aquatic Photosynthesis*. Malden, MA: Blackwell Science, 1997. 44-80. Print.
- Garcia-Pichel, F., J. Belnap, S. Neuer, and F. Schanz. "Estimates of Global Cyanobacterial Biomass and Its Distribution." *Algological Studies* 109.1 (2003): 213-27. Print.
- Grossman, A., M. Schaefer, G. Chiang, and J. Collier. "The Phycobilisome, a Light-Harvesting Complex Responsive to Environmental Conditions." *Microbiological and Molecular Biology Reviews* 57.3 (1993): 725-49. Web.
- Hawes, I., H. Giles, and P. Doran. "Estimating Photosynthetic Activity in Microbial Mats in an Ice-covered Antarctic Lake Using Automated Oxygen Microelectrode Profiling and Variable Chlorophyll Fluorescence." *Limnology and Oceanography* 59.3 (2014): 674-88. Web.
- Heinz, Walz, GmbH. "Underwater fluorometer Diving-PAM Handbook of Operation." Germany, 1998. Print.
- Jorgensen, B., Y. Cohen, and D. Marais. "Photosynthetic Action Spectra and Adaptation to Spectral Light Distribution in a Benthic Cyanobacterial Mat." *Applied and Environmental Microbiology* 53.4 (1987): 879-86. Web.

- Kaiser, M. *Marine Ecology: Processes, Systems, and Impacts*. Oxford: Oxford UP, 2005. Print.
- Klatt, C., J. Wood, D. Rusch, M. Bateson, N. Hamamura, J. Heidelberg, A. Grossman, D. Bhaya, F. Cohan, M. Kühl, D. Bryant, and D. Ward. "Community Ecology of Hot Spring Cyanobacterial Mats: Predominant Populations and Their Functional Potential." *The ISME Journal* 5.8 (2011): 1262-278. Web.
- Lawrenz, E., E. Fedewa, and T. Richardson. "Extraction Protocols for the Quantification of Phycobilins in Aqueous Phytoplankton Extracts." *Journal of Applied Phycology* 23.5 (2011): 865-71. Print.
- Lionard, M., B. Péquin, C. Lovejoy, and W. Vincent. "Benthic Cyanobacterial Mats in the High Arctic: Multi-Layer Structure and Fluorescence Responses to Osmotic Stress." *Frontiers in Microbiology* 3 (2012). Web.
- Lorenzen, C. "A Determination of Chlorophyll and Pheo-pigments: Spectrophotometric Equations." *Limnology and Oceanography* 12.2 (1967): 343-346. Print.
- Lugomela, C., E. Söderbäck, and M. Björk. "Photosynthesis Rates in Cyanobacteria-dominated Sub-tidal Biofilms near Zanzibar, Tanzania." *Estuarine, Coastal and Shelf Science* 63.3 (2005): 439-46. Web.
- MacIntyre, H., T. Kana, T. Anning, and R. Geider. "Photoacclimation of Photosynthesis Irradiance Response Curves and Photosynthetic Pigments in Microalgae and Cyanobacteria." *Journal of Phycology* 38.1 (2002): 17-38. Web.
- Maxwell, K., and G. Johnson. "Chlorophyll Fluorescence--a Practical Guide." *Journal of Experimental Botany* 51.345 (2000): 659-68. Print.

- Moreau R. "A review of limnological characteristics of Alpena, Michigan area flowing wells and sinkholes." In: Kimmel RA, Ed. Tectonics, structure, and karst in Northern Lower Michigan. Michigan basin geological society: field conference proceedings. (1983): 91–111.
- Niebauer, H.j., V. Alexander, and S. Henrichs. "A Time-series Study of the Spring Bloom at the Bering Sea Ice Edge I. Physical Processes, Chlorophyll and Nutrient Chemistry." *Continental Shelf Research* 15.15 (1995): 1859-877. Print.
- Nold, S., M. Bellecourt, S. Kendall, S. Ruberg, T. Sanders, J. Val Klump, and B. Biddanda. "Underwater Sinkhole Sediments Sequester Lake Huron's Carbon." *Biogeochemistry* 115.1-3 (2013): 235-50. Web.
- Olsson-Francis, K., and C. Cockell. "Experimental Methods for Studying Microbial Survival in Extraterrestrial Environments." *Journal of Microbiological Methods* 80.1 (2010): 1-13. Print.
- Pinckney, J., H. Paerl, and M. Fitzpatrick. "Impacts of Seasonality and Nutrients on Microbial Mat Community Structure and Function." *Marine Ecology Progress Series* 123 (1995): 207-16. Print.
- Rascher, U., M. Lakatos, B. Budel, and U. Luttge. "Photosynthetic field Capacity of Cyanobacteria of a Tropical Inselberg of the Guiana Highlands." *European Journal of Phycology* 38 (2003): 247-56. Web.
- Ruberg, S., D. Coleman, T. Johengen, G. Meadows, H. Van Sumeren, G. Lang, and B. Biddanda. "Groundwater Plume Mapping in a Submerged Sinkhole in Lake Huron." *Marine Technology Society Journal* 39.2 (2005): 65-69. Print.

- Sanders, T., B. Biddanda, C. Stricker, S. Nold. "Benthic macroinvertebrate and fish communities in Lake Huron are linked to submerged groundwater vents." *Aquatic Biology* 12 (2011). Web.
- Stavn, R. "Lambert-Beer law in ocean waters: optical properties of water and of dissolved/suspended material, optical energy budgets." *Applied Optics* 27.2 (1988): 222-231. Print.
- Vincent, W., D. Mueller, and S. Bonilla. "Ecosystems on Ice: The Microbial Ecology of Markham Ice Shelf in the High Arctic." *Cryobiology* 48.2 (2004): 103-12. Print.
- Warner, M., G. Chilcoat, F. McFarland, and W. Fitt. "Season Fluctuations in the Photosynthetic Capacity of Photosystem II in Symbiotic Dinoflagellates in the Caribbean Reef-building Coral *Montastraea*." *Marine Biology* 141 (2002): 31-38. Web.
- Whitton, B.A. "Cyanobacterial Responses to UV Radiation." *Ecology of Cyanobacteria II: Their Diversity in Space and Time*. Dordrecht: Springer, 2012. 481-502. Print.
- Zhao, K., R. Porra, and H. Scheer. "Phycobiliproteins." *Phytoplankton Pigments: Characterization, Chemotaxonomy, and Applications in Oceanography*. Cambridge: Cambridge UP, 2011. 375-411. Print.

CHAPTER 3

Experimental Studies of Lake Huron Sinkhole Microbial Mats Under Variable Light, Oxygen and Sulfide Conditions

ABSTRACT

Photophysiology of cyanobacteria-dominated mats from submerged sinkholes in Lake Huron were studied in laboratory experiments to understand how they acclimate to variable light quality and intensity. In a series of experiments, I examined photosynthetic efficiency using chlorophyll fluorescence and pulse amplitude modulation (PAM) to measure the effect of varying light intensities and spectral filtration. Four filter treatments (high-light, medium-light, chromatic filtration, and low-light with chromatic filtration) were used on oxygenated and anoxic samples from three study sites over a five day period to present samples with new light conditions. Another experiment analyzed photosynthetic yield and pigment concentration. Results showed that Fountain (FT) samples had increased photosynthetic yield while oxygenated - reflecting the more oxygenated environment they come from, and relied on changes in chlorophyll and phycobilin levels. El Cajon (EC) and Middle Island Sinkhole (MIS) showed little difference between anoxic and oxic conditions, and EC relied on changes in phycocyanin levels, while few significant pigment changes were detected at MIS. The characteristic ability of mats for sulfide tolerance also was demonstrated. These data provide insight into the highly adaptive capabilities of cyanobacteria under extreme changes in light intensity and quality as well as variable redox conditions. These results also may explain

the high functional diversity present in these unique ecosystems that contain surprisingly low taxonomic diversity – and provide important clues to their long-term survival strategies and evolutionary origins.

INTRODUCTION

Cyanobacteria have been shaping the Earth for the past 2.5 billion years by altering the biogeochemistry of the Earth from the depths of the ocean to the upper reaches of the atmosphere (Falkowski, 2008, Lyons *et al.* 2014). They are likely the first oxygen producing photosynthetic organisms to be present on the planet, originally inhabiting a world full of sulfide and lacking oxygen (Biddanda *et al.* 2012).

Atmospheric oxidation was a slow process that eventually culminated in the Great Oxidation Event nearly 2.3 bya, and may have been hindered by the prevalence of hydrogen sulfide – a photosystem II inhibitor. How photosynthetic organisms developed oxygenic photosynthesis as well as a tolerance for sulfide is currently unknown – especially over the early geologic period when oxygen was poisonous to the organisms then inhabiting the planet.

The principle of allocation, at an ecological level, is the idea that if an organism dedicates energy to a certain function, it then has less energy available for other functions (Gadgil and Bossert 1970). For example – organisms that must resist extreme temperatures are typically likely less capable of simultaneously tolerating extreme osmotic changes. Microbial life is interesting in that there have been microbes found in almost every environment discovered, and thus, have overcome many conditions that would have been thought to be too extreme for life to exist. The cyanobacteria in the current study are found across a range of light and are able to thrive in oxygenated as well as anoxic conditions - evidence of versatile adaptive capabilities.

Anoxygenic phototrophic bacteria, including purple sulfur bacteria, purple non-sulfur bacteria and green sulfur bacteria are typically anaerobic organisms requiring reduced materials as an electron donor (usually H₂S, H₂, or organic chemicals), and don't evolve oxygen. In contrast, cyanobacteria use a dual photosystem, evolving oxygen like green plants and using H₂O as an electron donor. While classified as a cyanobacteria, the organisms in this study are able to conduct both a oxygenic *and* anoxygenic photosynthesis. This is a rare, but previously well-documented phenomenon (Oren 1977; Cohen *et al.* 1986).

Another unique trait identified in some cyanobacteria (though not unique only to cyanobacteria) is phototaxis – the ability to coordinate movement in response to light. This has been observed in cyanobacteria inhabiting sinkholes around Alpena, Michigan. Communities from three locations are of interest in this study – Middle Island Sinkhole (MIS), El Cajon (EC) and the fountain (FT), each described in chapter 2. Studies with cyanobacteria from other locations have been conducted where filaments glide from darkened areas to areas of light more suitable to their energy needs. This can be done in simple experiments by covering a petri dish with foil and cutting out areas of the foil to allow light to pass through. The results are quite striking after only a few hours. Lit areas become more densely packed with cyanobacteria as they migrate towards the light, while the darkened areas remain sparse. It is unknown exactly how these cyanobacteria are able to aggregate in pinpoint locations that are many lengths longer than the individual filaments – simple random movement is insufficient in explaining this phenomenon (Hoiczuk 2000). It is more likely that a form of intercellular communication such as quorum sensing, which has been studied in microbial mats living in extreme conditions

(Montgomery *et al.* 2013). This light associated movement has been studied in other cyanobacteria, and their movement has even been modeled (Merz and Forest 2002; Tamulonis *et al.* 2011).

The purpose of this study was to characterize how changes in light intensity and spectra affect the photophysiology of these cyanobacteria-dominated mats, how sulfide affects photosynthetic efficiency and pigment content, and how cyanobacterial motility can be used for light optimization. We ask the question: “How do changes in light, oxygen and sulfide affect these mat communities?” Freshly collected mat samples were grown under a series of light filters used to mimic changes in natural light conditions. Changes in photosynthetic efficiency (Fv/Fm) were measured to assess the physiological state, and pigment extractions were performed to monitor changes in pigment synthesis. Furthermore, sensitivity to photosynthetic inhibitors such as hydrogen sulfide and 3-(3,4-Dichlorophenyl)-1,1-dimethylurea (DCMU) were assessed. Lastly, a simple petri dish experiment was conducted where photosynthetic efficiency was measured in areas of light and dark over a period of time as filaments travelled across the petri dish.

Our results may be helpful in describing the life strategies of sinkhole cyanobacteria. The wider study further characterizes the remarkable photosynthetic capabilities in a relatively novel ecosystem that is easily accessible, yet resides in a geographic area with increasing limestone mining and gas extraction activities taking place under a vulnerable geologic setting that puts these small and isolated ecosystems at risk from ongoing anthropogenic changes.

MATERIALS AND METHODS

Sampling

Samples were collected from the three sites previously described in chapter 2. FT samples were scraped from the basin at the bottom of the fountain and collected into zip lock bags. EC mat samples were pulled off of plants and debris surrounding the groundwater spring and placed into ziplock bags. SCUBA divers collected samples at MIS using plastic coring tubes with rubber stoppers. Coring tubes were filled with approximately 15cm of underlying sediment along with the cyanobacterial mats laying on top of the sediment in each sample. All samples from each site were stored upright on ice in coolers immediately following collection and during transportation back to the laboratory.

Mat slurry - stock preparation

Field samples were pooled (≈ 10 g dry weight) into 1L of groundwater and gently agitated by a stir bar (MIS samples were removed from the underlying sediment) to make homogeneous slurry stocks of the filaments in sinkhole-derived groundwater for each site. Stocks were prepared within 24-48hr of collection. All samples were prepared and grown in groundwater from the fountain site (which has a relatively similar water chemistry to the other sites) due to ease of collection and a significant absence of any other large particulate organic matter compared to the other sites (though this water was

not filtered, so some particulates or even microbes may have been present; see Chapter 2, Table 1 for groundwater chemistry information). Care was taken to exclude any extraneous particulate organic matter and invertebrates while preparing stock cultures. Cell suspensions were then distributed into 22mL scintillation vials and placed in a Fisher Scientific low-temperature incubator at 9.5 C° with an internal, independent thermometer check (Figure 1).



Figure 1: Samples were distributed into vials and placed in a matrix organizer underneath a common light source (top; upright cores on sides of incubator are MIS samples). Close up view of samples in scintillation vials (bottom: FT, EC and MIS samples, respectively).

Calibration studies

Preliminary tests were conducted the day of stock preparation in order to ensure that PAM readings were not skewed by differences in mat thickness, sample density or consecutive illumination time. MIS samples were not used due to scarcity of samples. 12mL of FT and EC stock cultures were distributed into scintillation vials and placed under constant illumination with no light filters for a 24hr period and measured with the Diving-PAM at 6, 12, 16, 20 and 24hr (n = 4). Another experiment aimed to expose effects of slurry concentration on PAM readings. EC and FT samples were prepared from their respective stocks by placing 1, 6, 12 or 15mL of stock in scintillation vials and then diluting the total volume to 15mL with fresh groundwater. Samples were allowed to acclimate and settle in the scintillation vials in the incubator for 1hr before PAM measurements were taken.

Filter study

Stock cultures of 12mL from each sampling location were distributed into scintillation vials according to the matrix in Table 1. The groundwater 'media' in each scintillation vial was replenished daily at the time of sampling. A 40 watt, GE incandescent bulb set on a 12:12 hr day:night cycle was used for illumination inside the incubator. These cultures remained untouched for 24 hr before any sampling occurred to allow acclimation to the microcosms and to allow reformation of the mat.

Filter treatments were placed over cultures to change the light intensity and/or quality. Light transmission was determined using a LiCor LI-192 underwater quantum

sensor (LiCor Biotechnology, Lincoln, Nebraska). The full light treatment allowed all the illumination from the overhead lightbulb and had no chromatic filter (100% -F). This was meant to roughly mimic the light conditions in EC which has no shading or chromatic filtration due to its shallow depth. The 50%-F+D treatment consisted of a single layer neutral density (D) screen mesh that cuts out ~50% of total illumination. This was meant to mimic the fountain which has some shading from the surrounding buildings and from the fountain itself. The blue treatment (BL) is a single layer of translucent plastic blue film that cuts out the longer wavelengths of light, simulating wavelength specific attenuation with depth in the water column. In addition, this filter cuts out roughly 80% of total photosynthetically active radiation (PAR). The lowest light treatment (5% +F+2D) has two layers of neutral density filters and one layer of blue filter which allows roughly 5% of bulb illumination while cutting out longer wavelengths. This was meant to mimic the light in MIS at a depth of 23m which has a significant reduction in illumination and significant chromatic filtration of longer wavelengths.

An initial measurement was made after the 24 hr acclimation period. Immediately afterwards, the light filters were placed over the vials in such a way that samples from all sites were exposed to the four treatments described below. The 12:12 day:night cycle began after the addition of filter treatments, and an initial (T0) photosynthetic yield measurement and small subsample for pigment analysis were taken. This cycle continued for 5 days where groundwater exchange, photosynthetic yield measurements and pigment subsamples were made one time, every day, at the end of the 12hr light period (note: due to the small sizes of these cultures, pigment samples were not analyzed for every day of the experiment). All sampling occurred after the light period so samples had the longest

Table 1: List of filter treatments used in the light filter study. +F and –F indicate the presence or absence, respectively, of a blue filter screen, and +D and –D the presence or absence of a neutral density filter, respectively (in the case of 2D, 2 neutral density filters were used). Note that the blue filter screen itself cuts out a significant amount of PAR as well. D refers to layers of neutral density filters that cut PAR by ~50%. Treatments are named based on the % light going past the filters and is available to the mats. All filter treatments were used with samples that were grown in oxygenated conditions as well as samples that were nitrogen purged.

Treatment	PAR ($\mu\text{mol s}^{-1} \text{m}^{-2}$)	Chromatic Filtration
100% -D-F	160	No
50% +D-F	60	No
20% -D+F	35	Yes
5% +2D+F	12	Yes

amount of treatment time just before sampling. A 1 hour dark adaptation period was allowed before PAM readings.

These treatments were further tested in oxic as well as anoxic conditions. Vials used for oxic treatments were left uncapped and open to the air in the incubator. All vials were covered with 1 layer of fully light-transparent plastic saran wrap to ensure that the air current in the incubator wouldn't cause evaporation of water overlying the mats. Treatments with blue filters were already protected from these effects but were covered anyways to ensure uniform treatment. For anoxic treatments, nitrogen purging was used.

A tubing manifold apparatus was constructed that delivered a steady stream of nitrogen to the media of each vial through a needle across a sealed membrane cap (Figure 2). After sampling, purging took place for 10min, the needles were then pulled out of the airtight membranes and purging was terminated.

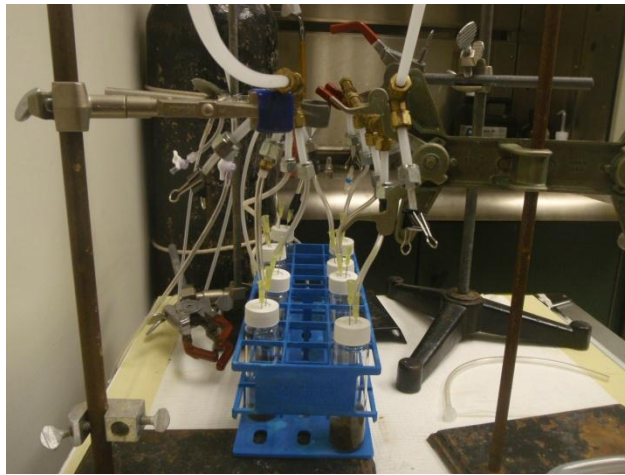


Figure 2: Tubing delivers nitrogen to samples and displaces oxygen. Tubing was connected to needles which delivered the nitrogen across a sealed membrane into each vial. The oxygen was then displaced and exited the vials via another needle open to room air.

Photosynthetic inhibitors

Samples from all sites were distributed into vials as previously described, open to incubator air (fully oxygenated) and placed under full light (no filter treatments). Two PSII inhibitors, $\text{Na}_2\text{S}\cdot 7\text{H}_2\text{O}$ (25 - 50 μM) and 3-(3,4-dichlorophenyl)-1,1-dimethylurea

(DCMU; 10 μ M) were added (plus a control) to cultures daily and sampled for 5 days as previously described. Buffers were not used, so reported inhibitor concentrations are estimated based off of a pH of 7-8. Cultures were allowed a full 24hr acclimation period, then an initial time point measurement was taken. Afterwards, inhibitor spikes were administered and cultures were allowed to sit for the full 24hr period before the next time point. Chemical inhibitors were always added after sampling such that samples were exposed to the chemical for 24hr before sampling. Upon re-addition of photosynthetic inhibitors, half of the media was removed and fresh groundwater added, and additional inhibitor added to bring concentration back to the desired level. Following this study, cultures were grown for several days only replenishing the groundwater media (no addition of photosynthetic inhibitors). Two days of baseline (no photosynthetic inhibition) were measured, followed by a time point of sulfide (62.5 - 125 μ M) and DCMU (25 μ M), and then higher concentration time point of sulfide (125 - 250 μ M) and DCMU (50 μ M), and a final time point of sulfide (62.5 – 125 μ M) and DCMU (25 μ M).

Cell motility

Samples from all sites were homogenized and distributed evenly across separate 10cm petri dishes (Figure 3). The lids were covered with aluminum foil and had 4 ~2cm circles cutout according to Figure 3. Initial Fv/Fm readings were made and then the lids were placed on the petri dishes. A light bulb was placed roughly 0.5m above the petri dish, pointing downwards. This allowed light to pass through the holes, while still having

areas of shade. Fv/Fm Measurements were made every 10min in the 4 light spots and 5 dark spots by turning off the light bulb, removing the petri dish lid, taking Diving-PAM measurements, and then replacing the lid and turning the light back on.

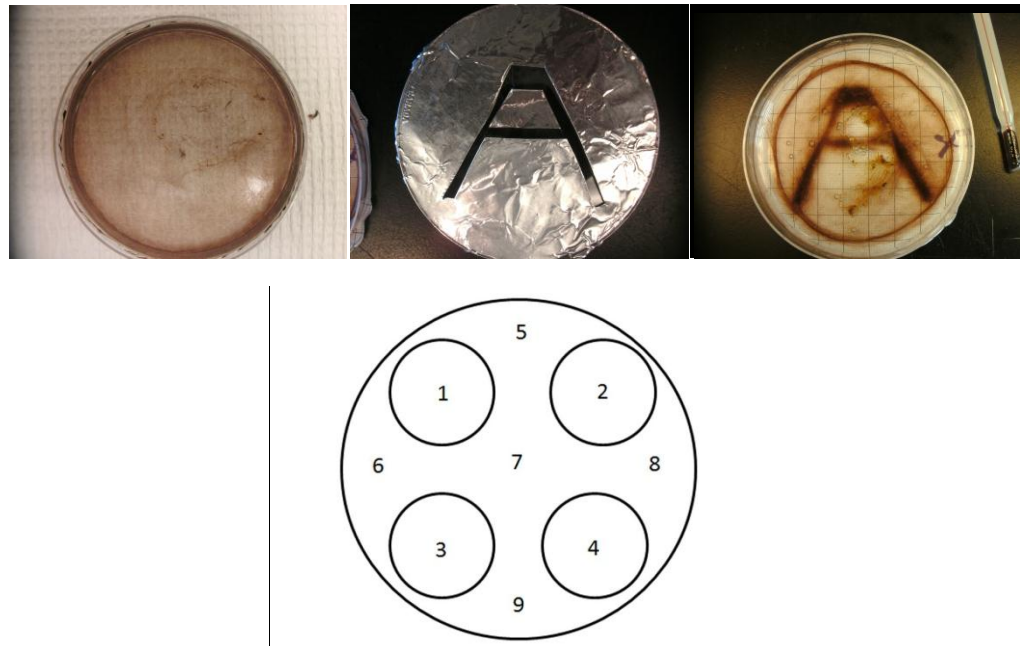


Figure 3: Top: Phototactic cyanobacteria can move to form the shape of oncoming light through an aluminum foil cutout. Left: The ‘before,’ cyanobacteria are homogenously distributed around a petri dish. Middle: A petri dish lid covered with aluminum foil has an “A” cutout to allow light through to the cyanobacteria. Right: After several hours, the cyanobacteria have conformed to the same shape as the aluminum foil cutout. Bottom: Diagram of cutout used in this motility experiment. Outer circle represents a 10cm petri dish that is covered in aluminum foil, the smaller circles are holes cut out in the foil to allow light to pass through to the cyanobacteria. PAM readings were taken in the lit areas of the petri dish (1 – 4), as well as the covered, dark areas (5 – 9) every 10min for 1hr.

Measurements

Fv/Fm measurements were made using the Diving-PAM by placing the fiber optic cable into the scintillation vial or petri dish and measuring from a set distance just above the mat (<5mm; Figure 4) taking care that the probe was not moved during measurement. PAM measurements were taken in dim lighting. Pigment samples were obtained by carefully removing a small piece of the mat and analyzed for chlorophyll, phycoerythrin and phycocyanin as described in chapter 2. Note that some time points are missing for pigment analyses. This was to conserve sample volumes throughout the duration of the experiment.



Figure 4: Recording DIVING-PAM measurements in the laboratory. The probe was placed into each vial and steadily held roughly 5mm from the mat surface and for each measurement.

Statistical analyses

All data was analyzed using R statistical software V2.15.3. All samples were analyzed with Shapiro-Wilk tests to determine if samples were normally distributed. The presence of numerous samples with non-normal distributions necessitated the use of non-parametric tests. Kruskal Wallis tests were applied to calibration studies, comparing all time points for changes in Fv/Fm, and comparing the different culture densities for changes in Fv/Fm. Kruskal Wallis tests were also applied to filter studies to compare both the filter treatments as well as the oxygen treatments. In the event of a statistically significant global Kruskal Wallis test, *post hoc* pairwise Wilcoxon tests were conducted with a Holm adjustment. Kruskal Wallis tests were also used for inhibitor studies to compare the two treatments and control group. Wilcoxon tests were applied to the cell motility experiment to compare areas of light and dark over the course of the hour long experiment.

RESULTS

Representative micrographs at different magnifications are displayed in Figure 5 for each site. For pictures and descriptions of the locations from which the samples were collected, refer to chapter 2. Two cell types appear to dominate these samples – the first being a thick filament with cells wider than they are long (roughly $15\mu\text{m} \times 5\mu\text{m}$), and the other a thin filament with roughly equal length and width dimensions ($5\mu\text{m} \times 5\mu\text{m}$).

Calibration study graphs are displayed in Figures 6 and 7. A slight effect of constant illumination was seen only in EC at a single time point – all other time points were similar within each site for FT and EC ($p = 0.901$ and 0.005 , respectively). Similarly, there was only one sample concentration from FT and none in EC that had any effect on Fv/Fm in the sample concentration study ($p = 0.024$ and 0.112 , respectively).

Assessments of normality for filter experiments are presented in Tables 2, 5 and 8, and the appropriate statistical results following in Tables 3, 6 and 9. Filter study graphs for comparisons within the N_2 and O_2 groups are displayed in Figures 8, 11 and 14. Bars represent the average values measured over a weeklong experiment. Comparisons of N_2 against O_2 groups are displayed in Figures 9, 12 and 15. As before, bars represent an average of measured values for a weeklong experiment. Following each set of figures are tables showing the weeklong time series of the preceding experiment (Figures 10, 13 and 16).

Most sample groups were normally distributed, but the sporadic presence of non-distributed samples necessitated the use of nonparametric statistics. For the sake of

consistency, these more conservative tests were used even in cases where all samples contained normal distributions. FT samples had higher photosynthetic yield and lower chlorophyll in the higher light treatments for both oxygenated and nitrogen purged samples (though only increased yield was statistically significant; Figure 8). Yield was higher in all oxygenated treatments (compared to nitrogen purged) except for the blue filter treatment. Both phycoerythrin and phycocyanin were significantly higher in the 100% light treatment for oxygenated samples.

No differences in yield were detected between filter or oxygen treatments in EC samples (Figure 11). Chlorophyll, phycoerythrin and phycocyanin were all higher in the 100% light treatment for both oxygen and nitrogen purged samples than in the low light treatments. Few effects were detected in comparisons between oxygenated and nitrogen purged samples – only chlorophyll was higher in oxygenated conditions with the blue filter treatment, while phycocyanin was lower in oxygenated conditions for the 50% light and blue filter treatments.

Photosynthetic yield was greater in higher light treatments (100% light) compared to lower light treatments (10% +F +ND), though yield was higher in oxygenated conditions (Figure 14). An apparent trend of increasing phycoerythrin and phycocyanin was present in increase light treatments, though this was not statistically significant.

Fv/Fm for most sites and most treatments seemed to have an initial increase in yield which then tapered off towards the end of the 5 day period. This trend, though not necessarily statistically significant, is most pronounced in MIS samples. This effect is

also often seen in pigment levels – an initial increase followed by a decrease towards the end of the experiment.

Inhibitor studies demonstrated a substantial effect of DCMU but not H₂S on Fv/Fm for all sites and concentrations used (Figures 17 – 25, and Tables 11 - 13). No significant differences were detected between inhibitor treatments for chlorophyll, phycoerythrin or phycocyanin. Time series of inhibitor experiments show fluctuations that may appear to be significant differences, but they are minimal and time integrated averages show that these differences are likely not significant. No time integrated values are available for the use of increased inhibitor concentration as many cultures died as a result of prolonged addition of DCMU. Despite a five-fold increase in both inhibitors, the trend of decreased yield for DCMU and no effect on H₂S continued.

Microscopy

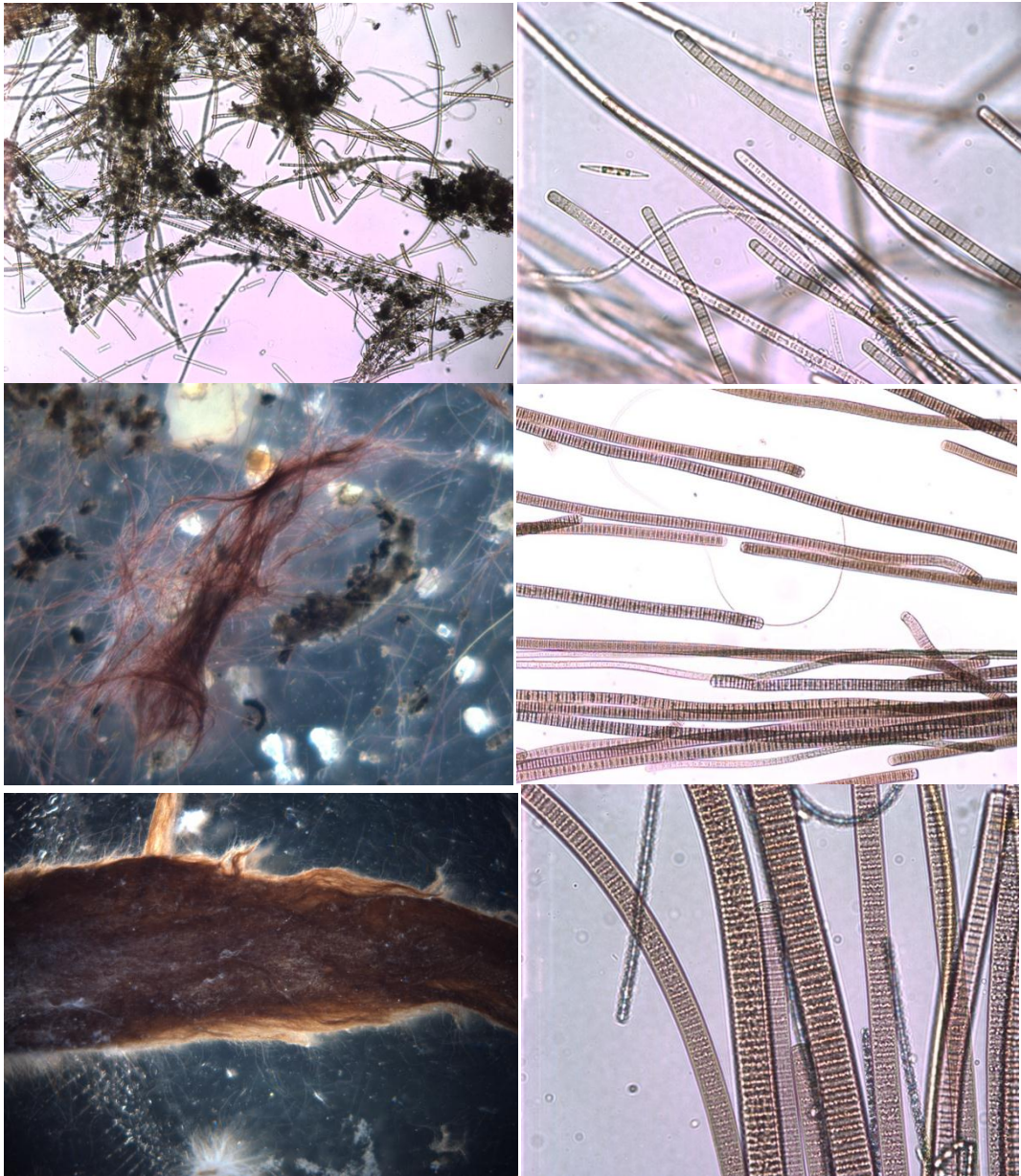


Figure 5: FT samples at 5X (top left), and 400X (top right), EC samples at 6.7X (middle left) and 400X (middle right), and MIS samples at 6.7X (bottom left) and 400X (bottom right).

Calibration studies

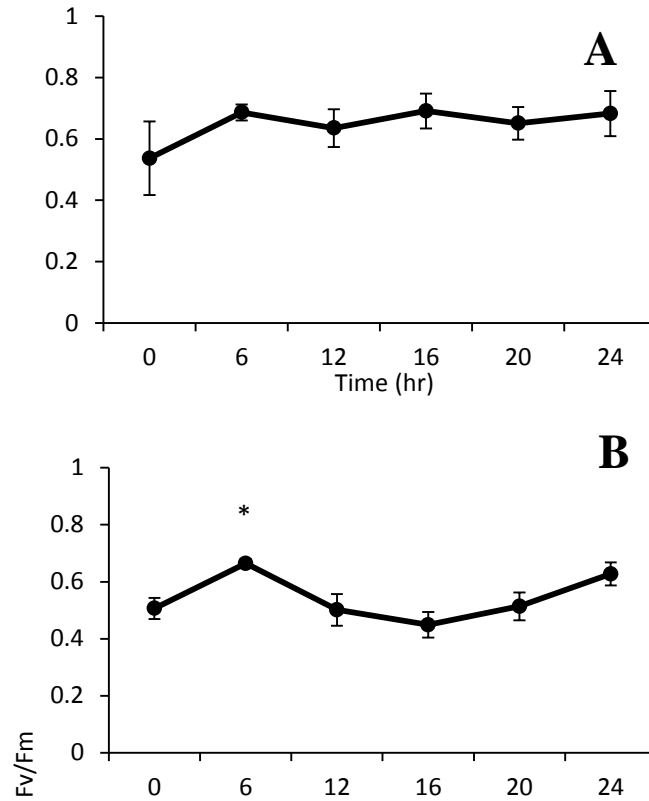


Figure 6: Yield was measured for a full 24hr period with FT (A) and EC (B) samples to observe the effect of continuous illumination. The only effect seen from ANOVA tests was an increase at 6hr for EC (indicated by “*”), while no significant differences were found for FT ($p = 0.005, 0.901$, respectively). $N = 4$ for each time point.

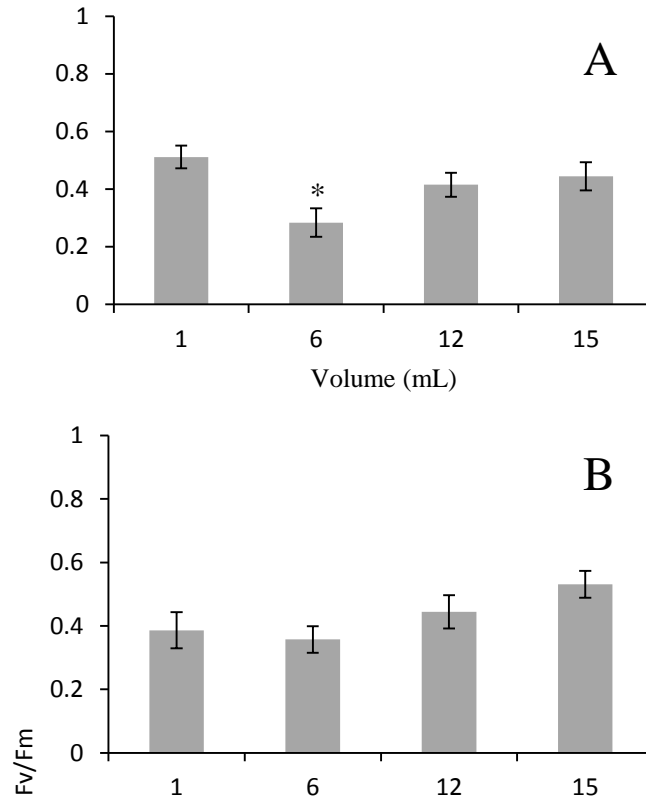


Figure 7: Stock solution concentration effect on Fv/Fm for FT (A) and EC (B). Volume indicates amount of slurry stock mixed with groundwater to make a total volume of 15mL (0mL of groundwater in the case of 15mL stock). No effect of volume was seen for EC ($p = 0.112$), but there was for FT ($p = 0.024$) for the 6mL treatment.

Filter studies

Table 2: p-value Results of Shapiro Wilk tests ($\alpha = 0.05$) for each FT treatment group. Values less than 0.05 are shown in bold and signify samples with non-normal distributions. Nitrogen purged samples are shown at left and oxygenated samples at right.

Filter	Y	Chl	PE	PC	Y	Chl	PE	PC
	Nitrogen				Oxygen			
Control	0.1707	0.1584	0.3338	0.4791	0.1707	0.1584	0.3338	0.4791
5%+2ND+F	0.7658	0.4723	0.0171	0.0880	0.0666	0.0113	0.0226	0.3753
20%-ND+F	0.2161	0.4149	0.1495	0.2635	0.1550	0.7884	0.0109	0.0377
50%+ND-F	0.4585	0.6842	0.0007	0.0007	0.0333	0.0088	0.0008	0.0021
100%-ND-F	0.1672	0.5173	0.0012	0.0009	0.3681	0.1117	0.0562	0.3252

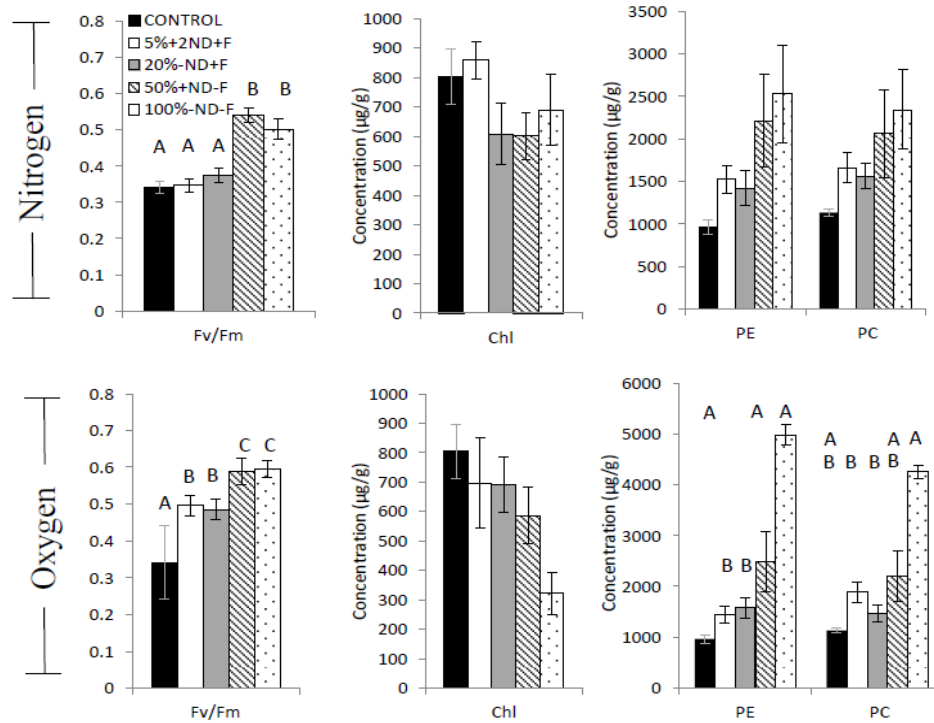


Figure 8: Comparisons of filter treatments for FT samples, grouped by all measured parameters: Fv/Fm, chlorophyll (Chl), phycoerythrin (PE), and phycocyanin (PC). The top row shows samples that were purged with nitrogen, and the bottom row shows samples that were fully oxygenated. Bars represent the average of the entire course of the experiment. Error bars represent standard error of the mean. Letters are shown above to indicate statistically significant different groups.

Table 3: Resulting p-values from Kruskal Wallis tests applied to FT filter comparisons ($\alpha = 0.05$). Significant values shown in bold and indicate that there was some effect on the measured parameter between filter treatments (groupings indicated in Figure 8).

Oxygen Condition	Fv/Fm	Chl	PE	PC
N ₂	<0.0001	0.3305	0.1715	0.4869
O ₂	<0.0001	0.0640	0.0002	0.0005

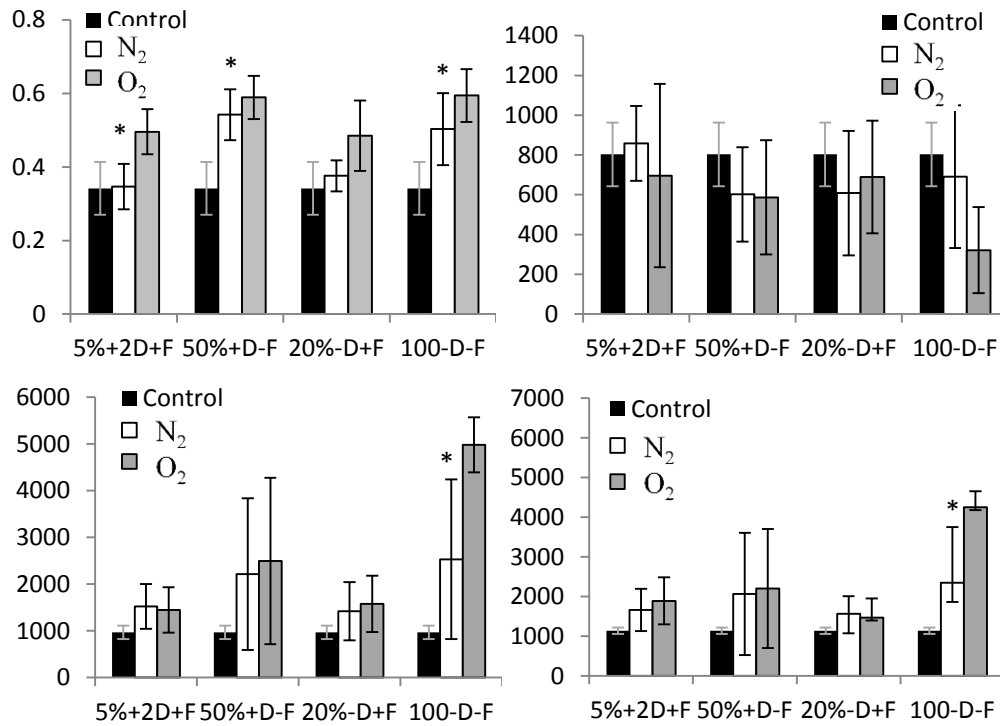


Figure 9: Comparisons between FT nitrogen purged and oxygenated samples for Fv/Fm (A), chlorophyll (B), phycoerythrin (C), and phycocyanin (D) over the course of the experiment at top left, top right, bottom left and bottom right, respectively. An “*” is displayed above treatments where N₂ and O₂ were found to be statistically different via *post hoc* Wilcoxon tests.

Table 4: p-values for Kruskal Wallis tests comparing FT nitrogen purged, oxygenated and control group samples ($\alpha = 0.05$). Significant values shown in bold.

Parameter	5%+2ND+F	50%+ND-F	20%- ND+F	100%-ND- F
Yield	0.0003	<0.0001	0.0006	<0.0001
Chl	0.9494	0.6600	0.6911	0.0260
PE	0.1811	0.0142	0.1480	0.0029
PC	0.1586	0.3273	0.2606	0.0020

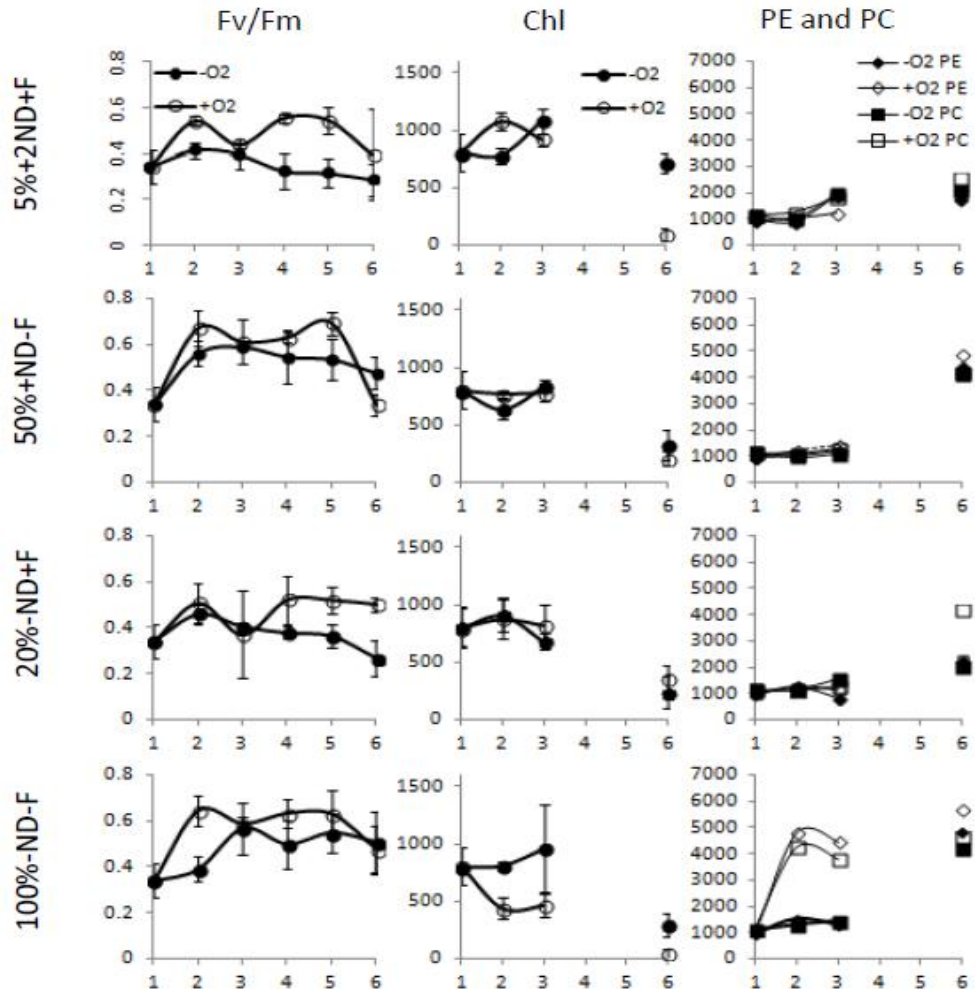


Figure 10: Plots of filter experiment for FT. Time (x axis) begins with the control that has had no exposure to filters. Time points were taken 24hr apart for 5 days after the control time point. Each Figures compares anoxic and oxic treatment groups for each filter treatment (horizontal rows; treatment indicated at left).

Table 5: p-value Results of Shapiro Wilk tests ($\alpha = 0.05$) for each EC treatment group. Values less than 0.05 are shown in bold and signify samples with non-normal distributions. Nitrogen purged samples are shown at left and oxygenated samples at right.

Filter	Y	Chl	PE	PC	Y	Chl	PE	PC
	Nitrogen				Oxygen			
Control	0.5688	0.3773	0.5704	0.5124	0.5124	0.3773	0.5704	0.5081
5%+2ND+F	0.5348	0.0561	0.8636	0.2816	0.2816	0.2612	0.8619	0.3218
20%-ND+F	0.0208	0.3774	0.2951	0.0055	0.0055	0.8452	0.4264	0.3142
50%+ND-F	0.0478	0.4599	0.3383	0.9882	0.9882	0.8603	0.4076	0.2392
100%-ND-F	0.2961	0.1501	0.8225	0.3878	0.3878	0.5216	0.7528	0.8321

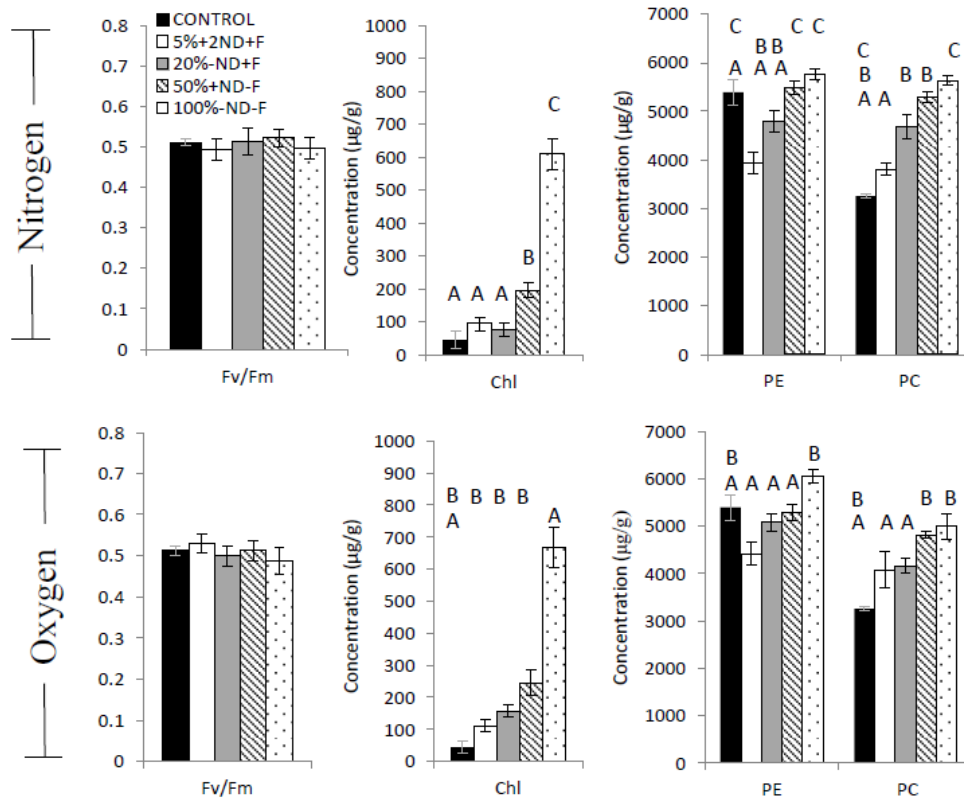


Figure 11: Comparisons of filter treatments for EC samples, grouped by all measured parameters: Fv/Fm, chlorophyll (Chl), phycoerythrin (PE), and phycocyanin (PC). The top row shows samples that were purged with nitrogen, and the bottom row shows samples that were fully oxygenated. Bars represent the average of the entire course of the experiment. Error bars represent standard error of the mean. Letters are shown above to indicate statistically significant different groups.

Table 6: Resulting p-values from Kruskal Wallis tests applied to EC filter comparisons ($\alpha = 0.05$). Significant values shown in bold and indicate that there was some effect on the measured parameter between filter treatments (groupings indicated in Figure 11).

Oxygen Condition	Fv/Fm	Chl	PE	PC
N ₂	0.9248	<0.0001	<0.0001	<0.0001
O ₂	0.9652	<0.0001	0.0003	0.0097

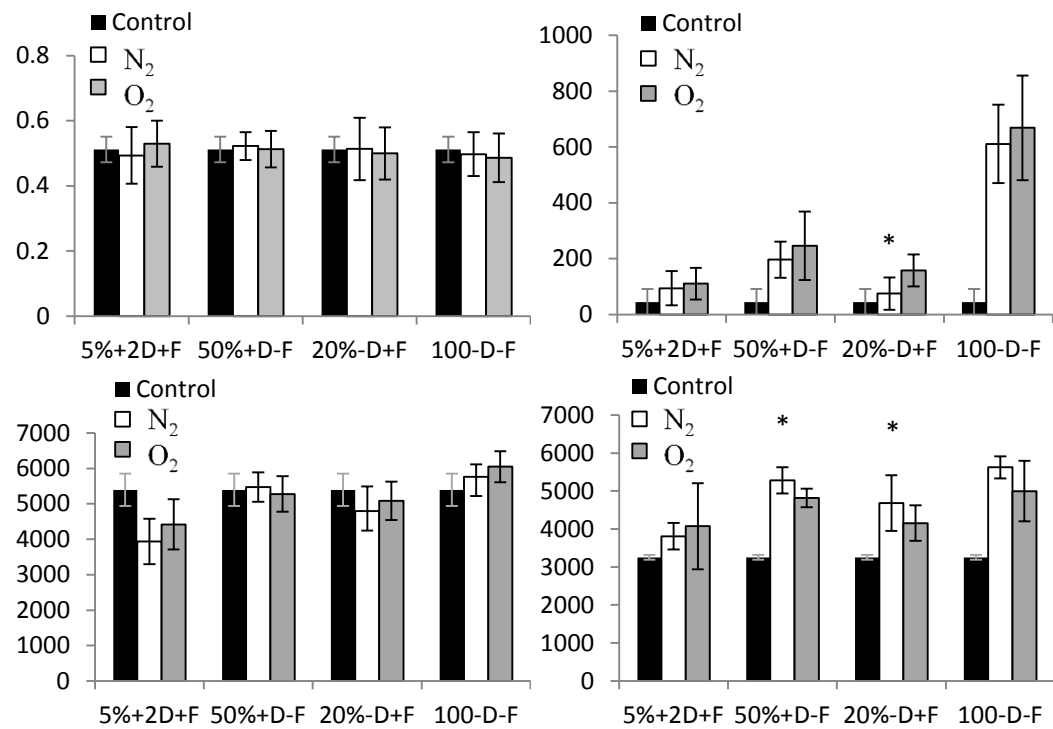


Figure 12: Summary graphs of EC filter studies representing average photosynthetic yield, chlorophyll, phycocyanin, and phycoerythrin over the course of the experiment at top left, top right, bottom left and bottom right, respectively. These plots ignore the effect of time.

Table 7: p-values for Kruskal Wallis tests comparing EC nitrogen purged, oxygenated and control group samples ($\alpha = 0.05$). Significant values shown in bold.

Parameter	5%+2ND+F	50%+ND-F	20%-ND+F	100%-ND-F
Yield	0.7759	0.7049	0.9635	0.9621
Chl	0.2474	0.0217	0.0152	0.0214
PE	0.0315	0.6338	0.4256	0.0960
PC	0.1859	0.0017	0.0090	0.0075

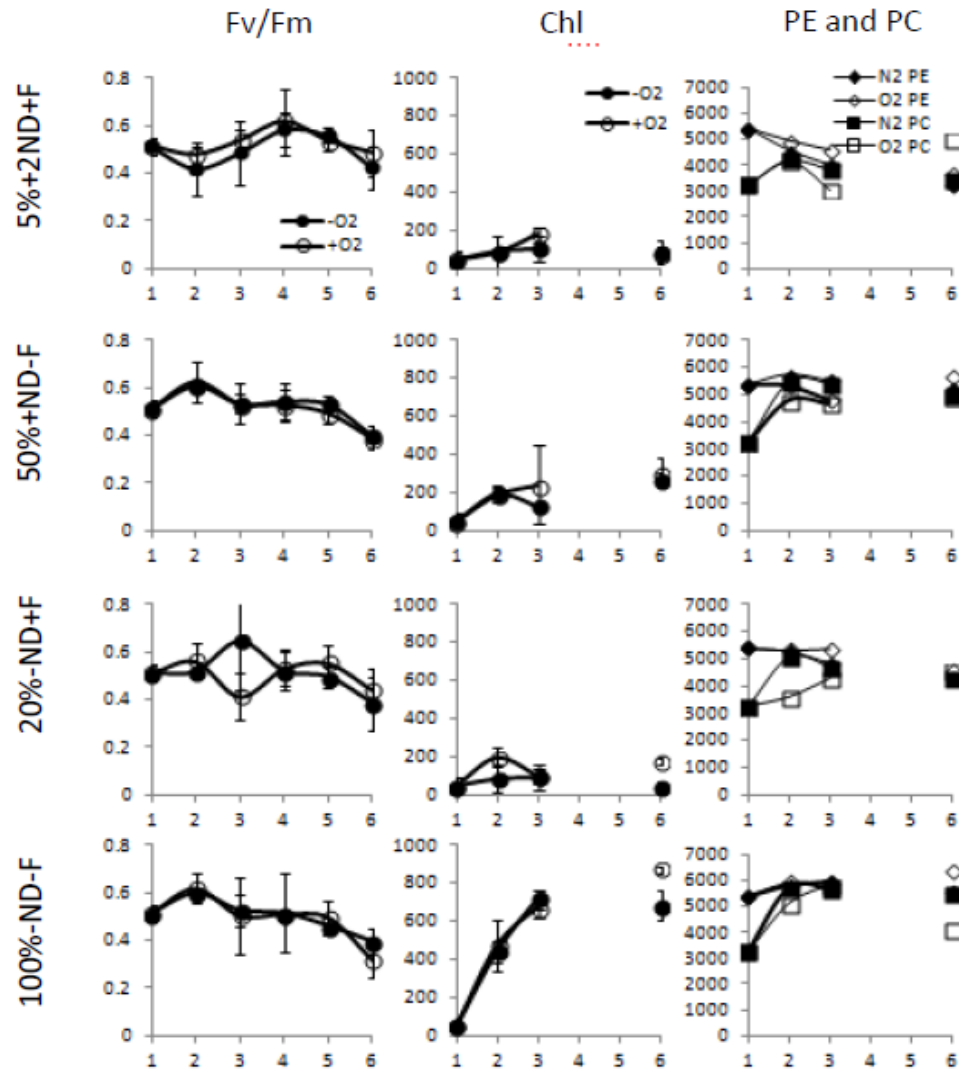


Figure 13: Plots of filter experiment for EC. Time (x axis) begins with the control that has had no exposure to filters. Time points were taken 24hr apart for 5 days after the control time point. Each Figures compares anoxic and oxic treatment groups for each filter treatment (horizontal rows; treatment indicated at left).

Table 8: p-value Results of Shapiro Wilk tests ($\alpha = 0.05$) for each MIS treatment group. Values less than 0.05 are shown in bold and signify samples with non-normal distributions. Nitrogen purged samples are shown at left and oxygenated samples at right.

Filter	Y	Chl	PE	PC	Y	Chl	PE	PC
	Nitrogen				Oxygen			
Control	0.3438	0.3762	0.9232	0.0556	0.3438	0.3762	0.9232	0.0556
5%+2ND+F	0.4345	0.5339	0.0038	0.1413	0.5853	0.3227	0.2982	0.3375
20%-ND+F	0.2726	0.7301	0.1399	0.2351	0.0603	0.6278	0.1543	0.8586
50%+ND-F	0.2965	0.8597	0.3013	0.7359	0.3093	0.8026	0.9775	0.5896
100%-ND-F	0.2641	0.5211	0.9705	0.5820	0.8454	0.7836	0.7840	0.6565

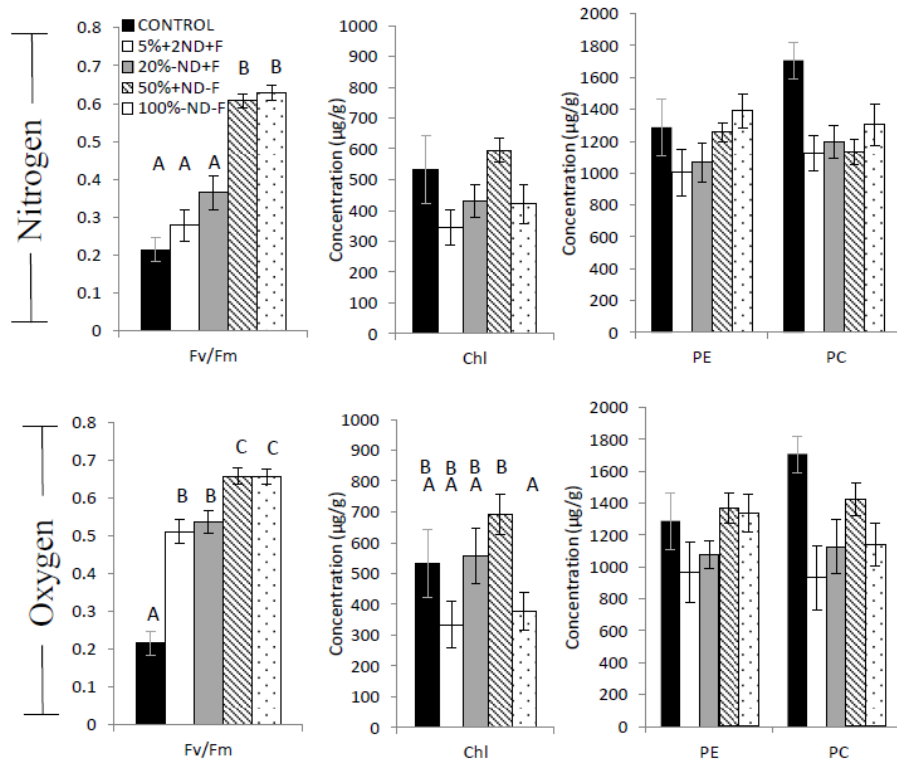


Figure 14: Comparisons of filter treatments for MIS samples, grouped by all measured parameters: Fv/Fm, chlorophyll (Chl), phycoerythrin (PE), and phycocyanin (PC). The top row shows samples that were purged with nitrogen, and the bottom row shows samples that were fully oxygenated. Bars represent the average of the entire course of the experiment. Error bars represent standard error of the mean. Letters are shown above to indicate statistically significant different groups.

Table 9: Resulting p-values from Kruskal Wallis tests applied to EC filter comparisons ($\alpha = 0.05$). Significant values shown in bold and indicate that there was some effect on the measured parameter between filter treatments (groupings indicated in Figure 14).

Oxygen Condition	Fv/Fm	Chl	PE	PC
N ₂	<0.0001	0.0428	0.0543	0.1518
O ₂	<0.0001	0.0178	0.2208	0.1214

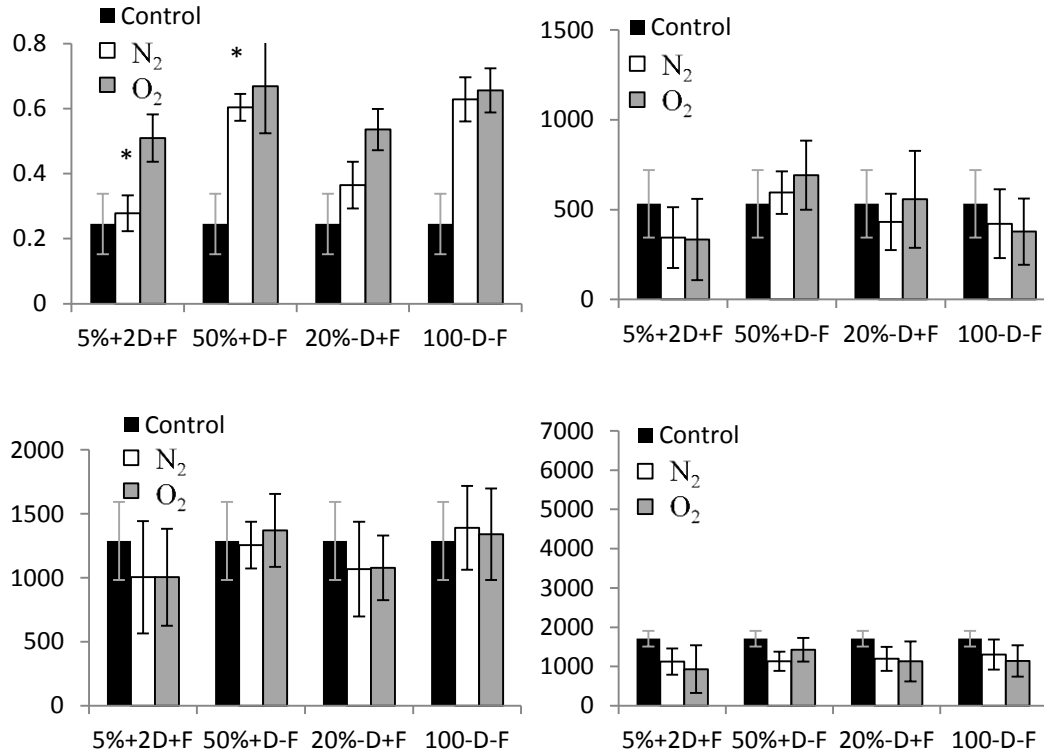


Figure 15: Summary graphs of MIS filter studies representing average photosynthetic yield, chlorophyll, phycocyanin, and phycoerythrin over the course of the experiment at top left, top right, bottom left and bottom right, respectively. These plots ignore the effect of time.

Table 10: p-values for Kruskal Wallis tests comparing EC nitrogen purged, oxygenated and control group samples ($\alpha = 0.05$). Significant values shown in bold.

Parameter	5%+2ND+F	50%+ND-F	20%-ND+F	100%-ND-F
Yield	<0.0001	<0.0001	<0.0001	<0.0001
Chl	0.3152	0.4614	0.2713	0.4111
PE	0.5239	0.4111	0.6338	0.8987
PC	0.0865	0.1077	0.0247	0.0917

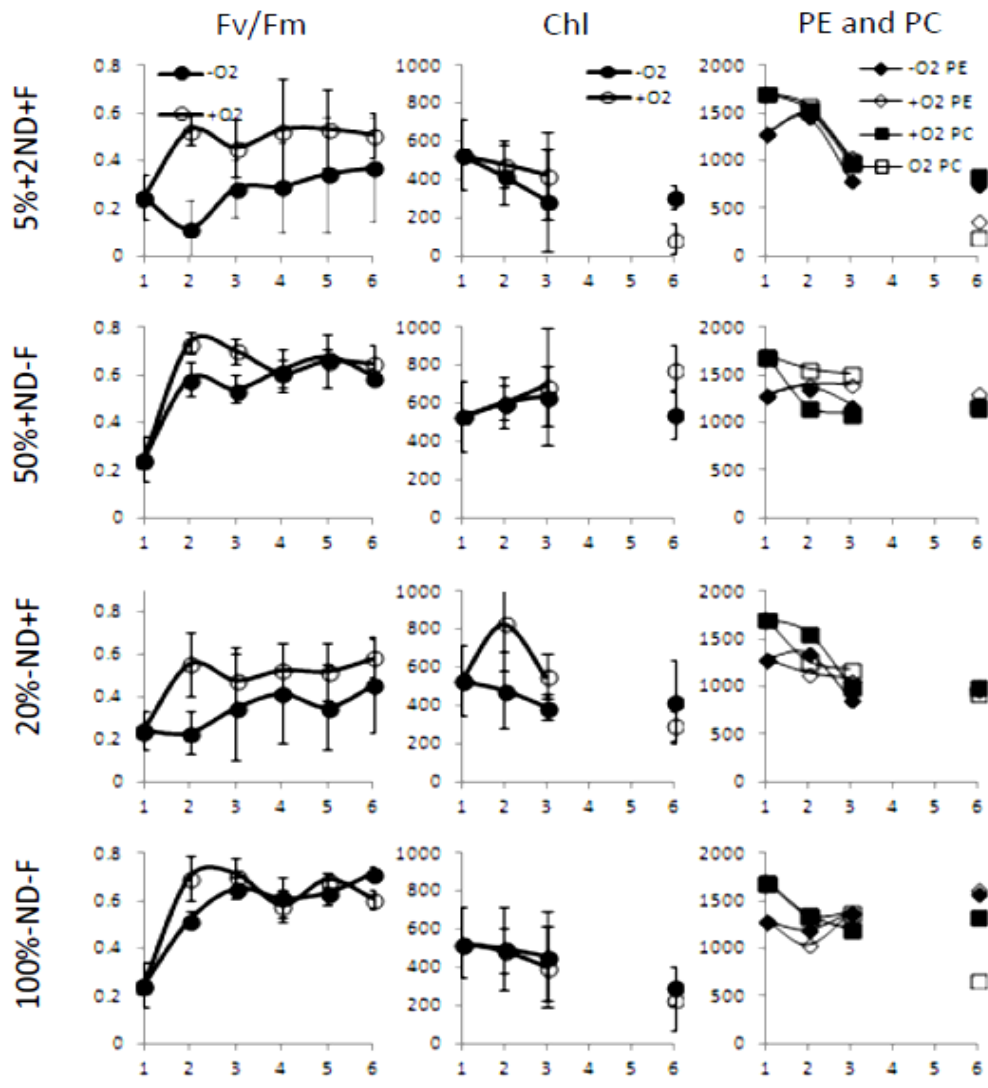


Figure 16: Plots of filter experiment for MIS. Time (x axis) begins with the control that has had no exposure to filters. Time points were taken 24hr apart for 5 days after the control time point. Each figure compares anoxic and oxic treatment groups for each filter treatment (horizontal rows; treatment indicated at left).

Inhibitor studies

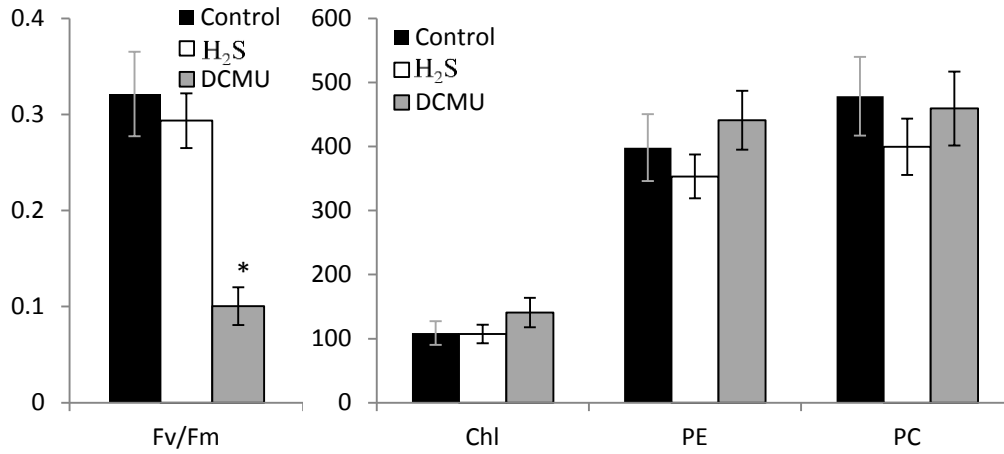


Figure 17: Measured Fv/Fm, chlorophyll (Chl), phycoerythrin (PE), and phycocyanin (PC) from addition of H₂S (25 - 50μM), DCMU (10μM), and a control on FT samples. Bars represent the average of all time points taken through the duration of the experiment and error bars represent the standard error of the mean. An “*” signifies a statistically significant group.

Table 11: Top - Shapiro Wilk Test p-value results for FT inhibitor studies.

Significant results shown in bold and indicate non-normal sample distribution.

Bottom - Kruskal Wallis test p-value results for inhibitor additions to FT samples ($\alpha = 0.05$). Significant values shown in bold, and indicate an effect of either H₂S and/or DCMU (the distinction between which treatment caused a positive test result is indicated by an “*” in Figure 17).

Treatment	Fv/Fm	Chl	PE	PC
Control	0.4389	0.7164	0.1162	0.3285
DCMU	0.0003	0.9090	0.9963	0.2183
H ₂ S	0.3830	0.9540	0.7173	0.3358
Kruskal Wallis Test	0.002	0.4691	0.2651	0.7173

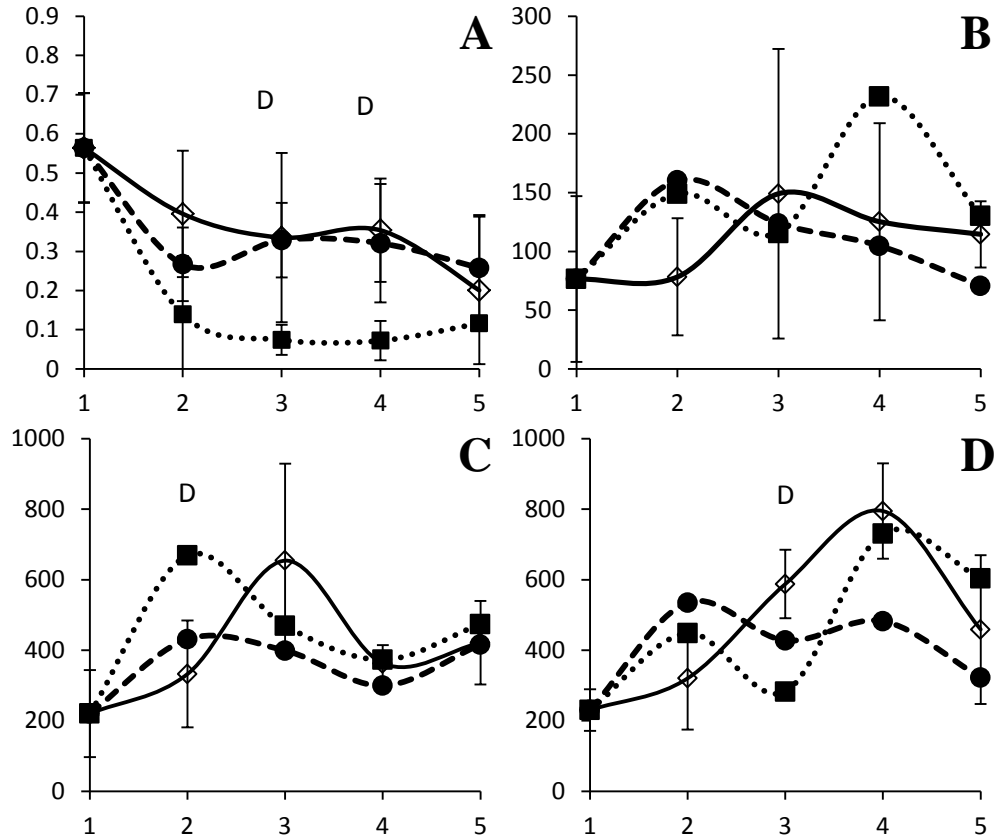


Figure 18: Time series results of FT inhibitor results. A.) Fv/Fm, B.) Chlorophyll, C.) Phycoerythrin, D.) Phycocyanin. H₂S: (●), DCMU: (■), Control: (◇). When applicable, the treatment that had a significant effect is marked above the time point with a symbol denoting which treatment had the effect (S: H₂S; and D: DCMU).

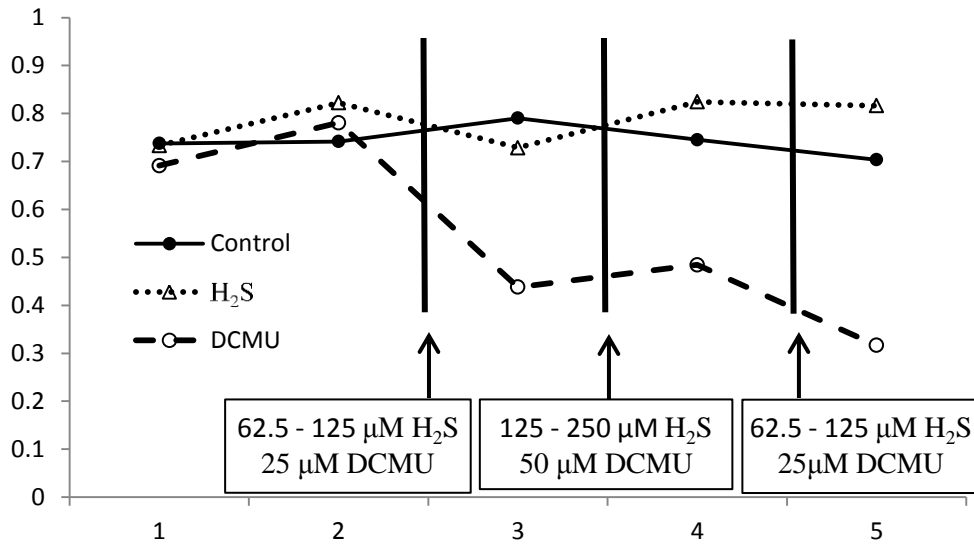


Figure 19: Time series of addition of increased inhibitor concentrations for FT samples. Two baseline, non-affected time points were measured before addition of inhibitors.

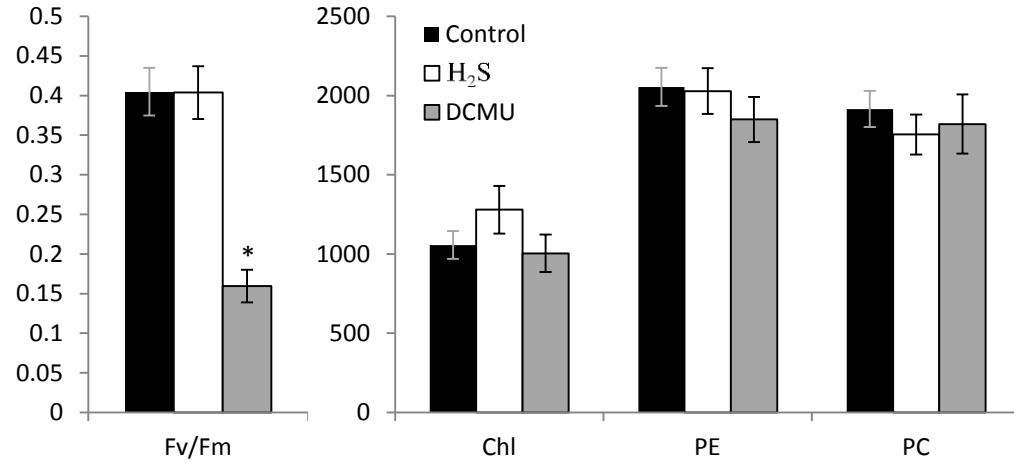


Figure 20: Measured Fv/Fm, chlorophyll (Chl), phycoerythrin (PE), and phycocyanin (PC) from addition of H₂S (25 - 50μM), DCMU (10μM), and a control on EC samples. Bars represent the average of all time points taken through the duration of the experiment and error bars represent the standard error of the mean. An “*” signifies a statistically significant group.

Table 12: Top - Shapiro Wilk Test p-value results for EC inhibitor studies.

Significant results shown in bold and indicate non-normal sample distribution.

Bottom - Kruskal Wallis test p-value results for inhibitor additions to EC samples (a = 0.05). Significant values shown in bold, and indicate an effect of either H₂S and/or DCMU (the distinction between which treatment caused a positive test result is indicated by an “*” in Figure 20).

Treatment	Y	Chl	PE	PC
Control	0.3866	0.6350	0.4121	0.9442
DCMU	0.0042	0.1664	0.1162	0.7158
H2S	0.4815	0.6879	0.1162	0.0586
Kruskal Wallis Test	<0.001	0.250851	0.494442	0.904678

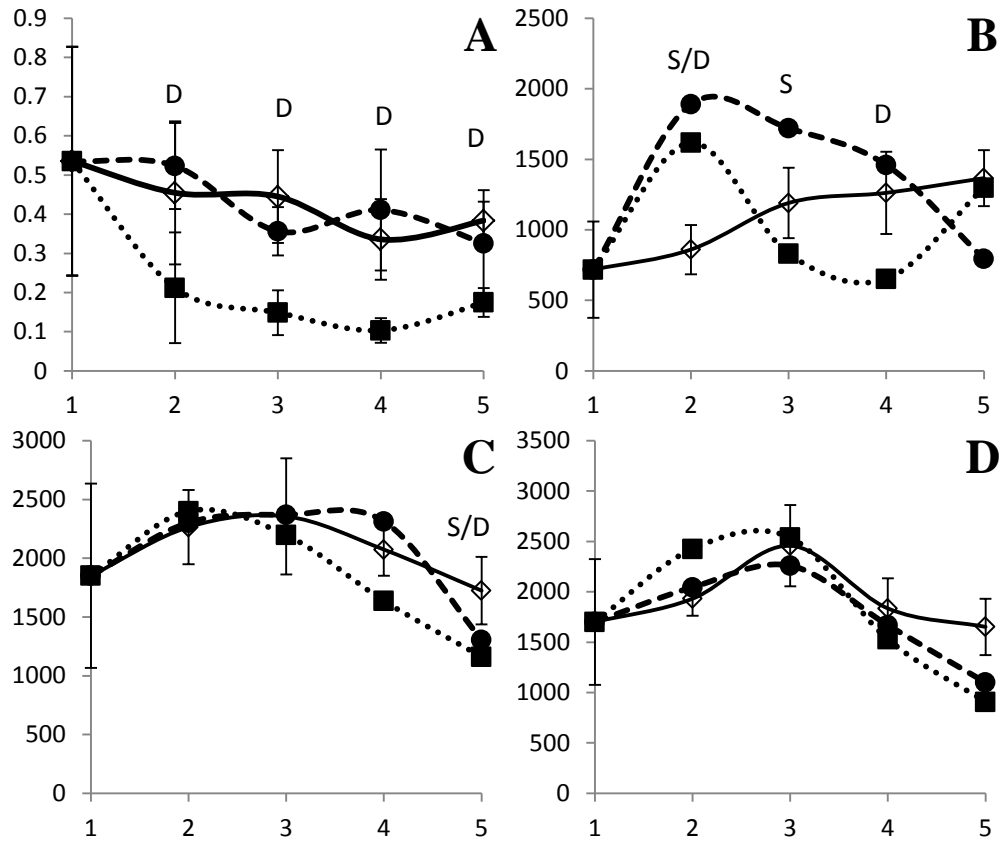


Figure 21: Time series results of EC inhibitor results.. A.) Fv/Fm, B.)

Chlorophyll, C.) Phycoerythrin, D.) Phycocyanin. H₂S: (●), DCMU: (■), Control: (◇). When applicable, the treatment that had a significant effect is marked above the time point with a symbol denoting which treatment had the effect (S: H₂S; and D: DCMU).

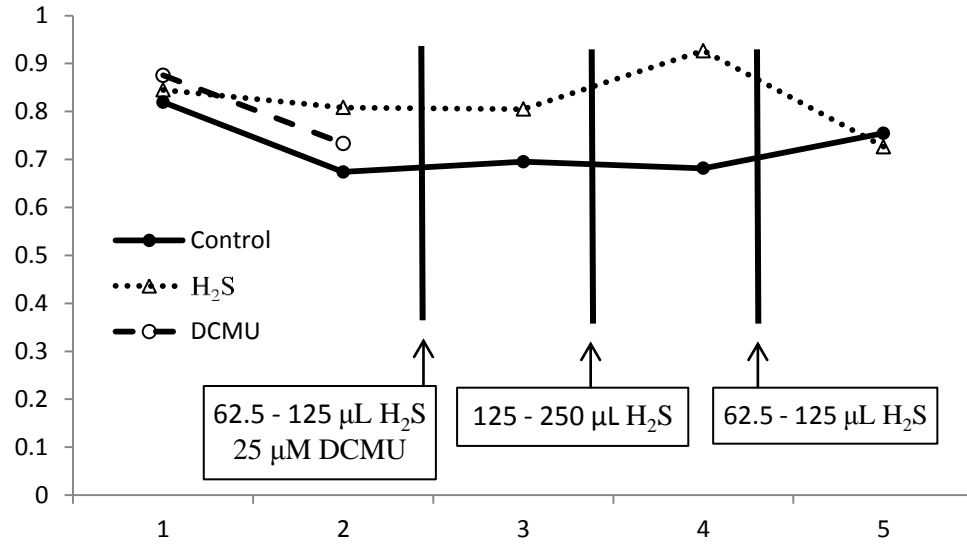


Figure 22: Time series of addition of increased inhibitor concentrations for EC samples. Two baseline, non-affected time points were measured before addition of inhibitors. Later time points for DCMU are missing as samples were too few after many cultures died.

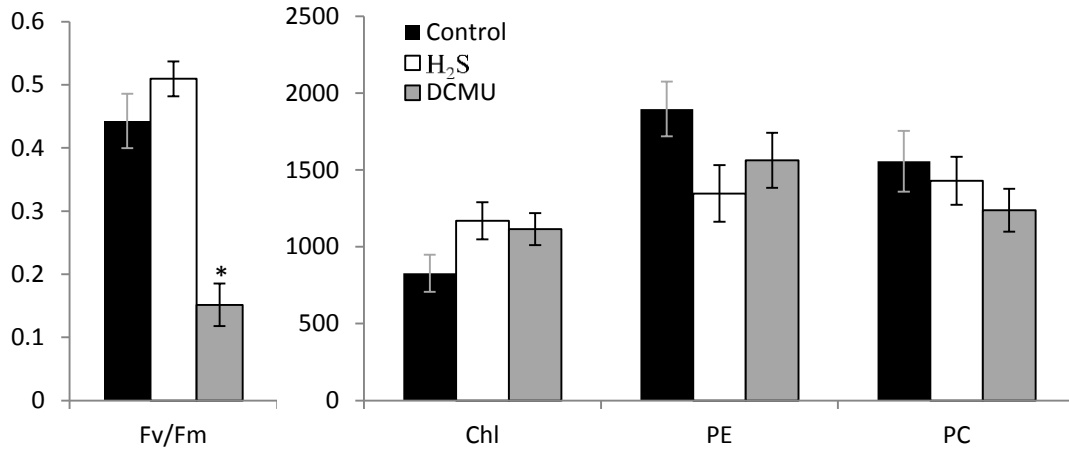


Figure 23: Measured Fv/Fm, chlorophyll (Chl), phycoerythrin (PE), and phycocyanin (PC) from addition of H₂S (25 - 50μM), DCMU (10μM), and a control on MIS samples. Bars represent the average of all time points taken through the duration of the experiment and error bars represent the standard error of the mean. An “*” signifies a statistically significant group.

Table 13: Top: Shapiro Wilk Test p-value results for MIS inhibitor studies.

Significant results shown in bold and indicate non-normal sample distribution.

Bottom: Kruskal Wallis test p-value results for inhibitor additions to MIS samples ($\alpha = 0.05$). Significant values shown in bold, and indicate an effect of either H₂S and/or DCMU (the distinction between which treatment caused a positive test result is indicated by an “*” in Figure 23). Note that the global Kruskal Wallis test found a positive p-value (>0.05) for chlorophyll, but the *post hoc* pairwise Wilcoxon test found no significant differences.

Treatment	Y	Chl	PE	PC
Control	0.0825	0.1572	0.8795	0.2074
DCMU	0.0223	0.1393	0.0500	0.7899
H ₂ S	0.0707	0.6381	0.4446	0.7951
Kruskal Wallis Test	<0.001	0.02216	0.1014	0.4275

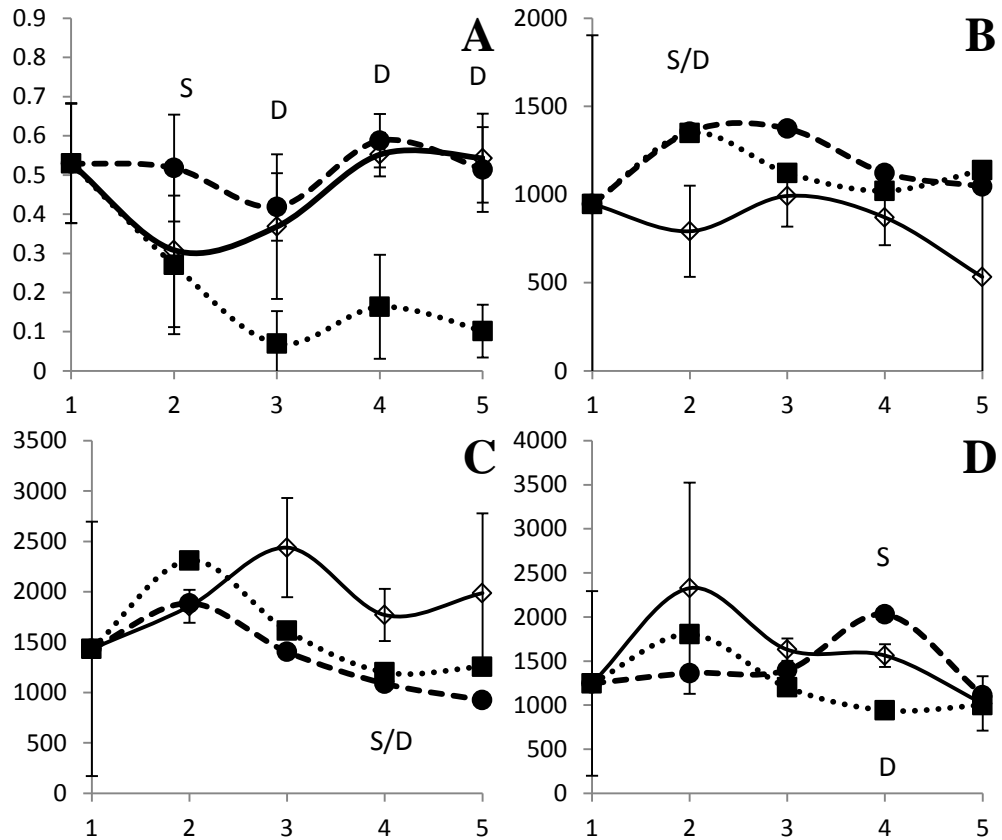


Figure 24: Time series results of MIS inhibitor results.. A.) Fv/Fm, B.) Chlorophyll, C.) Phycoerythrin, D.) Phycocyanin. H₂S: (●), DCMU: (■), Control: (◇). When applicable, the treatment that had a significant effect is marked above the time point with a symbol denoting which treatment had the effect (S: H₂S; and D: DCMU).

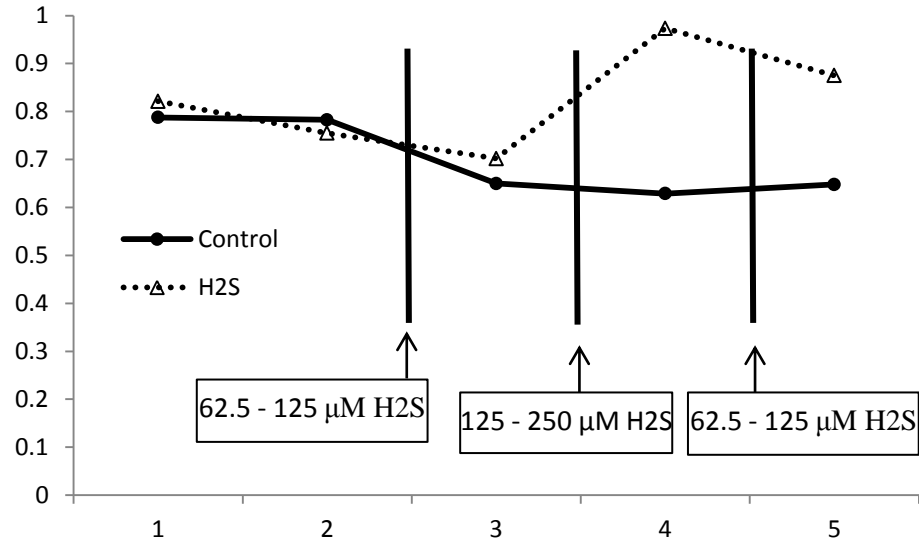


Figure 25: Time series of addition of increased inhibitor concentrations for MIS samples. Two baseline, non-affected time points were measured before addition of inhibitors. No DCMU treatments are presented as samples in this group were too few after samples died.

Cell motility experiment

The two treatments were normally distributed (Shapiro-Wilk test p-values of 0.0533 and 0.7014 for light and dark treatments, respectively). A 2 sample t-test yielded a p-value of 0.0091. For congruity with previous experiments, a Wilcoxon sign ranked test was conducted and yielded a significant p-value of 0.0045.

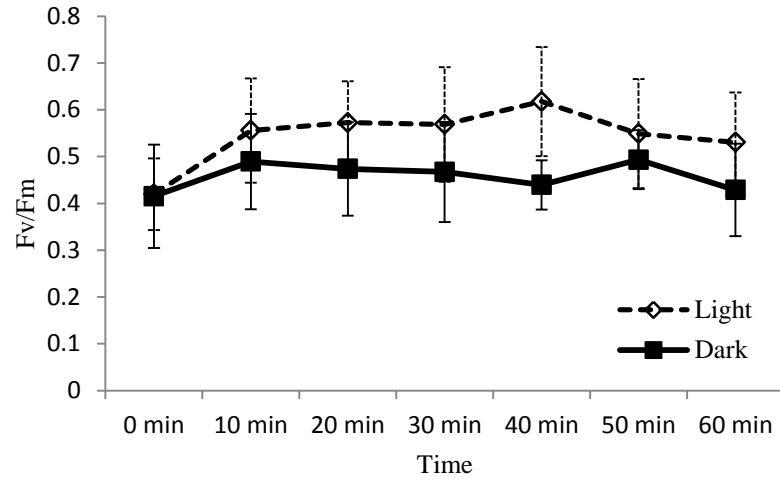


Figure 26: Time series results from cell motility experiment. This study was conducted for one hour and Fv/Fm was measured at 10min intervals in both the light sections and dark sections of the petri dish.

DISCUSSION

Cyanobacteria inhabit a vast range of habitats from temperature, chemical, light and pH extremes, and thus represent much diversity in physiology to adapt to their environment (Whitton 2012). My results characterize yet another example of a cyanobacterial community living in extreme conditions that is able to tolerate vast changes in both light and redox. Hydrogen sulfide tolerance is also described below.

Mats are dominated by 2 morphotypes

Morphologically identical cell types were identified in all three study sites. The dominant cells were straight, unbranched purple filaments. Of these filaments, most fell into two broad categories: wide filaments (~15 μ m) containing cells with greater width than length (~5 μ m), and thin filaments (5 μ m) containing cells that have roughly equal length and width. These descriptions fit the characteristics of *Oscillatoria*-like cyanobacteria described by Komareck *et al.* (2003), and also follow the description of *Thiothrix*-like and *Phormidium*-like cyanobacteria described by Voorhies *et al.* (2012) (then referred to as *Oscillatoria*). The thicker, *Thiothrix*-like filaments appeared to represent the greater majority of cell types present, though this was in contradiction to Voorhies *et al.* (2012) which found that *Phormidium*-like cyanobacteria was the dominant organism using genetic methods. While heterogeneity has been documented in cyanobacterial mats, these samples appeared to be relatively homogenous (Vilalta and Sabater 2005). Other organisms were present in collected samples (not pictured),

including diatoms, nematodes, and white filaments of what are believed to be sulfur-oxidizing bacteria – however, these organisms appeared to constitute only a small fraction of the organisms present. Care was taken to not include these macroscopic organisms, though these and other impurities could have increased dry weight values which would artificially lower pigment concentrations. While cyanobacteria collected from all study sites are morphologically similar, their genetic similarity is currently unknown. It is often the case that morphology can mask physiological or genetic diversity (Ward *et al.* 2012).

Calibration studies demonstrate stability of Fv/Fm

The only time point that stands out in the constant illumination calibration study is at the 6hr mark for the EC group. Both groups show an increase from the 0 to 6hr mark, though the FT group's 6hr point was not significantly different from all other time points. This initial increase may reflect an increase in photosynthesis related proteins as cultures had previously been in the dark (Foyer *et al.* 2012). These results show that after an initial acclimation period, cultures reached a relatively stable point after which measurements were not affected by the total illumination time. Note also that the results show that there is not an 'innate' diurnal cycle independent of light levels. If there was, a noticeable curve would be seen in Fv/Fm, and consistent timing of future yield measurements would have been critical. While such cycles have been recorded in nature, they likely follow PAR over the course of the day, while in this study light was constant, and as such so was Fv/Fm (Stibal *et al.* 2007; Mackey *et al.* 2008). The following

experiments were conducted after 12hr treatments periods which falls within the stable region of this study.

While F_v/F_m is a relative parameter, the effect of the thickness/density of mat samples on F_v/F_m was studied to ensure that sample thickness or density had no effect. Interestingly, 6mL stood out from the other chosen concentrations, but only for FT, yet 1, 12, and 15mL all responded with higher yield. There was no obvious increasing or decreasing trend (linear or otherwise). As a result of this, all subsequent experiments used culture volumes of 12mL.

Light and redox studies show high levels of cyanobacterial versatility

There appeared to be a variable effect of oxygenated and deoxygenated conditions. Photosynthetic yield was higher in oxygenated conditions for FT and MIS, but not at EC, while pigment levels were largely unaffected by oxygen conditions (Figures 9, 11, and 15). Yield tended to stay slightly higher in oxic conditions for all filter treatments, but where a significant difference was detected for pigments, sometimes the oxic and sometimes the anoxic treatment had higher pigment concentration. Overall there appears to be an effect of anoxic conditions on F_v/F_m , chlorophyll, phycocyanin and phycoerythrin such that oxygenated conditions are preferable for FT and MIS mats.

The site from which FT samples were collected contains the highest levels of oxygen, and therefore may be expected to better handle oxygenated conditions. *In situ*, these samples are essentially exposed to air while EC and MIS are perennially submerged, and mostly in anoxic waters. Periods of mixing may expose EC and MIS

mats to higher oxygenated water, but this is likely a minority of the time and still would only expose them to oxygen levels far less than that of air. FT samples are likely more adapted to oxygen, and therefore less adapted to anoxic conditions, as our lab results show a higher Fv/Fm under oxygenated conditions. This is likely due to the energetic boost that comes with oxygenated conditions – autotrophic organisms must respire the carbon that they have fixed, and the presence of oxygen allows this to occur through respiration.

In the FT full light treatment (100%-F), chlorophyll decreased in oxygenated conditions (though this finding was not statistically significant), while phycobilins both increased. These conditions are most similar to FT's natural conditions, and these results highlight how FT mats may survive in conditions with stark changes in PAR. Phycobillin synthesis often changes with changes in the light spectrum, but this trend was difficult to see in this data (Bennet 1973). Chlorophyll, being a more structurally integral pigment than accessory pigments, often takes longer to synthesize and degrade, thus high levels of chlorophyll could be hazardous to cellular health when there is very high light – it would therefore be expected that chlorophyll would be low for a mat from a high light environment, and more response from phycobillins may be seen (Reger and Krauss 1970). However, these simulated conditions have much lower PAR than *in situ*, so this may not be the case. We do see, however, some evidence that FT samples are physiologically stronger in oxygenated conditions, based off of Fv/Fm results. Phycobilins likely play a role in this, as well as the respiratory advantage that comes from the presence of oxygen.

EC samples, on the other hand, showed no differences in Fv/Fm between oxic and anoxic conditions. This data suggests a degree of physiological versatility which may be due to fluctuations in oxygen conditions from mixing events in the shallow location from which the samples are found. This is currently unknown, however, as all *in situ* oxygen concentrations were found to be quite low and longer periods of measurement would show if periods of oxygenation occur. Further, respiration in the presence of oxygen as well as motility likely play large roles in survival across redox gradients (Minz *et al.* 1999).

Pigment changes occurred mostly in phycocyanin for all EC filter treatments. This, like FT, suggests an element of maintaining homeostasis through regulation of accessory pigments, in this case, phycocyanin. This means of control could be through a phycobilin associated state transition that effectively redirects harvested light energy from PSII to PSI or vice versa (Bailey and Grossman 2008). Two of the three study sites (FT and MIS) contained mats that showed higher yield with oxygen present. Studies of *Chloroflexus aurantiacus*, a filamentous anoxygenic phototrophic bacterium, showed that bacteriochlorophyll synthesis decreases when oxygen is present – a useful function to aid in PSI associated anoxygenic photosynthesis, as anoxygenic photosynthesis only occurs in the absence of oxygen for many anoxygenic phototrophs, including *Cf. aurantiacus* (Sprague *et al.* 1981; Feick *et al.* 1982). This mechanism may exist in the mats from the present study, and may be a factor that helps to regulate the metabolic switch from oxygenic and anoxygenic photosynthesis.

MIS samples showed a slight effect of anoxic and oxic treatments, and oxygenated samples generally had higher photosynthetic yield. Pigment levels were

largely unaffected. MIS mats do not undergo much variation in PAR *in situ*, and the range of PAR for filter treatments most closely resembles PAR at MIS, which may account for so few changes in yield and pigment levels. MIS mats may be less adapted to altering pigment levels due to the relatively stable conditions at Middle Island, yet appear to be quite tolerant of changes in oxygen. *In situ* MIS samples likely rarely experience oxygenated water, except in cases where the chemocline may dip, and/or oxygen evolution is at a maximum during the day. For samples from all sites, there was the potential that the saran wrap that was used to prevent evaporation could have limited gas exchange for the oxic treatments. This would potentially help explain the lack of drastic differences between oxic and anoxic groups.

It was expected that treatments containing the chromatic filter would show changes in phycobilin levels – however, no clear trends were observed in MIS experiments. *In situ*, MIS mats are likely exposed to light of only a narrow band of wavelengths between 500 and 600nm (Figure 12). This wavelength coincides well with the peak absorption range of phycoerythrin and phycocyanin. The lack of an increase in phycobilin levels under chromatic filtration could be due to light being sufficiently high in all treatments such that synthesis of new phycobilins is not necessary. Phycoerythrin will typically increase preferentially under suboptimal levels of PAR, so it is likely that PAR levels were not low enough for this to occur (Kana and Gilbert, 1987). The increase of phycocyanin occurs with increasing depth as the shorter wavelengths (blue, 400nm) are filtered and only the longer wavelengths (red, 700nm) remain. Phycocyanin absorbs light of wavelengths longer than those absorbed by phycoerythrin, and a shift in the phycobilin ratio towards phycocyanin would be expected. Unfortunately, neither the

depths at which the samples were collected, nor the range of light spectra used, were likely to be from a large enough range to observe these sort of changes. The light bulb used was an incandescent bulb which emits well past 700nm, which generated heat that made higher light treatments impossible due to the incubator not being able to maintain a stable temperature. Further, incandescent bulbs do not emit light similar to the emission spectra of sunlight (Figure 27). The light used was therefore not relevant to what is present in the field. There was also a strong disparity between the range of light used in the experiments to that present in the field. This considerably smaller range of PAR may have created little need for acclimation.

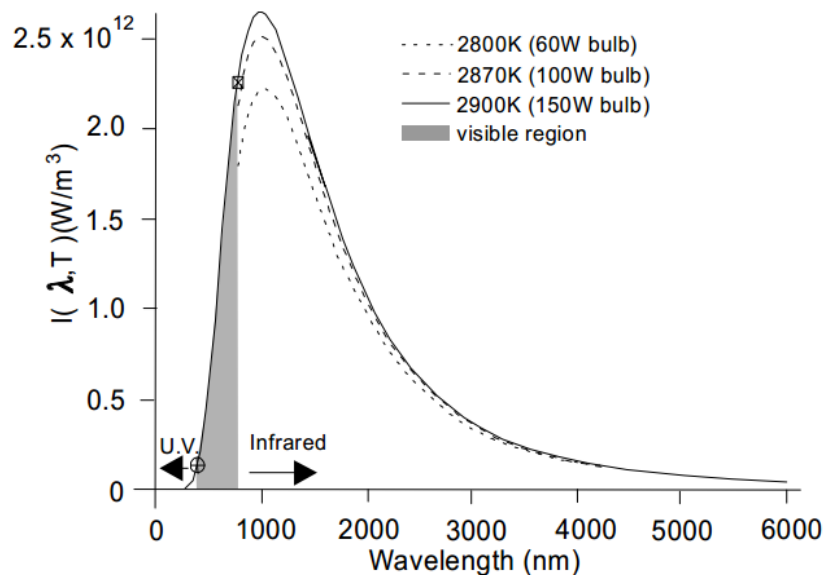


Figure 27: Emission spectra of incandescent light bulbs at three different wattage ratings. The bulb used in this study was a 40W bulb, close to the 60W bulb represented in the figure. The visible spectrum is colored gray. (MacIsaac 1999).

The pigment level of samples was directly influenced by the environment from which they were collected (Figure 28), which in itself lends to the idea of differential responses. If there is an optimal pigment distribution and samples from different sites start with different amounts, they must respond differently. Figure 27, differs from field measures quite significantly (i.e., chlorophyll is actually higher for FT samples here, where in the field they were significantly lower). This is likely an artifact of sampling as these figures represent one period of sampling, while field measures represent two years worth of data.

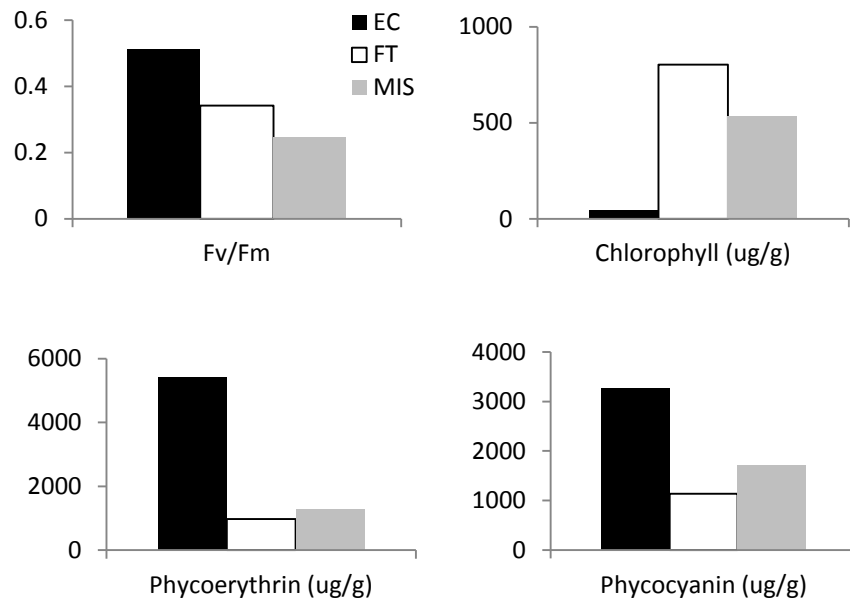


Figure 28: Control groups for samples from the three study sites. These values represent parameters measured in the lab, but before experimental treatments were applied.

The small range of PAR used in these experiments may have made filter treatments less effective than expected. Absolute PAR values ranged from 12 – 160 $\mu\text{mol s}^{-1} \text{ m}^{-2}$, whereas in the field values from all sites ranged from 100 to nearly 2000 $\mu\text{mol s}^{-1} \text{ m}^{-2}$. Higher light treatments were attempted, but the cultures were bleached and died. This may have been partly due to the incubator being unable to keep the temperature low at the higher light levels. Further, greater care should have been taken to ensure that ambient light was not present while making PAM measurements. This inconsistency could have significantly affected the measurements made, and masked effects of light conditions, oxygen conditions, or the presence of inhibitors.

Sulfide tolerance of sinkhole cyanobacteria

Strong evidence is presented showing significant photosynthetic inhibition by DCMU, but not by H_2S . The concentration of *in situ* H_2S is between 100 and 250 μM (Costello and Dick – personal communication), within the range of concentrations used in these experiments, so photosynthetic inhibition does not occur at levels of H_2S present in these sinkholes. Both chemicals used were photosystem II inhibitors, but some organisms, including those studied here, have strategies to tolerate H_2S . DCMU inhibits photosynthesis by binding to and blocking the plastoquinone binding site of PSII, which then blocks passage of electrons from PSII to the electron transport chain. The most common adaptation to sulfide is through the activation of sulfide dependent PSI, which often allows concurrent anoxygenic and oxygenic photosynthesis, or at least acts as a

detoxifying mechanism to allow continuation of PSII operation. Still others will simply convert to a purely anoxygenic form of photosynthesis, allowing stoppage of PSII.

Sulfide tolerance in cyanobacteria has been categorized into 4 broad groups: 1. Sulfide sensitive (oxygenic photosynthesis inhibited at $<75\mu\text{M}$), 2. Oxygenic photosynthetic cyanobacteria incapable of anoxygenic photosynthesis that are able to tolerate significant levels of sulfide (up to $350\mu\text{M}$), and oxygenic photosynthesis is even stimulated over certain ranges of sulfide, 3. simultaneous sulfide-insensitive oxygenic photosynthesis (with low carbon assimilation activity measured up to levels of $1000\mu\text{M}$) with sulfide driven anoxygenic photosynthesis, and 4. asynchronous oxygenic and anoxygenic photosynthesis where PSII activity is fully inhibited at $80\mu\text{M}$, and anoxygenic photosynthesis could operate between 200 and $1000\mu\text{M}$ (Cohen *et al.* 1986 and Stahl 1995).

The mats found in these 3 sites are likely a combination of groups 2 and 4. It is known that sulfide driven anoxygenic photosynthesis occurs, and Voorhies *et al.* 2012 found no oxygenic photosynthesis in intact cores (no/low oxygen) – this does not exclude the possibility of group 2 cyanobacteria, though if present likely play a minor role. Any oxygenic photosynthesizers of this type would only be active in microclimates of low sulfide, which is likely rare. If or when this oxygenic photosynthesis was to occur, the oxygen produced would be used immediately so that oxygen build up would not occur. The absence of oxygenic photosynthesis found in intact cores suggests that simultaneous anoxygenic and oxygenic photosynthesis do not occur, precluding group 3. Mats from all 3 sites were treated with and were able to tolerate sulfide levels 10 times higher than that found in the Zodletone sulfur spring, concurrent with previous findings that the mats use

sulfide for anoxygenic photosynthesis (Buhring *et al.* 2011; Voorhies *et al.* 2012). A similar *Oscillatoria*-like cyanobacteria was describe in Lake Arcas that performed sulfide dependent anoxygenic photosynthesis with relatively sulfide tolerant oxygenic photosynthesis (Camacho *et al.* 1996). Further, differential phycobilin synthesis was found in their study, though not in my experiments.

The ability for simultaneous sulfide and oxygen tolerance would have been a key factor for survival during the prolonged oxygen transition era where oxygen gradually increased over the course of a couple billion years. Further, the simultaneous presence of both anoxygenic and oxygenic photosynthesis is likely a factor that prolonged the oxygenation of the atmosphere (Johnston *et al.* 2009).

Cell motility

The lit areas of the petri dish showed a higher photosynthetic yield. The trend of increasing yield in the light areas increased throughout most of the hour long experiment. This suggests that in only a matter of 10 – 15min, filaments were capable of finding themselves in an area better optimized for light harvest. The lighter areas remained at a higher yield while the dark areas still contained filaments with lower yield. This phototactic movement is important for filaments *in situ* as cells, especially at EC, are able to relocate themselves to better optimize their light harvesting potential (either ‘hiding’ from light that is too intense, or seeking out light patches in the dark). At MIS, detecting light, and being able to relocate is important in the case of objects (such as detritus) falling on the mat and obstructing light from reaching the mat surface. The presence of

stromatolites suggests that microbial phototaxis has been present for billions of years. The cyanobacteria in the present study have displayed horizontal phototaxis, and are believed to undergo vertical phototaxis *in situ*.

Conclusion

Phycobilins likely play a crucial role in the survival and life strategy of these microbial communities to effectively optimize energy harvesting from light. As presented, photosynthetic pigments respond differently in mats collected from sites with varying conditions (no measured responses in MIS, changes in all pigments for EC and FT). The extreme changes caused by fluctuations in phycobilins have even resulted in anecdotal evidence of filaments rapidly changing color from purple to green. This is potentially a result of complimentary chromatic adaptation (Bennet 1973). The presence of phycobilins, an advantageous trait in these conditions, likely spread very quickly via horizontal gene transfer, as has been previously shown in cyanobacteria (Tooming-Klunderud *et al.* 2013).

The samples collected from different sites likely responded differently to treatments because they are adapted to the environment from which they were collected. This may mean that the samples have different baseline levels of pigment concentration, and the manner in which they respond to changes in light and redox is altered as they are adapted to different sets of changes (i.e. rapid and extreme fluctuations in light at FT, and only a narrow range of PAR at MIS). Throughout all of these changes in pigment levels, photosynthetic efficiency remained relatively unchanged, even between sites. This shows

that changes in pigmentation are used to maintain homeostasis – a stable photophysiological state despite fluctuating light conditions. Despite variable responses, it is not possible to tell from my data if the samples collected from different sites are genetically different. If they were found to be genetically different it would show that different communities were selected for based on different selective pressures. If the communities are genetically similar, it means that the same organisms are able to acclimate to a vast range of conditions and the different responses from samples from different sites is likely explained by different baseline levels of pigments.

While our results suggest sulfide tolerance and maintenance of light harvesting via accessory pigmentation, our instrumentation could not assess anoxygenic photosynthetic activity, but rather only the absence of oxygenic photosynthetic activity. This assumption of active anoxygenic photosynthesis is based on the empirical findings of Voorhies *et al.* (2012). The physiological versatility (high and low light tolerance as well as sulfide and oxygen tolerance) represents the rich functional diversity present in these systems. This high functional diversity is vital to these communities' survival as they contain very low taxonomic diversity (Nold *et al.* 2010; Voorhies *et al.* 2012), especially in habitats that are highly dynamic. Accessory pigments, although not recently discovered, are becoming an increasingly complex and large role in the overall picture of how photosynthesis functions (Liu *et al.* 2013). The presence of anoxygenic photosynthesis under sulfidic conditions is reminiscent of the earliest known microbial mats (Buhring *et al.* 2011), and these cyanobacterial mats within modern day sinkholes may provide a glimpse into Earth's deep history.

LITERATURE CITED

- Bailey, S., and A. Grossman. "Photoprotection in Cyanobacteria: Regulation of Light Harvesting." *Photochemistry and Photobiology* 84.6 (2008): 1410-420. Web.
- Bennett, A. "Complementary Chromatic Adaptation In A Filamentous Blue-Green Alga." *The Journal of Cell Biology* 58.2 (1973): 419-35. Web.
- Bühning, S., S. Sievert, H. Jonkers, T. Ertefai, M. Elshahed, L. Krumholz, and K. Hinrichs. "Insights into Chemotaxonomic Composition and Carbon Cycling of Phototrophic Communities in an Artesian Sulfur-rich Spring (Zodletone, Oklahoma, USA), a Possible Analog for Ancient Microbial Mat Systems." *Geobiology* (2011): No. Web.
- Biddanda, B., S. Nold, G. Dick, S. Kendall, J. Vail, S. Ruberg, and C. Green. "Rock, Water, Microbes: Underwater Sinkholes in Lake Huron Are Habitats for Ancient Microbial Life." *Nature Education Knowledge* 3.13 (2012). Web.
- Camacho, A. "Adaptation to Sulfide and to the Underwater Light Field in Three Cyanobacterial Isolates from Lake Arcas (Spain)." *FEMS Microbiology Ecology* 21.4 (1996): 293-301. Print.
- Cohen, Y., B. Jorgensen, N. Revsbech, and R. Poplawski. "Adaptation to Hydrogen Sulfide of Oxygenic and Anoxygenic Photosynthesis among Cyanobacteria." *Applied and Environmental Microbiology* 51 (1986): 398-407. Web.
- Falkowski, P., T. Fenchel, and E. Delong. "The Microbial Engines That Drive Earth's Biogeochemical Cycles." *Science* 320.5879 (2008): 1034-039. Web.

- Feick, R., M. Fitzpatrick, and R. Fuller. "Isolation and Characterization of Cytoplasmic Membranes and Chlorosomes from the Green Bacterium *Chloroflexus Aurantiacus*." *Journal of Bacteriology* 150 (1982): 905-15. Web.
- Foyer, C., J. Neukermans, G. Queval, G. Noctor, and J. Harbinson. "Photosynthetic Control of Electron Transport and the Regulation of Gene Expression." *Journal of Experimental Botany* 63.4 (2012): 1637-661. Web.
- Gadgil, M., and W. Bossert. "Life Historical Consequences of Natural Selection." *The American Naturalist* 104.935 (1970): 1. Web.
- Johnston, D., F. Wolfe-Simon, A. Pearson, and A. H. Knoll. "From the Cover: Anoxygenic Photosynthesis Modulated Proterozoic Oxygen and Sustained Earth's Middle Age." *Proceedings of the National Academy of Sciences* 106.40 (2009): 16925-6929. Web.
- Hoiczyk, E. "Gliding Motility in Cyanobacteria: Observations and Possible Explanations." *Archives of Microbiology* 174.1 (2000): 7-11. Web.
- Kana, T., P. Gilbert. "Effect of Irradiances up to 2000 μ E on marine *Synechococcus*." *Deep Sea Res.* 34 (1987): 479 – 495. Print.
- Komarek, J. "Filamentous Cyanobacteria." Ed. R. G. Sheath. *Freshwater Algae of North America: Ecology and Classification*. Ed. J. D. Wehr. Amsterdam: Academic, 2003. Print.
- Liu, H., H. Zhang, D. Niedzwiedzki, M. Prado, G. He, M. L. Gross, and R. E. Blankenship. "Phycobilisomes Supply Excitations to Both Photosystems in a Megacomplex in Cyanobacteria." *Science* 342.6162 (2013): 1104-107. Web.

- Lyons, T., C. Reinhard, and N. Planavsky. "The Rise of Oxygen in Earth's Early Ocean and Atmosphere." *Nature* 506 (2014): 307-15. Web.
- Macisaac, Dan. "Basic Physics of the Incandescent Lamp (lightbulb)." *Physics Teacher* 37.9 (1999): 520. Web.
- Mackey, K., A. Paytan, A. Grossman, and S. Bailey. "A Photosynthetic Strategy for Coping in a High-light, Low-nutrient Environment." *Limnology and Oceanography* 53.3 (2008): 900-13. Web.
- Merz, A., and K. Forest. "Bacterial Surface Motility: Slime Trails, Grappling Hooks and Nozzles." *Current Biology* 12.8 (2002): R297-303. Web.
- Minz, D., S. Fishbain, G. Muyzer, Y. Cohen, BE Rittman, and DA Stahl. "Unexpected Population Distribution in a Microbial Mat Community: Sulfate-reducing Bacteria Localized to the Highly Oxidic Chemocline in Contrast to a Eukaryotic Preference for Anoxia." *Applied and Environmental Microbiology* 65 (1999): 4659-665. Web.
- Montgomery, K., J. Charlesworth, R. Lebar, P. Visscher, and B. Burns. "Quorum Sensing in Extreme Environments." *Life* 3.1 (2013): 131-48. Web.
- Nold, S., J. Pangborn, H. Zajak, S. Kendall, R. Rediske, and B. Biddanda. "Benthic Bacterial Diversity in Submerged Sinkhole Ecosystems." *Applied and Environmental Microbiology* 76.1 (2010): 347-51. Web.
- Oren, A. "Quantum Yields for Oxygenic and Anoxygenic Photosynthesis in the Cyanobacterium *Oscillatoria Limnetica*." *Proceedings of the National Academy of Sciences* 74.5 (1977): 2152-156. Web.

- Reger, B., and R. Krauss. "The Photosynthetic Response to a Shift in the Chlorophyll a to Chlorophyll B Ratio of *Chlorella*." *Plant Physiology* 46.4 (1970): 568-75. Web.
- Sprague, S., L. Staehelin, and R. Fuller. "Semiaerobic Induction of Bacteriochlorophyll Synthesis in the Green Bacterium *Chloroflexus Aurantiacus*." *Journal of Bacteriology* 147: 1032-039. Web.
- Stibal, M., J. Elster, M. Abackå, and K. Kaåltovskål. "Seasonal and Diel Changes in Photosynthetic Activity of the Snow Alga *Chlamydomonas Nivalis* (Chlorophyceae) from Svalbard Determined by Pulse Amplitude Modulation Fluorometry." *FEMS Microbiology Ecology* 59.2 (2007): 265-73. Web.
- Tamulonis, C., M. Postma, and J. Kaandorp. "Modeling Filamentous Cyanobacteria Reveals the Advantages of Long and Fast Trichomes for Optimizing Light Exposure." Ed. Christopher V. Rao. *PLoS ONE* 6.7 (2011): E22084. Web.
- Tooming-Klunderud, A., H. Sogge, T. B. Rounge, A. J. Nederbragt, K. Lagesen, G. Glockner, P. K. Hayes, T. Rohrlack, and K. S. Jakobsen. "From Green to Red: Horizontal Gene Transfer of the Phycoerythrin Gene Cluster between *Planktothrix* Strains." *Applied and Environmental Microbiology* 79.21 (2013): 6803-812. Web.
- Vilalta, E., and S. Sabater. "Structural Heterogeneity in Cyanobacterial Mats Is Associated with Geosmin Production in Rivers." *Phycologia* 44.6 (2005): 678-84. Web.
- Voorhies, A., B. Biddanda, S. Kendall, S. Jain, D. Marcus, S. Nold, N. Sheldon, and G. Dick. "Cyanobacterial Life at Low O₂: Community Genomics and Function

Reveal Metabolic Versatility and Extremely Low Diversity in a Great Lakes Sinkhole Mat." *Geobiology* 10.3 (2012): 250-67. Print.

Ward, D., R. Castenholz, S. Miller. "Cyanobacteria in Geothermal Habitats," in *Ecology of Cyanobacteria II: Their Diversity in Space and Time*. Dordrecht: Springer, 2012. Print.

Whitton, B. "Part I: Environments." *Ecology of Cyanobacteria II: Their Diversity in Space and Time*. Dordrecht: Springer, 2012. Print.

SYNTHESIS

The present work characterizes some of the remarkable characteristics of extremely versatile cyanobacteria that reside in Lake Huron's submerged sinkholes. By studying these communities in the field we have shown that microbial mats thrive across a range of light conditions. In laboratory studies, I further analyzed these field trends and characterized their sulfide tolerance as well as behavioral attributes that appear to give them an edge in survival under light-limiting conditions and result in significant carbon sequestration.

Our three study sites were analyzed for physico-chemical properties, and in them we discovered similar characteristics including perennially low oxygen, low pH, constant low temperature, high conductivity and high sulfate conditions. These conditions were relatively stable throughout the measured dates as well as through the winter at MIS. Oxygen levels are likely higher at FT due to the shallow water level which is likely coupled with greater influence of ambient temperatures. This site also had the highest level of PAR paired with the highest amount of variability in PAR due to periods of direct, unfiltered sunlight to shading from the neighboring buildings. EC cyanobacteria have natural macrophyte vegetation and other structures that can provide moderate shading in oversaturating light conditions using phototactic movement (discussed below). MIS samples experiences only a small range of low PAR values.

Microbial mats show seasonally variable photosynthetic characteristics

An apparent inverse relationship was seen between F_v'/F_m' and PAR for all sites (Figure 1). PAR had a greater effect on F_v'/F_m' than any of the other biological parameters studied. F_v'/F_m' was more similar between MIS and EC, the sites with some water column depth that allowed for filtration of PAR, and, as a result, had a higher F_v'/F_m' . FT likely had a lower F_v'/F_m' due to increased levels of PAR, which, during periods of direct sunlight likely caused photoinhibition. Pigment levels also appeared to show seasonal characteristics, and chlorophyll specifically may have directly influenced F_v'/F_m' which had positive, significant relationships in FT and MIS. Pigment levels between sites were statistically indistinguishable except for chlorophyll, where FT had a significantly lower amount, likely due to periods of extremely high PAR. This was the main pigmentation difference seen in *in situ* samples, and the most likely to explain F_v'/F_m' .

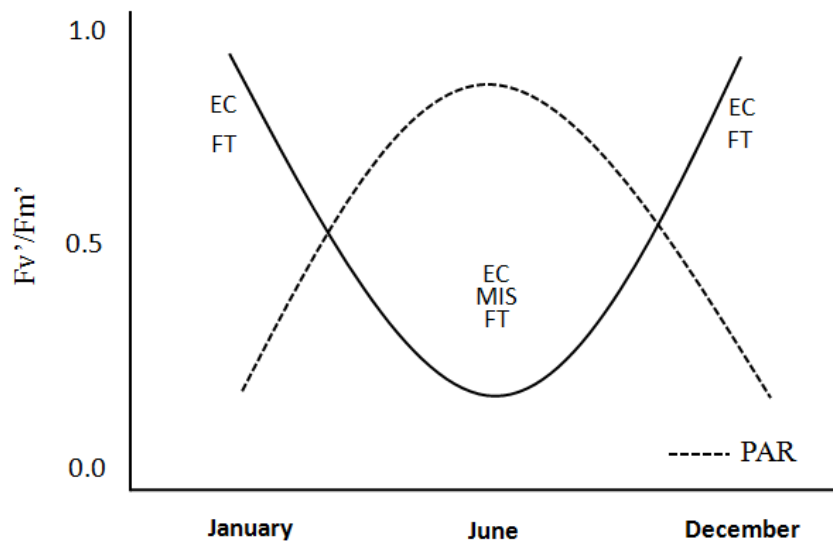


Figure 1: Overview of seasonality of F_v'/F_m' measured *in situ* in three sinkhole ecosystems.

F_v'/F_m' is affected by PAR, but in order to maintain homeostasis, cells must keep F_v'/F_m' within some optimal range. Staying within this range must be done at least in part by pigment regulation. Indeed, my data typically shows increases in F_v'/F_m' that are paired with increased chlorophyll, and increased chlorophyll with decreased PAR (Figure 2; also see Chapter 2). Phycobilins seemed to show the same relationship, though were only significant with EC samples for phycocyanin. This general relationship of decreased F_v'/F_m' has been recorded in other studies in sites around the globe (Figure 3).

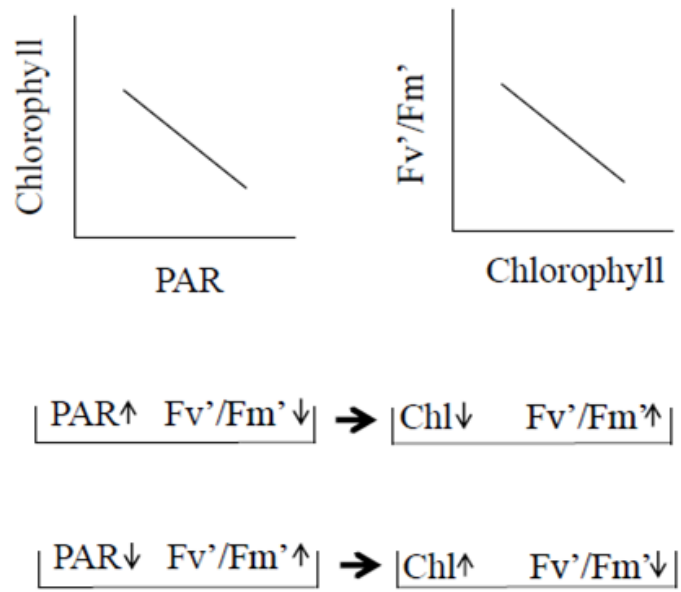


Figure 2: Top -- Conceptual diagrams of the relationship between chlorophyll, PAR, and Fv'/Fm'. Bottom – theoretical model of regulatory response to changes in PAR to maintain homeostasis. As PAR increases, Fv'/Fm' decreases. The response is to decrease chlorophyll pigment which then increases Fv'/Fm'.

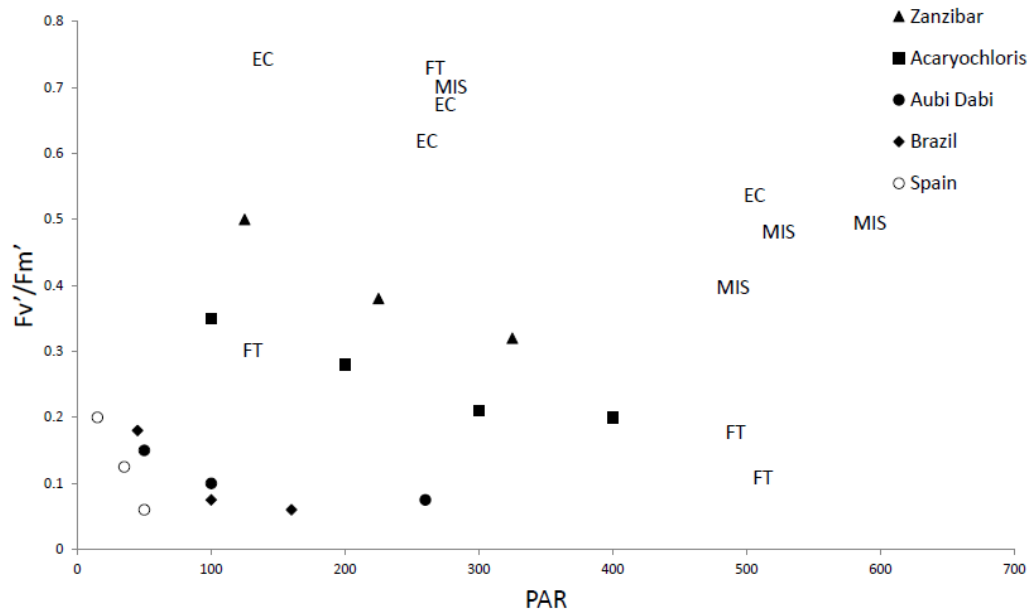


Figure 3: Comparison of Fv'/Fm' values between my study and other studies around the world. Source: Zanzibar (Lugomela *et al.* 2005), *Acaryochloris* (Kuhl *et al.* 2005), Aubi Dabi, Brazil and Spain (Al-Najjar *et al.* 2014).

This relationship was not directly corroborated by the laboratory experiments where, in general, higher light treatments yielded higher yield. The mismatch likely comes from the much lower PAR values used in experimental treatments. If much higher PAR values had been used, pigmentation likely would have decreased and yield would have decreased.

Key physical differences between sites may have strongly influenced the biological parameters I measured. FT, a man made structure, was located between buildings which influenced the amount of PAR received. This site featured flowing water (making motility difficult or impossible) that requires the mats to adhere to the concrete

floor of the fountain or risk going down the fountain drain. There are no natural structures that provide shade from direct sunlight.

EC received, on average, lower PAR. The cyanobacterial communities here live in an area where relocation may be possible for light optimization. Naturally occurring phenomenon may help to reduce the risk of over saturating light – such as relocation or greater growth accumulation in shaded areas. The effect of microhabitat shading in any of these study locations was not specifically studied and would be an interesting area of investigation.

MIS mat communities exist at a depth of 23m which significantly decreased the total range of PAR from only 0 - 100 $\mu\text{mol s}^{-1} \text{m}^{-2}$. As such, F_v'/F_m' remained high.

Microbial mats tolerate extreme redox changes

FT mats were found to have higher photosynthetic yield under oxygenated conditions, likely reflecting the higher prevalence of oxygen from the site from which they were obtained. EC mats showed no changes in photosynthetic yield, potentially due to episodic mixing events where oxygen is present at EC. Phycocyanin responded to changes in oxygen levels by generally increasing in the presence of oxygen. MIS had no strong response in either pigment levels or photosynthetic yield to changes in oxygen level. These results show that these mat communities respond differently to changes in redox even outside of their natural environment. This could be a result of differing functional genomic profiles and would be worth further investigation.

Sinkhole cyanobacteria have moderate sulfide tolerance

Mat communities from all study sites showed moderate tolerance of H₂S and consistent intolerance for DCMU. These results help confirm previous findings of the mat communities' ability for anoxygenic photosynthesis and oxygenic photosynthesis, and that the mats are likely dominated by cyanobacteria capable of asynchronous oxygenic and anoxygenic photosynthesis. These data help to place these communities into a broader historical context – physiological tolerance of both H₂S and oxygen would hypothetically put these communities into the “mixed/versatile” era in the evolutionary timeline of photosynthesis (Figure 4).

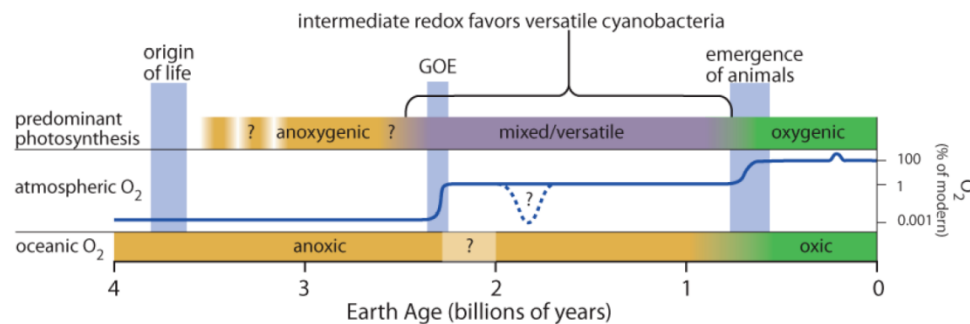


Figure 4: Timeline of Earth history showing atmospheric levels of molecular oxygen, significant biological landmarks, and the predominant type of photosynthesis. Cyanobacteria are believed to be responsible for the sharp rise in O₂ 2.3bya, known as the Great Oxidation Event (Biddanda *et al.* 2012).

Photophysiological filament motility and sedimentary carbon burial

The microbial communities studied use a combination of intercellular changes (photophysiology, pigments) as well as extracellular function (motility, phototaxis). The combination of these two phenomenon in concert allow individual cells as well as whole communities to optimize themselves for light harvesting. At Middle Island Sinkhole, motility allows cyanobacteria to climb to the surface of the mat to better reach sunlight – a phenomenon long known in stromatolites. Motility has even greater implications for the ecology at Middle Island Sinkhole where it has been documented that the microbial mats sequester overlying planktonic carbon by crawling over planktonic detritus that has fallen on the mat surface (Biddanda et al. 2012; Nold *et al.* 2013). This effectively buries and preserves the carbon due to the low oxygen conditions underlying the mat. These observational, stable C isotope tracer studies, as well as C:N analysis of sediment, show the underlying sedimentary organic matter to be more similar to phytoplankton in the overlying water column than the microbial mat itself. This shows a functional need for light directed motility. It is important to note that mat building stills occurs in the absence of light, quorum sensing probably aids mat building, which can then aid light directed motility (Montgomery *et al.* 2013). There is likely an important interplay between these two abilities. Further investigation into this phenomenon will help to better understand the link between motility and photophysiological changes, both of which have a significant effect on the overall ecology of these submerged sinkhole ecosystems.

These insights add to our understanding of the role of cyanobacterial communities on Earth. Seasonal acclimation to a range of PAR seems to be vital to sinkhole cyanobacteria survival. Tolerance of a range of redox as well as the presence of

photosynthetic inhibitors doesn't seem to have a negative effect on the photophysiology of the communities studied. Additionally, understanding the photophysiology of these communities in the modern context helps to better understand possible linkages to Earth history and the evolution of photosynthesis.

LITERATURE CITED

- Al-Najjar, M., A. Ramette, M. Kuhl, W. Hamza, J. Klatt, and L. Polerecky. "Spatial Patterns and Links between Microbial Community Composition and Function in Cyanobacterial Mats." *Frontiers in Microbiology* 5 (2014): n. pag. Web.
- Biddanda, B., S. Nold, G. Dick, S. Kendall, J. Vail, S. Ruberg, and C. Green. "Rock, Water, Microbes: Underwater Sinkholes in Lake Huron Are Habitats for Ancient Microbial Life." *Nature Education Knowledge* 3:13 (2012). Web.
- Kühl, M., M. Chen, P. Ralph, U. Schreiber, and A. Larkum. "Ecology: A Niche for Cyanobacteria Containing Chlorophyll D." *Nature* 433.7028 (2005): 820. Web.
- Lugomela, C., E. Söderbäck, and M. Björk. "Photosynthesis Rates in Cyanobacteria-dominated Sub-tidal Biofilms near Zanzibar, Tanzania." *Estuarine, Coastal and Shelf Science* 63.3 (2005): 439-46. Web.
- Montgomery, K., J. Charlesworth, R. Lebard, P. Visscher, and B. Burns. "Quorum Sensing in Extreme Environments." *Life* 3.1 (2013): 131-48. Web.
- Nold, S., M. Bellecourt, S. Kendall, S. Ruberg, T. Sanders, J. Klump, and B. Biddanda. "Underwater Sinkhole Sediments Sequester Lake Huron's Carbon." *Biogeochemistry* 115.1-3: 235. Web.